People's Democratic Republic of Algeria

Ministry of Higher Education and Scientific Research

University M'Hamed Bougara –Boumerdes-

Faculty of Engineering

Department of Electrical Engineering and Electronics

Memoire

Presented in Partial Fulfillment of the Requirements of the Degree of

MAGISTER

In Electronic Systems Engineering

Title

Energy Efficiency Optimization of Induction Motors

By

Mr. Yassine YAKHELEF

Before the jury:

Pr. L. REFOUFI	Professor at Univ. of Boumerdes	Supervisor.
Pr. DJ. BENAZZOUZ	Professor at Univ. of Boumerdes	President.
Dr. H. BENTARZI	Senior Lecturer at Univ. of Boumerdes	Examiner.
Dr. H. ZEROUG	Senior Lecturer at USTHB	Examiner.

Energy Efficiency Optimization of Induction Motors.

By

Yassine YAKHELEF

ELECTRICAL AND ELECTRONIC ENGINEERING DEPARTMENT.

BOUMERDES UNIVERSITY.

2007.

DEDICATION´

To my lovely parents, to those without whome my existence would be meaningless.

To my wife who sacrificed all her time to help me doing this work and who encouraged me throughout its achievement.

To my children Mohamed Abdelbasset and Nour El-Imene

To all my brothers and sisters

To all my friends

I dedicate this modest work.

TABLE OF CONTENTS

Chapter 3: The Induction Motor Fed From Non-Sinusoidal Power Supply and Converter Loss Calculation

Chapter 4: Power Factor Energy Optimal Control of Induction Motor

Chapter 5: Model-Based Energy Optimal Control Of Induction Motor

Chapter 6: Comparison Between Power Factor and Model-Based Controllers Performances

Acknowledgements:

First of all, i would like to thank my supervisor: **Prof. L. REFOUFI** for his help and patience during the last and most important period of this work and his guidance of the thesis along the right path.

My sincere and deep gratitude is due to the president of the jury **Pr. DJ. Benazzouz** and the members of the jury **Dr.H. Bentarzi** and **Dr.H. Zeroug** for their acceptance to evaluate this work.

Precious thanks also go to all my teachers of electrical and electronic engineering department of university of Boumerdes.

My sincere thanks go to **Dr. A. Khaldoune** and **Mr. R. Naamane** for their help and encouragement.

I do not forget to thank the staff of the department library for making different materials under our disposal.

.

ملخص:

إن التكلفة العالية و الاستهلاك المتزايد للطاقة الكهربائية إضافة إلى الحاجة الحيوية لاحتواء تأثيراتها السلبية على البيئة أضحت من العوامل القوية الدافعة لتنقيص فقودات الطاقة وتحسين الفاعلية العملية للمحركات الكهربائية .

تعتبر المحركات الحثية الأكثر استخداماً, فهي تمثل حوالي 60 % من مجموع الطاقة الكهربائية المستهلكة, مما يتطلب اهتمام خاص بتحسين الفاعلية الطاقوية بالنسبة للمحركات الحثية ذات القدرة الصغيرة و المتوسطة (اقل من 52 kW) والتي تستخدم في تطبيقات التسخين, التهوية والتكييف.

في هذا العمل يتم دراسة مفصلة والمقارنة لطريقتين من طرق التحسين المثلى للفاعلية الطاقوية للمحركات الحثية المتغيرة السرعة.

الطريقة الأولى تسمى بالضابط المثلى للفاعلية بواسطة معامل القدرة , حيث ترتكز على حساب قيمة معامل القدرة الأساسي مستخرج من الدارة الكهربائية المكافئة للطور الواحد للمحرك ثم ضبطه ثابتا على قيمته المقننة محققا بدلك أقصى قيمة للفاعلية على مدى مجال تغير السرعة المستخدم.

أما التقنية الثانية فتعرف بتقنية التحكم بنموذج الفقد القاعدي ، هذه الطريقة تعتمد على بناء نموذج الفقودات للمحرك الحثي في المعلم (d-q) حيث تم حل مسألة تحسين المردود الطاقوي بتحقيق تكافؤ بين الفقد الطاقوي بالنسبة للمحور (d) والفقودات بالنسبة للمحور (q) وهذا عند كل نقطة من نقاط التشغيل اقل من شروط الحمولة الكاملة .

النتائج المحصل عليها كانت متقاربة بالنسبة لكلا الطريقتين حيث نسجل نسبة 18% كتحسين في الفاعلية الطاقوية بالنسبة لكل المحركات الحثية التي أخضعت للدراسة في حالات الحمولة الجزئية.

Abstract:

The high cost of energy, its ever-increasing consumption and the vital need to curb harmful energy related effects on the environment are strong incentives to reduce the energy losses and improve the operating efficiency of electric motor drive systems. Further more, reduced losses not only reduce operating cost but also reduce capital cost of utility systems supplying electric power to their consumers. Induction motors are dominant loads, they account for about 60 % of the electricity consumed, for this reason, it is important to concentrate on optimizing the efficiency of induction motors, in particular small and medium size motors below 52 kW, whose load are Heating, Ventilation and Air Conditioning (HVAC) application.

In this work, two energy efficiency optimization techniques that minimize the total copper and core losses in a variable speed induction motor are studied and compared.

The power factor efficiency optimizer is based on the calculation of induction motor displacement power factor from its complete per-phase equivalent circuit, and which leads to a maximum operating efficiency when it is kept constant throughout the range of speed variation.

The model-based control technique, on the other hand, is based on induction motor loss model built in a d-q reference frame, where the optimization problem is solved by achieving a balance between the d- and q- loss components throughout the range of speed variation.

Results are showing that the two control techniques for the induction motors population studied indicate an overall comparable level of performance for both controllers. Achievable efficiency improvement at partial loads can reach 18 %.

Résumé:

Le prix élevé et la consommation croissante de l'énergie électrique, ainsi que le besoin vital de maîtriser ses effets néfastes sur l'environnement représentent des facteurs forts nous incitant à réduire les pertes énergétiques et donc améliorer le rendement des moteurs asynchrones. La réduction des pertes non seulement réduit les coûts de fonctionnement mais aussi les coûts d'investissement des systèmes énergétiques d'alimentation électrique.

Le moteur asynchrone représente le type de charge le plus important, pour cette raison, il est important d'améliorer son rendement énergétique et, en particulier, pour la population des moteurs asynchrones inférieurs à 52 kw utilisés dans les charges des chauffage, ventilation et climatisation (HVAC).

Le présent travail concerne une étude détaillée de deux techniques de commande optimale de l'efficacité énergétique appliqués aux moteurs à induction à vitesse variable.

La technique du facteur de puissance est d'abord étudiée. Cette méthode est basée sur le calcul du facteur de puissance des composants fondamentaux du courant et tension de l'alimentation (par référence au circuit équivalent du moteur à induction développé pour ce but).

En maintenant ce facteur de puissance constant à sa valeur maximale, l'amélioration du rendement de système est possible dans la plage de variation de vitesse désirée.

La deuxième méthode est appelée model-based, est basée sur l'obtention d'un modèle de perte pour le moteur asynchrone dans le repère (d-q). En utilisant cette méthode, le problème d'optimisation est résolu en assurant l'égalité des pertes correspondant aux deux composants (d- et q-) pour tous points de fonctionnements inférieurs à la vitesse nominale.

Les résultats montrent que les performances des deux méthodes de commande sont, globalement, comparable, où l'amélioration de 18 % de rendement énergétique est prédite pour les moteurs étudiés en charges partielles.

CHAPTER

1 *Introduction*

Throughout the twentieth century, most of the drives for industrial processes, commercial equipments, and domestic appliances have been designed to operate at essentially constant speed, mainly because of the ready availability of economical induction motors operating on the available constant frequency AC power supply. For many mechanical loads, it is recognized that a variable speed drive would provide improved performance, productivity, and energy efficiency [1]. However, until recently, the provision of continuously variable speed has been considered too expensive for all but special applications, for which constant speed was not acceptable [2]. Examples of such drives are: elevators, steel mill drives, machine tools, and robots. This situation is first changing, and particularly, in recent decades, as electric drives have been undergoing a major evolution as a result of two factors:

1) The availability and continuously decreasing cost of variable frequency electric power supplies resulting from advances in power electronic switching devices and in microprocessing based controls;
2) The increased concern about the present and future cost and availability of electric energy.

Consequently, variable speed drives are being designed into new systems and are being fitted to existing systems, permitting improved optimization of both quality of the system's output and its energy efficiency [3], [4].

1.1. Induction Motor and Energy Consumption:

The induction motor, especially the squirrel cage type, is widely used due to its several distinct virtues in comparison with d.c machines. These relate to lower cost and weight, lower inertia, improved ruggedness and reliability, low maintenance requirement and the capability to operate in a dirty and explosive environment due to the absence of commutators and brushes [5], [6]. Some of these virtues are of paramount importance, which make the induction motor drive system mandatory in several areas of applications.

Because of these advantages and its wide use, the induction motor is likely to remain the major electrical energy consumer for many years to come.

Due to that fact, a large part of electrical energy used in various places including households, industry, commerce, public services, traction and agriculture, is consumed by induction motors. It is found that the electrical motors consume around 56 % of the total consumed electrical energy, and of this, induction motors account for 96 %, this shows that around 54 % of the total electrical energy is consumed by induction motors [7].

To achieve energy savings in induction motor drives, an analysis of the use of the induction motor especially the cage motor is required. The intention is to concentrate the work in a field of motor drives where most of the energy is used and, more importantly, where it is wasted. Fig.1.2 shows the distribution of the use of energy by induction motors, divided into five motor size classes [7]. The data is based on statistics of the energy use in Denmark, and the tendency is valid for most industrialized countries and can be extended to be used for the developing countries like Algeria.

Analysis of these statistical results shows that the greater amount of energy is consumed by induction motors in the power range below 52 kW. Most important is the distribution of motor energy losses to the right of the figure. It shows that about 67% of the energy loss is dissipated in motors with a power rating below 52 kW. The tendency here is clear: if the aim is to save energy in induction motor drives, then, we need to concentrate the work on motor drives below 52 kW rated power.

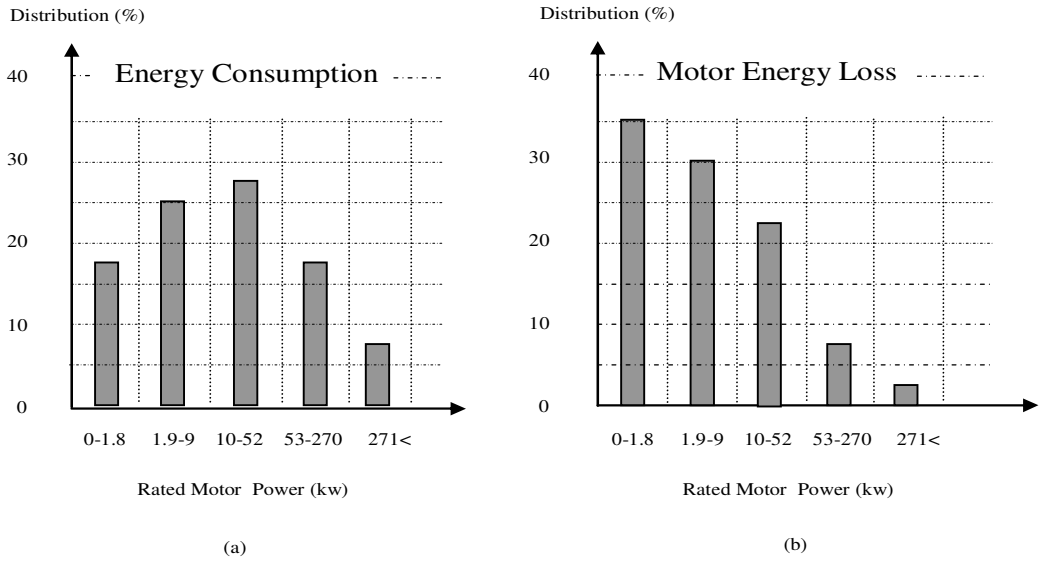

Fig.1.2 (a) Distribution of energy used by induction motors,
(b) Distribution of energy loss in induction motors [7].

It can be deduced that if losses in this population of motors can be reduced by just a few percent, it will have a major impact on the total electrical energy consumption. In a more precise statement, if the aim is to save energy in induction motor drives, then, we need to concentrate the work on motor drives below 52 kW rated power.

Accordingly, the present study is based on the squirrel cage induction motor power rating of 1.5 kW, 4.0 kW, 7.5 kW, 25 kW and 50 kW, with their parameters are listed in appendix B.

1.2-Induction Motor Drives and Load Types:

In order to have a consistent evaluation of induction motor drive energy control, it is very important to know the characteristics of the load [8], [9]. Practically, the induction motor can drive the following three load types, which are different in their characteristics:

- Fan and pump type loads,
- Constant torque loads, like conveyors and position displacement or reciprocating pumps, and
- Constant horse-power loads, such as winding machines.

1.2.1- Fan and Pump Type Loads:

These are variable torque loads which include, mainly, the heating, ventilation and air conditioning (HVAC) systems. Because in these load applications the torque is proportional to the square of the operating speed, they are characterizing by low torque requirements at low motor operating speeds [9].

1.2.2- Constant Torque Loads:

Constant torque loads require the same amount of torque at low speeds as at high speeds. The torque, in this load type, remains constant throughout the speed range, where as, the horse-power increases and decreases in direct proportion with the speed. As a result, special consideration must be given to the motor, especially its temperature rise during the operating time. In this context, special duty motors may be required which include a constant speed blower on the motor.

1.2.3-Constant Horsepower Loads:

For the constant horse-power load-type, the torque required at low speed is high, whereas at high speed, this torque is low, with the total required horse-power remains constant at any speed.

Each of these load types has its characteristics, which impact the amount of energy savings and process control that can be expected with the addition of adjustable speed drive.

1.3. Induction Motor / HVAC Drive Energy Efficiency Optimization:

When working on induction motor drive energy efficiency optimization, it is particularly interesting to consider the HVAC load type, because it is the group of applications that is often used in connection with induction motor [10], [11].

Recently, variable speed drives (VSDs) have been intensively applied in several HVAC systems, where the reduction in the cost of control electronics has made energy savings of 40% - 60% possible in these applications [11]. But when the speed is reduced to meet the load requirements, the load efficiency can be maintained high while the induction motor efficiency drops off as it becomes lightly loaded. Therefore, an energy optimal control method is required for further drive efficiency improvement under light load conditions.

1.4. Energy Optimal Control Methods of Induction Motor under Light Load Conditions:

Several small and medium size induction motor drive efficiency improvement methods have been reported in the literature. In general, they can be divided into two categories. The first category is the so-called loss-model based approach. It is also termed the loss-model controller (LMC), consisting of computing the losses by using the induction motor model and selecting the flux level that minimizes these losses.

The second one is termed as the power-measure- based approach, known also as search controllers (SCs). In this approach, the flux (or its equivalent variable) is decreased until the electrical input power settles down to the lowest value for a given torque and speed.

In the first approach, different loss models can be found in the literature. Alexander Kusko *et al* [12] in their works of reducing the energy losses in industrial and

transportation system adjustable speed electric motor drives addressed the method of adjusting the a.c motor stator voltage and frequency to minimize the electromagnetic controllable losses based on the induction motor equivalent circuit model including the core losses. Based on this loss- model, the objective function of the induction motor total losses is obtained and the minimization problem is solved numerically for the frequency corresponding to minimum losses. Garcia *et al.* [13], [14] proposed a simple loss model using the induction machine equivalent circuit in d-q coordinates. The loss model consists of computing the iron loss, copper losses (rotor and stator) in function of stator currents i_{qs} and i_{ds} in d-q frame. For a given speed and torque, the solution of the loss model yields the flux current i_{ds} for which the total loss is minimal.

In the second approach, the input power is first measured and then minimized by different ways. Moreira *et al.* [15] used the information of the third harmonics component of the air gap flux in the process of reducing the flux current, i_{ds}, in order to minimize the input power.

Sausa and Bose [16] proposed the technique of fuzzy logic based on-line efficiency optimization controller for a drive that uses the indirect vector controlled induction motor speed control system. The fuzzy logic controller adaptively decrements the flux-producing current on the basis of measured minimum input power, and for a given load torque and speed, the pulsating torque problem, generated through the iterative process, has been addressed by implementing a feed-forward torque compensator and the controller leads to an effectively induction motor drive efficiency improvement when operating under light load conditions.

In connection to the same approach, Cao-Minh *et al.* [17] reported their results on a new control algorithm for efficiency maximization of induction motor drives when operating at light load conditions. The algorithm uses the – golden section – technique to improve the convergence rate in the process of searching the optimal value of flux component of stator current, for which the electrical input power of the system is minimum at a given torque and speed. Because the flux component current is reduced in stepwise manner, torque pulsation problem is encountered. This undesirable problem, especially for induction motor low speed operation, is overcome by using a second order low-pass filter in the output of the efficiency optimization routine. The

application of the algorithm in the direct vector control environment has led to a substantial power saving and corresponding efficiency improvement.

In general the first approach is fast but depends largely on the motor parameters, which are very difficult to be exactly obtained due to the parameter sensitivity to operating conditions.

The second approach, on the other hand, is simpler and can include all kinds of losses; including the converter losses since the power entering to the system is measured and used in the optimization algorithm. However, it is relatively slow due to the search process. In addition it is difficult to precisely measure the input power in some practical cases. Therefore, measurement of d.c link power instead of input power represents an attractive solution.

The present study addresses the problem of efficiency optimization of induction motor in HVAC application where load dynamics are not demanding but efficiency improvement margins can be very important, with the objective of arriving at a simple reliable controller.

In order to achieve this objective, the steady state performances of induction motor when connected to a three phase sinusoidal, balanced power supply with detailed presentation of induction motor losses are addressed in chapter two. In chapter three, we have considered the induction motor when powered by a three phase sine wave PWM-VSI power supply, where the aim is to estimate the converter losses for squirrel cage induction motor for different power levels below 52 kW.

Chapters four and five are, respectively, devoted for the study and application of the two energy optimal control approaches, which constitute the power factor controller and model-based energy optimal controller with the corresponding simulation results. A brief comparison between the two controllers is done in chapter six. At the end we have concluded about the results that we have obtained throughout this study.

CHAPTER

2

Analysis of Steady-State Performances of Induction Motor Fed by Sinusoidal Power Supply

2.1. Introduction:

Work on energy efficiency optimization of squirrel cage induction motor variable frequency drive system requires, at first, computation of the steady state performance characteristics of the motor alone, which is the subject of this chapter. The main objective is to evaluate the different loss components of the induction motor assuming that it is connected to a three phase sinusoidal, balanced power supply.

2.2. The Operation Principle of Induction Motor:

When a set of balanced three phase voltages is applied to the distributed three phase primary windings, the resulting three phase currents establish a rotating m.m.f wave that results in a flux wave of constant amplitude rotating in the air gap at a constant speed known as synchronous speed (ω_s) [18]. The value of the synchronous speed is fixed by two parameters:

1) The supply frequency (f_1), cycles per second or Hertz;
2) The number of pole pairs (p) for which the primary is wound.

These parameters are appeared in the definition of synchronous angular speed as:

$$\omega_s \text{ (rev/sec)} = 2\ f_1 / p \quad \text{or;}$$

$$\omega_s \text{ (rev/mn)} = 120.\ f_1 / p \qquad (2.1).$$

The revolving field also links the rotor conductors, and since these linkages change, a voltage is induced in this latter. Currents then flow in the rotor and the interaction of these currents with the stator revolving flux results in a mechanical developed torque causing the rotor to turn in the same direction as that of the stator field at a speed (ω_m) [19], [20].

An induction motor runs at a shaft speed (ω_m) that is less than the synchronous speed (ω_s), the speed difference ($\omega_s - \omega_m$) is called the slip speed. The ratio of the slip speed to the synchronous speed is the most important variable in induction motor operation and is called the per-unit slip (s) [21]:

$$s = \frac{(\omega_s - \omega_m)}{\omega_s} \qquad (2.2).$$

2.3. Induction Motor Per-Phase Equivalent Circuit:

The study of electrical steady-state performances of induction motor under all operating conditions is achieved by developing an equivalent circuit which can fully describe the way it works, and which accounts for the various voltage and current components illustrating the transfer of power from stator to rotor, to be converted, there after, into mechanical form [22]. From the equivalent circuit also, a set of equations which define the operation of the induction motor can be deduced to enable the performance of the motor to be calculated.

Referring to Fig.2.1, when a three-phase sinusoidal, balanced voltage of r.m.s value V_1 is applied to the stator, an r.m.s current (I_1) flows in the stator windings and a part of the voltage is absorbed by the stator winding resistance (R_1); part is absorbed by the stator leakage reactance (X_1), which corresponds to the flux linkages that do not cross the air gap to couple rotor and stator windings together. The remainder of the stator voltage is absorbed by the counter voltage generated by the revolving field: E_1. The current I_1 has two components: the no load (or exciting) current I_0 and the reflected rotor current I_2. The no load current has two components: the magnetizing current I_m and the current I_c, which caries the power from the source to cover the iron core losses, represented by the resistor R_c. The magnetizing current builds the air gap flux, the measure of which is the main reactance X_m.

The resistor R_c is connected in parallel to the main reactance, and the voltage drop across them is equal to E_1 because the iron core losses are proportional to the square of the main flux magnitude, which is proportional to the amplitude of the induced voltage E_1 [20]. These relations are expressed, for one-phase Y connected induction motor, as:

$$V_1 = E_1 + R_1 I_1 + jX_1 I_1 \qquad (2.3).$$

$$E_1 = R_c I_c = X_m I_m \qquad (2.4).$$

Where the subscript '1' is used to describe the stator quantities, and by these equations, the stator equivalent circuit is defined.

On the other hand, the revolving field, which generates E_1 in the stator, would also generate the voltage ($sE_2^{'}$) in the rotor side. Since the rotor conductor bars are closed (short-circuited), this generated voltage is absorbed by the current ($I_2^{'}$), passing through the rotor circuit resistance ($R_2^{'}$) and the leakage reactance ($sX_2^{'}$).

We have then the equation expressing this relation as:

$$sE_2^{'} = R_2^{'}I_2^{'} + jsX_2^{'}I_2^{'} \qquad (2.5).$$

Which is the equation that defines the per-phase rotor equivalent circuit of the Y-connected induction motor, where the subscript '2' is used, in this case, to describe the rotor quantities.

When the equations (2.3), (2.4) and (2.5) are combined, the steady-state per-phase exact equivalent circuit of the induction motor under the real operating conditions can be obtained. This is illustrated in Fig.2.1.

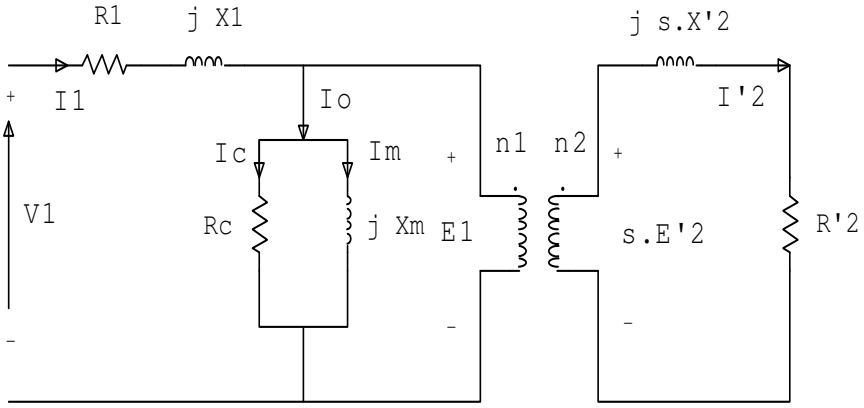

Fig.2.1. Per-Phase Exact Equivalent Circuit of Induction Motor under Real Operating Conditions.

Where (n1) and (n2) are the respective turns per-phase on the primary and secondary windings. Although this equivalent circuit can be used to assess the motor performances, it is not easy to do so due to the two different frequencies of the circuit; the stator frequency (f_1) and the rotor (slip) frequency $\left(f_2 = s.f_1\right)$. So it is normal to simplify further the circuit by referring, at the same time, all the rotor parameters to the stator winding.

To do so, we divide both sides of the expression (2.5) by the slip s, then, we reflect the rotor parameters to the stator side according to the relations [19]:

$$E_2 = \frac{n1}{n2}.E_2^{'} \qquad (2.6).$$

$$I_2 = \frac{n1}{n2}.I_2^{'} \qquad (2.7).$$

$$R_2 = (\frac{n1}{n2})^2.R_2^{'} \qquad (2.8).$$

$$X_2 = (\frac{n1}{n2})^2.X_2^{'} \qquad (2.9).$$

Concerning the transformation ratio $\left(\frac{n1}{n2}\right)$, it is found that, as long as the induction wound rotor motor is concerned, this ratio is usually greater than unity and is typically in the range of 1.1- 1.3 [21]. However, this ratio is taken approximately equals to unity for the squirrel cage induction motor type [23].

Under these considerations, the end result of the simplifications performed on the circuit of Fig.2.1 is represented by the circuit of Fig.2.2, which is the traditional per-phase exact equivalent circuit of an induction motor, where the necessary referred rotor parameters are usually available from the manufacturers to match this figure in any specific case and all voltage quantities given here are valid regardless of the frequency of operation, in that, the synchronous speed (ω_s) is given explicitly [22].

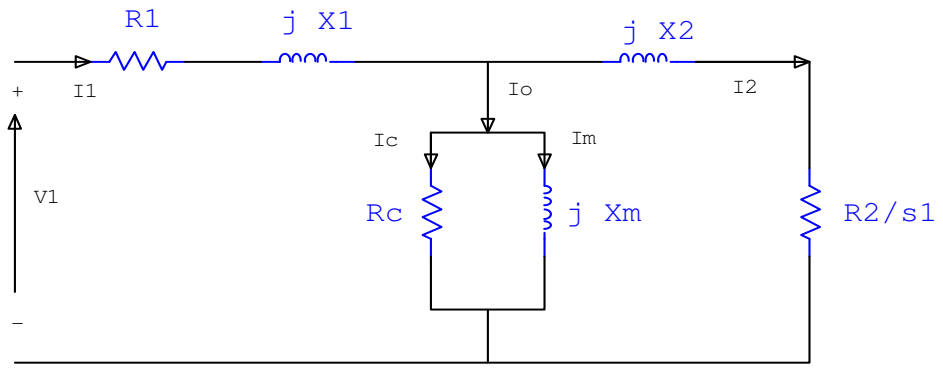

Fig.2.2 Per-Phase Steady State Equivalent Circuit of a Three-Phase Induction Motor.

Where:

R_2 : is the actual rotor resistance per phase referred to the stator (Ω).

X_2 : is the actual rotor leakage reactance per phase referred to the stator (Ω).

R_1 : is the stator resistance per phase (Ω).

X_1 : is the stator leakage reactance per phase (Ω).

X_m : is the magnetizing reactance (Ω).

And the losses in the magnetic circuit; iron (or core) losses are represented by the presence of the resistor Rc.

The usefulness of this equivalent circuit in the analysis and assessment of the squirrel cage induction motor steady-state performance characteristics is based on the knowledge of the impedance parameters. These are the result of the following tests that can be carried out on the induction motor:

(1) No-load test to determine the mechanical and magnetic losses.

(2) Short-circuit or blocked-rotor or locked-rotor test to determine the effective total resistance, the rotor resistance, or the electrical resistance losses (copper losses).

(3) Stator resistance test to determine the stator resistance separately from the rotor resistance.

It is very important, however, to say that the induction motor impedance parameters appeared in the steady-state equivalent circuit are not constant. Besides, the variation of the ohmic resistances with temperature, the parameters may be expected to change with the loading conditions, where the major cause in this change consists in the saturation[53].

2.4. Induction Motor Power Loss Calculations:

The per-phase exact equivalent circuit of the induction motor developed earlier is used to assess the steady-state performance characteristics of the induction motor. If it is assumed that the induction motor is fed from a balanced sinusoidal three-phase power supply, hence the validity of the equivalent circuit, and all circuit parameters are deduced from the conventional tests, in addition to the availability of the input or output conditions, (input voltage and operating slip may be given), the assessment and

analysis of the induction motor performances require, first, an acceptably accurate quantification of its losses.

2.4.1. Induction Motor Power Losses:

The induction motor losses can be classified as follows:

a) Stator copper losses,

b) Rotor copper losses,

c) Iron (core) losses,

d) Stray losses, and

e) Mechanical (friction + windage) losses.

By referring to the per-phase induction motor equivalent circuit of Fig.2.2, three of the five component losses can be identified.

2.4.1.1. Copper Losses:

The electrical windings will always have a finite resistance, however small, it will cause power losses which are generally proportional to $(I^2.R)$, where I is the current flowing through it, and they are also called the electrical losses or joule losses [24].

The value of the winding resistance will increase with temperature and this will depend on the current loading and the effectiveness of the overall cooling of the machine. To be on the save side, the resistance at rated temperature should be used in loss calculations.

When the induction motor is powered by a sinusoidal supply, these copper losses consist of two types:

- ***Stator copper loss;***

$$P_{sc} = I_1^2.R_1 \qquad (2.10).$$

- ***Rotor copper loss;***

$$P_{rc} = I_2^2.R_2 \qquad (2.11).$$

Where:

R_1 and R_2 are respectively the stator and rotor resistances ;

I_1 and I_2 are respectively the stator and rotor currents (the RMS values).

2.4.1.2. Iron (Core) Losses:

In every cycle of operation, the flux in the core of the induction motor will be reversed causing a small loss of energy usually called hysteresis loss illustrated by the area of $\frac{B}{H}$ hysteresis loop, which is typically shown in Fig.2.3. The value of this power loss component depends on the quality of the iron being used, the value of the flux density over which it is being used and the frequency of operation. An empirical expression for it in a core taken through 'f_1' cycle of magnetization (operation) per second is [25] :

$$P_h = K_h . f_1 . B_m^x \qquad (2.12).$$

Where:

B_m : is the maximum induction reached (flux density),

K_h : is the hysteresis constant depending on the molecular quality and structure of the core material, and

x : depends also on the core quality and which normally varies between 1.5 and 2.5.

Traditionally x equals 2 has been used for the general unspecified case for AC magnetic circuits [26].

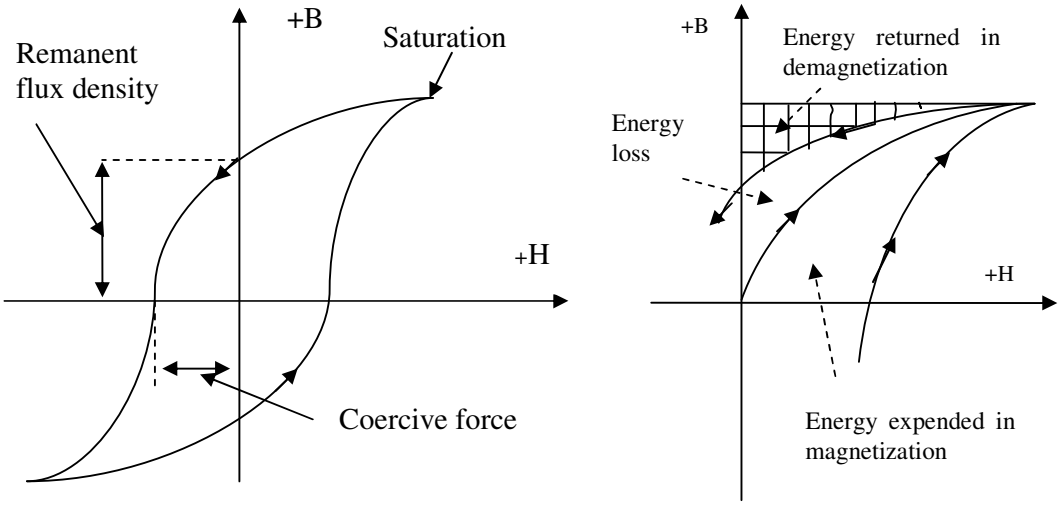

Fig.2.3. Hysteresis Energy Loss.

The total iron losses also contains an other component, it is the eddy current loss due to the induced current flowing in the core. In order to reduce this loss to relatively small proportions, a.c magnetic circuits are laminated using thin insulated sheets clamped together.

There will still be a small eddy current loss and for a specific iron circuit, it can be given by:

$$P_e = K_e.t^2.f_1^2.B^2 \qquad (2.13).$$

Where the constant K_e depends on the resistivity of the core material and 't' being its thickness.

This compound of eddy and hysteresis losses is represented in the induction motor equivalent circuit model by:

$$P_c = I_c^2.R_c \qquad (2.14).$$

The core losses were represented only in the motor stator side, because the rotor core loss varies with rotor frequency (f_2), and hence with the slip.

Under running, steady-state conditions, the design B squirrel cage induction motor slip, s, do not exceed 5 % [27] and therefore, the rotor frequency will be about (does not exceed) the value 2.5 Hz, which makes the rotor core loss very small that can be neglected throughout the steady-state analysis of the induction motor [28].

2.4.1.3. Mechanical Losses:

These are the friction and windage power losses, where the friction power losses are the result of friction between the moving parts and the windage power loss is the result of the air circulating inside the motor for cooling purposes., which can be implemented by some simple fan blades attached to the shaft inside the machine housing and very large machines require external cooling systems (blowers).

In general, both friction and windage losses are proportionally dependent on the motor operating speed. Therefore they will drop to very low levels under low speed operating conditions [29].

2.4.1.4. Stray Load Losses: Ps

The friction, windage, core and copper (I^2R) losses can be estimated from no-load and short-circuit tests that can be performed on the induction motor. The measured loss on the loaded induction motor, however, is invariably greater by the amount called stray load losses.

These losses consist of additional iron and copper losses due to the quasi-sinusoidal field distribution in the air gap, and the additional losses caused by stator slot effects and skin effect in conductors [19].

Consequently, the use of a suitable slot ratio and the insulation of the rotor bars in their slots can substantially reduce the stray losses [30].

Although its importance, the quantification of these losses is not the concern of the present study.

2.5. Induction Motor Power Flow:

The mechanical output power (P_{mech}) from the motor is the product of the motor developed torque (T_e) and the operating shaft speed (ω_m).

In (SI) units, there is no multiplying constant, and:

$$P_{mech} = T_e.\omega_m \qquad (2.16).$$

Where P_{mech} in watts, T_e in Newton meters and ω_m in rad /sec.

By combining (2.2) and (2.16) we obtain the output power in terms of per-unit slip:

$$P_{mech} = T_e.\omega_s(1-s) \qquad (2.17).$$

The output power has to overcome the forces due to bearing and brush friction (usually small) [31] and due to the ventilation windage (which may be considerable) as well as driving the load. If it is necessary to identify the load torque T_l and the windage torque T_{fw} separately, (2.16) may be written as:

$$P_{mech} = (T_o + T_{fw}).\omega_m \qquad (2.18).$$

Where T_o represents the output torque of induction motor which is equal to the load torque, T_l , at the stable operating point [32].

The portion of the internal electrical power per-phase that is converted to mechanical output power is:

$$P_{mech} = I_2^2.R_2\frac{(1-s)}{s} \qquad (2.19).$$

The total power per-phase delivered to the motor secondary windings through the air gap is:

$$\begin{aligned} P_g &= P_{mech} + I_2^2.R_2 \\ &= I_2^2.R_2.\frac{1}{s} \\ &= T_e.\omega_s \end{aligned} \qquad (2.20).$$

Where P_g is the air gap power which is the power transferred from the stator to the rotor of the induction machine through its air gap, and which is related, according to equation (2.20), to the motor parameters mentioned in the complete per-phase equivalent circuit of Fig. 2.2.

This air gap power has two components:

1. ***The copper losses in the rotor circuit*** P_{rc}***:***

$$P_{rc} = I_2^2.R_2 \qquad (2.21).$$

2. ***The mechanical power*** P_{mech}

$$P_{mech} = I_2^2.R_2.\frac{(1-s)}{s} \qquad (2.22).$$

Knowing the air gap power, we can express the rotor copper losses, P_{rc}, by utilizing equation (2.20) and equation (2.21) as:

$$P_{rc} = s.P_g \qquad (2.23).$$

The mechanical power as a function of the air gap power is obtained from (2.20) and (2.23) as;

$$P_{mech} = (1-s).P_g \qquad (2.24).$$

If the rotor current is calculated, the electromagnetic developed torque can be expressed as a function of air gap power as:

$$T_e = \frac{P_g}{\omega_s} \qquad (2.25).$$

On the other hand, the input power per-phase entering the machine terminals is given by:

$$P_{in} = V_1.I_1.\cos(\varphi_1) \qquad (2.26).$$

Where φ_1 is the phase shift angle between V_1 and I_1 , which is constant for a given supply frequency (f_1).

A portion of the input power P_{in} is converted into the stator winding copper losses, and an other portion covers the stator iron (core) losses P_c . The remaining input power is supplied to the rotor as the air gap power P_g .

The air gap power is divided into the rotor copper losses and the mechanical output power as a function of the rotor slip, s. When the friction and windage losses are subtracted from the mechanical output power, the power on the motor shaft P_o is obtained.

According to this description, the power flow within the squirrel-cage induction motor is shown in Fig.2.4.

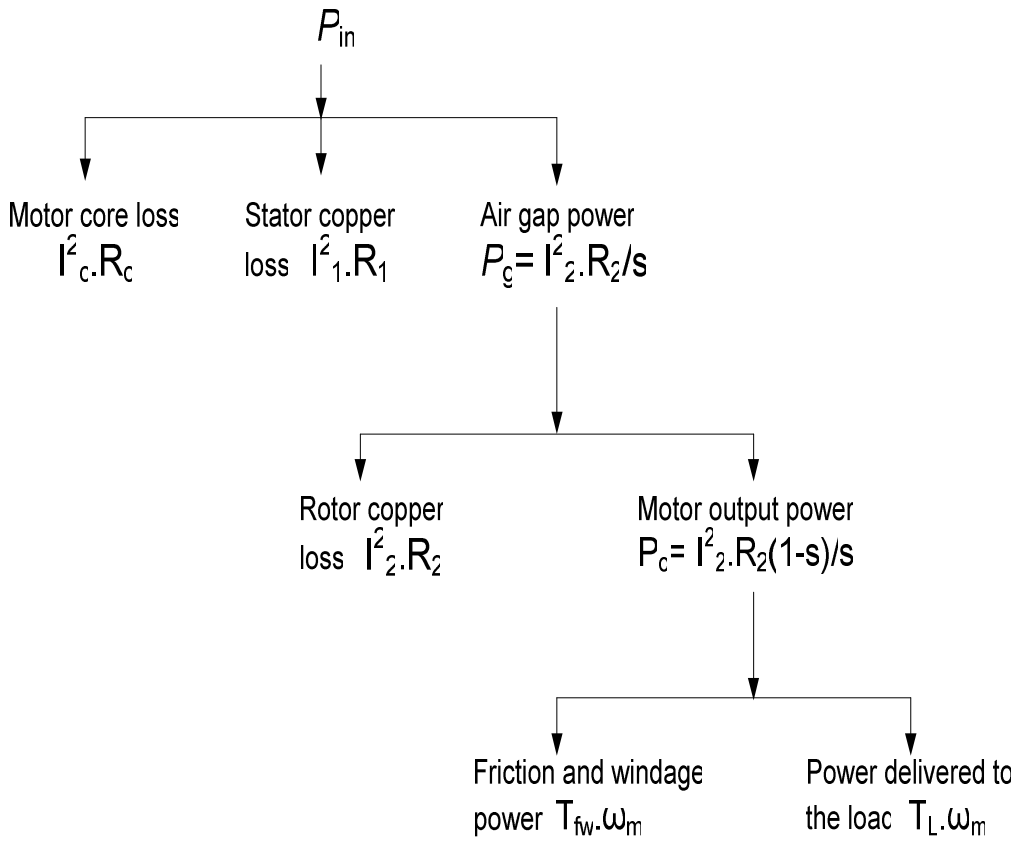

Fig.2.4. Per-Phase Motor Power Flow [21].

2.6. Induction Motor Steady State Performances Calculations:

Based on the induction motor losses analysis presented in the previous section, and by referring to the steady-state per-phase exact equivalent circuit, the motor steady-state performance calculation and analysis can now be performed.

In general, these performances are characterized by the following briefly discussed factors:

1) The efficiency;
2) The power factor;
3) The starting current;
4) The starting torque and
5) The pull-out (or maximum) torque

2.6.1. Induction Motor Efficiency:

The efficiency of the induction motor is simply its output power divided by its input power where they are in the same units [33]. The shaft output power is the input power minus the various accumulated losses. Similarly, the input power is the shaft output power plus the same losses. Mathematically, this is formulated as:

$$\eta = \frac{P_o}{P_{in}} = \frac{P_{in} - \sum losses}{P_{in}} = \frac{P_o}{P_o + \sum losses} \qquad (2.27).$$

With: $\sum losses = P_{sc} + P_{rc} + P_c + P_{fw} + P_s$.

Where:

η: Efficiency,

P_{in} and P_o are respectively, the input and output power.

P_{sc}, P_{rc} and P_c are, respectively stator copper losses, rotor copper losses and core losses and,

P_{fw} and P_s are respectively, friction and windage losses and stray load losses.

2.6.2. Induction Motor Power Factor:

The power factor is defined as the quotient of the input power to the volt-ampere quantity. This is expressed as:

$$PF = \frac{P_{in}}{V_1.I_1} \qquad (2.28).$$

For the induction motor fed from sinusoidal balanced three phase power supply, the power factor is given as:

$$PF = \frac{V_1.I_1.\cos(\varphi)}{V_1.I_1} = \cos(\varphi) \qquad (2.29).$$

With φ is the phase angle between the phase voltage and current of the induction motor.

When a balanced three-phase voltage is applied, the induction motor will operate at a lagging power factor, which will vary over the load range of the motor. The power factor displayed by a typical three phase induction motor is very poor during part-load conditions [34].

2.6.3 Induction Motor Current and Developed Torque Characteristics:

There are really three different points where the actual value of the induction motor torque is needed: the starting torque, the maximum torque and the load torque or the rated torque. The knowledge of how to determine these torque values enables us to fit the motor to its load in the most economical manner [35].

The maximum torque that a squirrel cage induction motor can develop is variously known as the break-down torque, or the pull-out torque. In squirrel cage induction motor (SCIM), this torque is ordinarily substantially higher than the starting torque, the maximum torque is usually developed at from half to three-quarters the synchronous speed and it is about three to four times the rated full load torque [23].

The plots torque-speed characteristics obtained for the population of induction motors studied indicate that the developed torque, with a fixed supply voltage, will drop at little to the minimum pull-up torque as the motor accelerates, and then rises to the maximum pull-out torque at almost full speed and drops to zero at the synchronous speed.

When it is connected to a supply voltage, the induction motor draws a very high starting current. The starting current of the induction motor, with a fixed voltage, will drop very slowly as the motor accelerates and will only begin to fall significantly when the motor has reached at least 80 % full speed, as it is seen in the corresponding plots.

The curves of induction motor starting current and torque characteristics are dependent on the terminal voltage and the motor (rotor) design characteristics, which are NEMA design classifications assigned for establishing the operating specifications for different motor types. These design classes are defined by the letters A, B, C, and D, where the design letter is used to indicate the motor's torque characteristic which is an important selection consideration.

Most squirrel cage induction motors (SCIMs) are design B, with design A being the second common type [27]. Table 2.1 lists the key characteristics of NEMA design B squirrel cage induction motors.

NEMA Design	Starting carrent	Starting Torque	Breakdown torque	Percent Slip	Applications
A, B	medium	Medium Torque	high	Max. 5 %	Low inertia, high acceleration (fans, blowers, centrifugal pumps and machine lools).
C	Medium	High torque	medium	Max. 5 %	High starting torque, compressors crushers, boring mills, conveyor equipment, textile machinery, wood working equipments.
D	medium	Extra High Torque	Low	5 % Or more	Bulldozers, shearing machines, punch presses, stamping machines, hoists.

Table 2.1 NEMA Polyphase Induction Motor Designs.

The steady-state performance characteristics, which are previously described, are shown in the following figures for 1.5 kW, 4.0 kW, 7.5 kW, 25 kW and 50 kW induction motors.

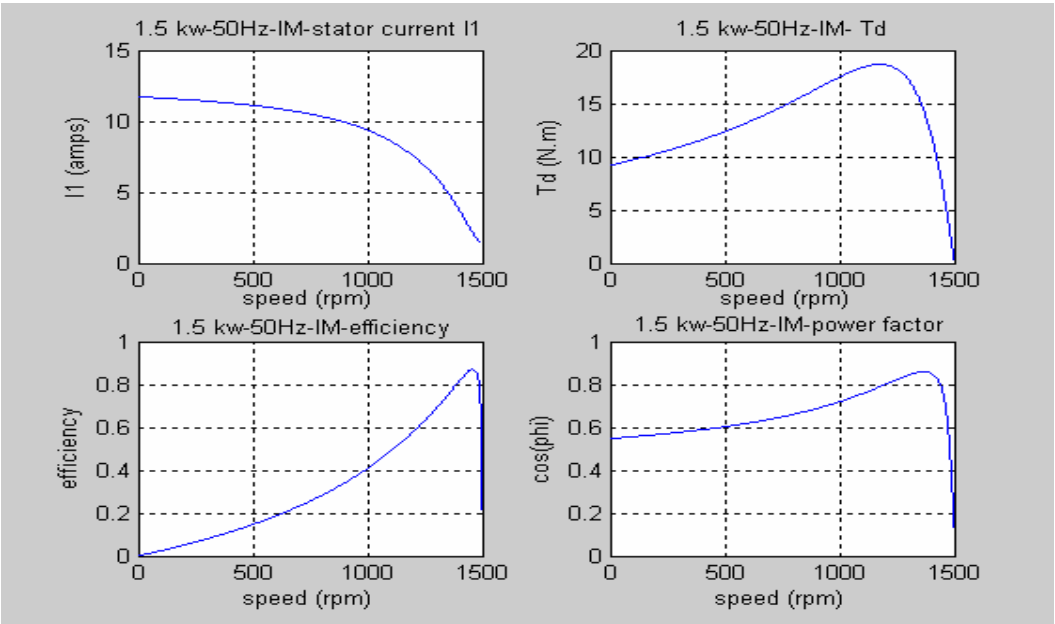

Fig.2.5. Steady-State Developed Torque, Stator Current, Efficiency and Power Factor of 1.5 kW.

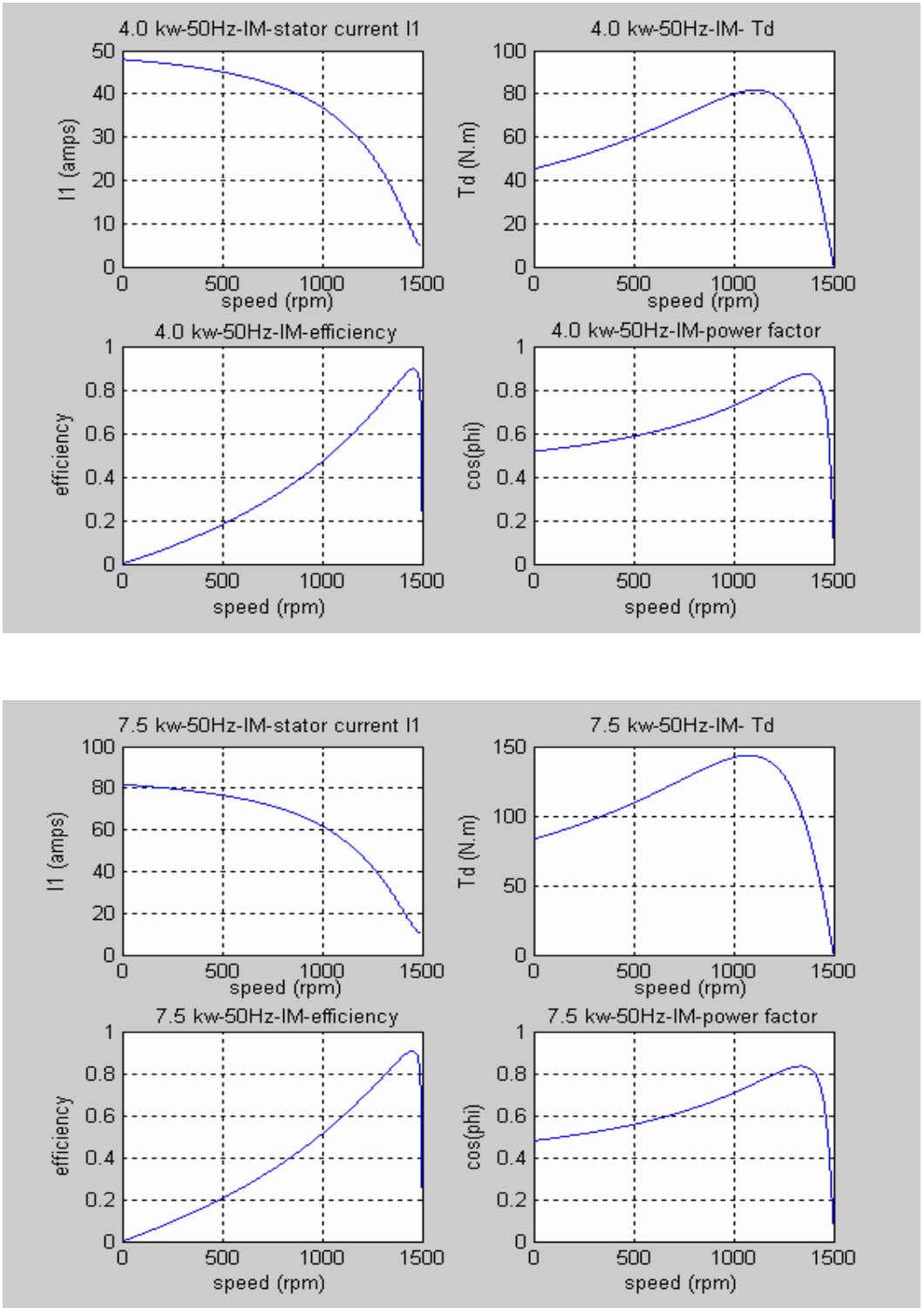

Fig.2.6. Steady-State Developed Torque, Stator Current, Efficiency and Power Factor of 4.0 kW and 7.5 kW Induction Motor.

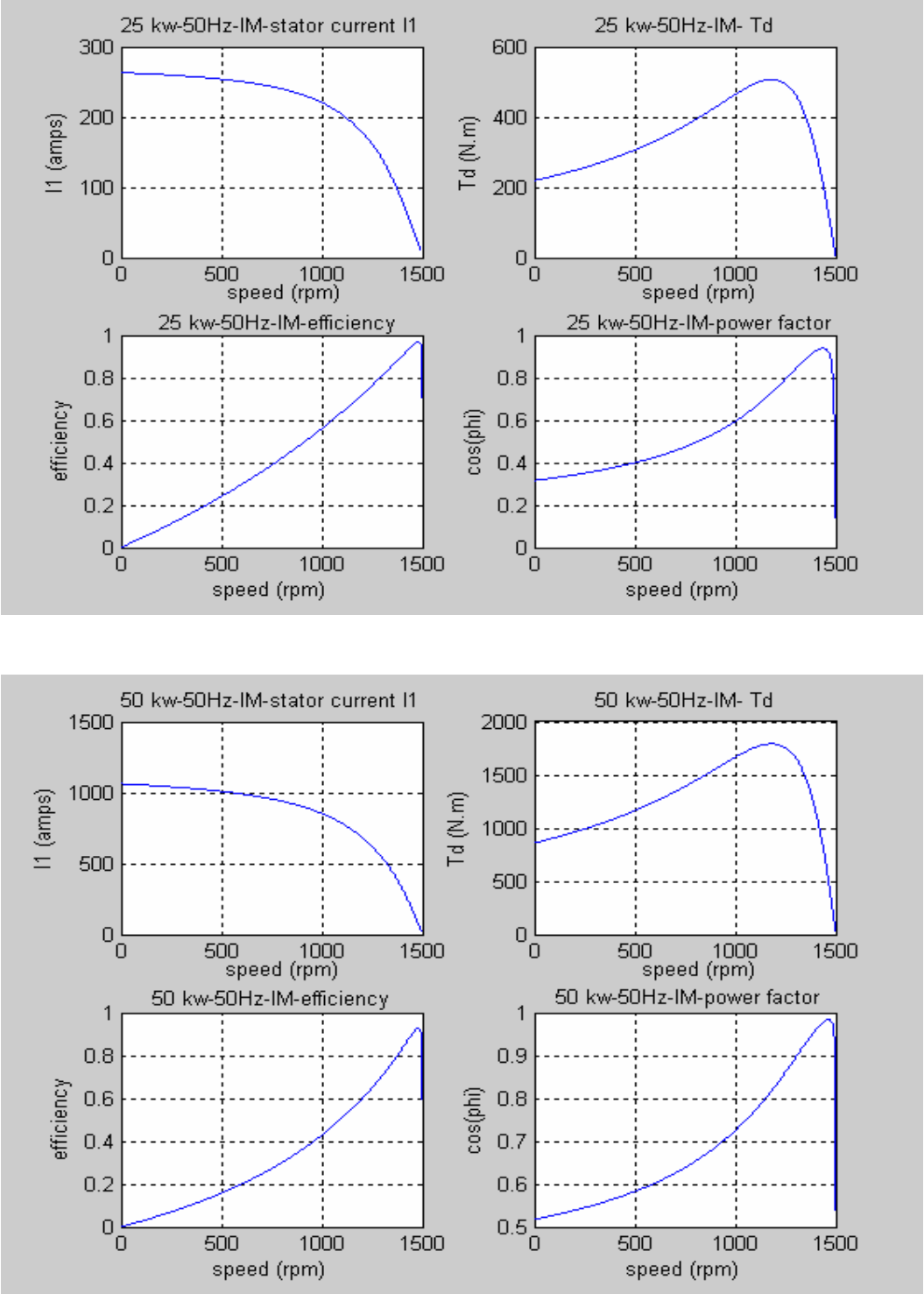

Fig.2.7. Steady-State Developed Torque, Stator Current, Efficiency And Power Factor of 25 kW and 50 kW Induction Motor

The curves show very clearly that the conditions to the right of the pull out torque point are very much better than at other speeds; the efficiency is high, the power factor is high, the torque per amp is high, for these reason, the induction motor is always used near to the synchronous speed with the actual speed of the operation being dependent on the torque demanded by the load [29].

On the other hand, a three-phase induction motor fed from a constant voltage, constant frequency source is inherently inefficient at low speeds, a fact that can be easily educed in all these plots.

2.7. Conclusion:

The steady-state performance characteristics of the squirrel cage induction motor are calculated and simulated for the five induction motor power ratings: 1.5 kW, 4.0 kW, 7.5 kW, 25 kW and 50 kW. The simulated design B induction motors are taken to represent a population of small and medium size induction motors, which are widely used to drive a type of load applications known as heating, ventilation and air conditioning (HVAC) systems.

This analysis, is based on the per-phase exact equivalent circuit , known also as the six-parameters equivalent circuit of the induction motor, where the motor is assumed to be fed from a balanced three-phase sinusoidal power supply and the motors parameters are assumed constant.

CHAPTER

3

The Induction Motor Fed by a Non-Sinusoidal Power Supply and Converter Loss Calculation

3.1. Introduction:

In the preceding chapter, the induction motor steady state performances are studied and analyzed by assuming that the motor is supplied from a three-phase sinusoidal, balanced power supply. The present study concerns the energy efficiency optimization of induction motor drives, it is therefore necessary to study the performances of induction motor when it is supplied from three-phase balanced non-sinusoidal power supply; in other word, when fed by a power electronic converter (P.E.C). Besides, the converter loss is calculated in view of they can be neglected or not in relation to the optimization problem.

3.2. The Induction Motor Fed from P.E.C:

If the induction motor is supplied from a variable frequency, variable voltage source, there can be an infinite number of sets of torque-speed curves like those obtained at the end of chapter two for each induction motor. The result shows that: it is possible to always operate in the area of the right of the peak torque point, i.e. in the area of maximum efficiency, maximum power factor and maximum torque per amp and inherent stable operation, what ever the speed the motor runs at. With such a variable supply, therefore, the motor can always be operated under its most advantageous conditions at any speed from the standstill.

To allow the induction motor to operate under variable frequency, variable voltage conditions, power electronic converter systems should be inserted between the mains and the motor.

3.3. Inverters for Adjustable Speed Induction Motor:

The class of converters that converts d.c power to a.c power is defined as inverters, and it is the inverter that creates variable frequency from the d.c source which is used to drive an induction motor at a variable speed [36].

Inverters can broadly be classified either as voltage-source or current-source inverters, with the two types are totally different in their behaviour.

3.3.1. The Voltage Source Inverter (VSI) Drive:

The voltage-fed, or voltage-source inverter (VSI) is powered from a stiff, or low-impedance, d.c voltage source, such as a battery or a rectifier, the output of which is smoothed by an LC filter. The large filter capacitor across the inverter input terminals

maintains a constant d.c link voltage. The inverter is, therefore, an adjustable-frequency voltage source, the output voltage of which is essentially independent of load current. This type of inverters is, in turn, found as Six-Step -VSI and PWM-VSI.

3.3.1.1. The Three-Phase Bridge Six-Step VSI:

The three-phase six-step, or quasi-square wave, inverter is a voltage-source inverter that has been widely used in commercial adjustable-speed a.c motor drives. Conventional thyristors have been used in many six-step inverters. However, any semiconductor device with self-turn off capacity can be used, such as GTO, power MOS FET, or transistor, where the semiconductor must have a sustained gating, or firing, signal throughout the half-cycle, during which conduction may occur, because the exact instant at which conduction commences is load dependent [21].

When an induction motor is powered by a six-step VSI, the motor current waveforms show a significant harmonic content whose influence on motor performances is apparent.

On the other hand, in a six-step inverter, the output voltage waveform does not vary with frequency and there is a fixed ratio between the magnitudes of the d.c link voltage and the a.c output voltage, where the control of the a.c output voltage is achieved by varying the d.c link voltage which is commonly provided by phase-controlled thyristor converter with an LC filter on the output. The filter is used to smooth the rectified voltage but introduces a time lag which slows the transient response of the system [36]. A typical structure of six-step VSI is given in Fig.3.1.

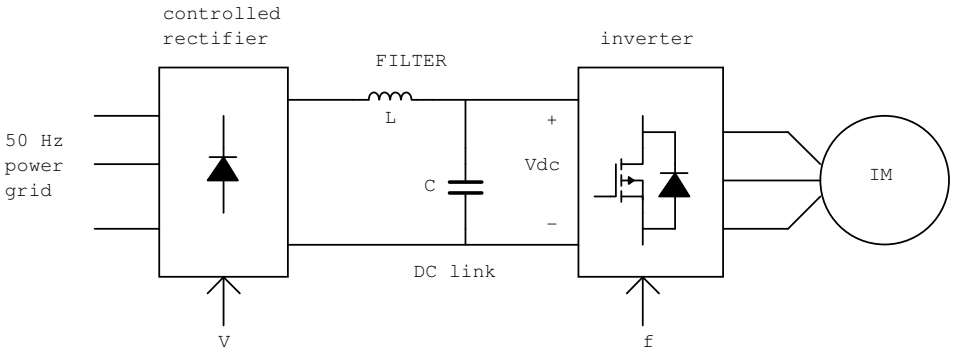

Fig.3.1. General Structure of the Six-Step Voltage Source Inverter.

3.3.1.2. The Three-Phase Bridge PWM-VSI:

The three-phase bridge inverter circuit for PWM waveform generation is identical to that of six-step inverter circuit, but the switching sequence is more complex [31], [37]. Voltage control is achieved by modulating the output voltage waveform within the inverter and hence an adjustable-voltage d.c link is not required. Consequently, an uncontrolled diode bridge rectifier is used, and the fast switching speed of power transistor, such as IGBT, is advantageous in PWM inverter, but thyristors or GTOs are necessary at high power levels [21].

The output frequency control is accomplished, as usual, by varying the switching rate of the inverter devices. Thus, output voltage and frequency can be rapidly altered within the inverter circuit, and the PWM inverter drive, therefore, has a transient response which is much superior to that of the six-step inverter drive. A typical circuit structure of the inverter is given in Fig.3.2.

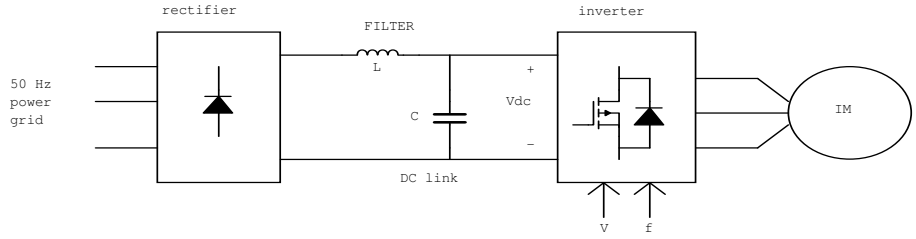

Fig.3.2. General Form of the PWM Voltage Source Inverter.

When a sophisticated PWM strategy is adopted, there are no low-order harmonics in the motor current and low-speed torque pulsations and cogging effects are eliminated [31]. However, the switching frequency of the PWM inverter is substantially higher than that of the six-step inverter, as a result, inverter switching losses may be significant.

As far as the three-phase PWM inverter is concerned, a variety of modulation techniques has been devised, among which, we distinguish:

- ❖ The square-wave PWM inverter, and
- ❖ The sinusoidal PWM inverter.

Adjustable-frequency operation of a sine wave PWM inverter for a.c induction motor control requires a generation of a set of three-phase sine wave reference voltages of adjustable amplitude and frequency. But if the motor is to operate at very low speeds down to standstill, the reference oscillator must have a corresponding low- frequency capability down to zero frequency. Consequently, many of the early PWM inverter drives were adapted to the square-wave PWM strategy because the electronic circuit design of an adjustable-frequency square-wave oscillator is relatively straight forward. However, the implementation of sinusoidal PWM has been facilitated by modern digital circuit techniques utilizing programmed memory or custom-designed large-scale integrated (LSI) circuit [31].

3.3.2. The Current Source Inverter Drive:

Since induction motors have traditionally designed to operate from a voltage source, the voltage source inverter was developed and used first to approximate the waveform presented to the motor by the utility. The current source inverter, on the other hand, is very different in concept.

Current-fed inverter drives have been in use slightly more than 20 years [37]. They have, however, several properties which make them attractive as well as an inevitable number of undesirable effects [38]. As the name implies, the inverter switches of a CSI are fed from a constant current source. While a true constant current source can never be a reality, it is reasonably approximated by a rectifier or a chopper with a current control loop, as well as a voltage d.c link inductor to smooth the current.

An important limitation in the application of a CSI drive is the fact that open-loop operation in the manner of VSI is not possible. For more details on the topic the reader can refer to [21], [36], [37].

While the use of either of these controlled circuits (VSI, CSI) is dictated by the type and the characteristics of the application, however, by the availability of such electronic systems, the speed and /or torque of the induction motor can now be varied (controlled) and therefore, satisfying the requirements of an important load type applications known as variable torque loads to which the fan loads are belonging.

Due to their characteristics, especially the quadrature proportionality property between the torque and the speed, in the present study we have chosen to use the sine wave PWM-VSI to feed the induction motor drive.

3.4. Harmonic behaviour of induction motor:

When sine wave PWM-VSI is used to feed the induction motor, it generates an output voltage or current waveforms with harmonic content due to the switching action of the inverter.

3.4.1. Positive, negative and zero sequence harmonics:

In the presence of non-sinusoidal voltage V_k or current I_k, the k^{th} harmonic components in the phase currents produce a time harmonic mmf wave rotating forward or backward at speed $k\omega_s$ [39]. In general, the direction of rotation of the harmonic field is determined by the phase sequence of the harmonic currents, where, harmonics of order (6n+1), with 'n' an integer, have the same phase sequence as the fundamental currents, and hence produce mmf waves that rotate in the same direction as the main field. These harmonics are called positive sequence harmonics.

Conversely, the harmonic currents of order (6n-1) are called negative sequence harmonics. The harmonic currents of order (6n-3) do not produce any fundamental air gap mmf and they are called zero sequence harmonics, these harmonics are also termed triplen harmonics.

3.5. Induction Motor Harmonic Equivalent Circuit:

When the induction motor absorbs the inverter output current waveforms, the k^{th} harmonic component produces a time harmonic mmf wave rotating forward or backward. The resulting rotor slip is given by [39]:

$$s_k = \frac{k\omega_s \mp \omega_m}{k\omega_s} \qquad (3.1).$$

Where the negative sign is given for positive sequence harmonics and the positive sign is given for the negative sequence harmonics.

In order to understand the harmonic behaviour of the induction motor, we need to build its harmonic equivalent circuit. This circuit is obtained by taking a copy of the fundamental equivalent circuit of Fig.2.2, with the appropriate harmonic parameters designation.

The induction motor per-phase harmonic equivalent circuit is shown in Fig.3.3.

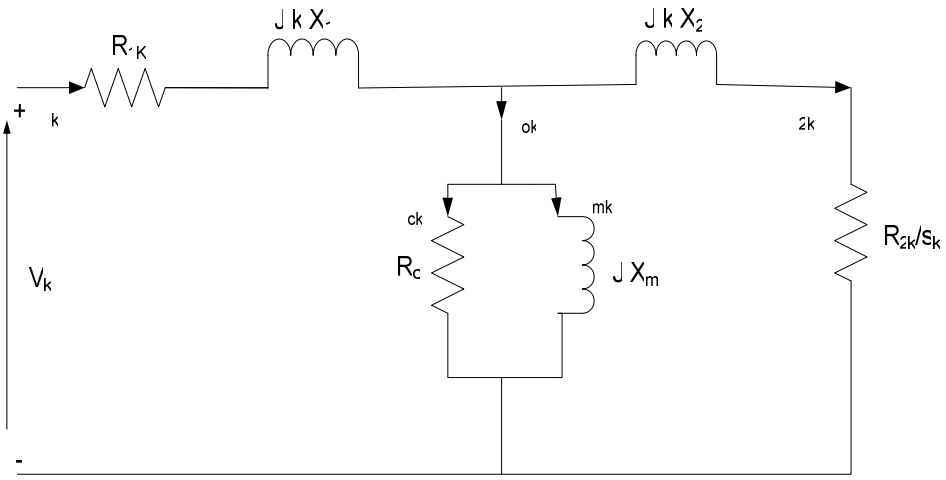

Fig.3.3. Per-phase Induction Motor equivalent circuit for the k^{th} time harmonic.

Where the harmonic slip s_k is substituted for the fundamental slip, s_1, and all inductive reactances are increased by a factor 'k'. The stator and rotor resistances are also larger due to skin effect at the harmonic frequency, which is taken negligible in our study.

3.5.1. Induction Motor Harmonic Currents:

The induction motor currents under non-sinusoidal power supply can be found by using the principle of superposition and calculating each harmonic current component, I_k, (at harmonic k), from the per-phase harmonic equivalent circuit.

Therefore, if V_k denotes the k^{th} harmonic component of the supply voltage, the corresponding stator harmonic current is $I_k = \frac{V_k}{Z_k}$, where Z_k is the k^{th} harmonic input impedance.

When three-phase sinusoidal PWM inverter with frequency ratio $p = \frac{f_c}{f_1} = 21$ and the modulation index $M = \frac{V_1}{V_c} = 0.9$, where f_c and V_c are the carrier signal frequency and amplitude respectively, is used, the dominant harmonics will be those of order $(k = 2p \mp 1)$ and $(k = p \mp 2)$, therefore, the harmonics to be considered are

$k = 19,23,41,and\,43$ [21]. The evaluation of the harmonic currents can be obtained as follows:

$$I_{har} = \sqrt{I_{19}^2 + I_{23}^2 + I_{41}^2 + I_{43}^2} \qquad (3.2).$$

If I_1 is the fundamental r.m.s current, the total r.m.s stator current is:

$$I_{rms} = \sqrt{I_1^2 + I_{har}^2} \qquad (3.3).$$

The same principle is used to calculate the motor rotor current I_{2k} .

3.6. Induction Motor Losses on Non-Sinusoidal Power Supply:

When the induction motor is fed by a non-sinusoidal supply, there is an additional losses that take place, but the use of sine wave PWM inverter reduces these losses significantly bellow the value of that of six-step inverter.

The following induction motor harmonic losses can be calculated:

- ***Harmonic stator copper losses:***

  When skin effect is neglected, the total stator copper losses are:

  $$P_{sc,T} = 3I_{rms}^2 R_1 \qquad (3.4).$$

  Where I_{rms} is total rms stator current, and R_1 is the per-phase stator resistance.

- ***Harmonic rotor copper losses:***

  The total rotor copper losses are:

  $$P_{rc,T} = 3I_{2,rms}^2 R_2 \qquad (3.5).$$

  Where $I_{2,rms}$ is the total rms rotor current, and R_2 is the per-phase rotor resistance.

- ***Harmonic core losses:***

  We consider that the core loss in the induction motor powered by a non-sinusoidal supply is also increased, and is calculated as:

  $$P_{c,T} = 3I_{c,rms}^2 R_c \qquad (3.6).$$

  Where $I_{c,rms}$ is the total rms core loss current, and R_c is the core loss resistance.

3.7. PWM-VSI Losses Calculation:

In the previous sections we have detailed in describing the induction motor power losses when it is fed by sinusoidal and non-sinusoidal power supplies. Since the present study addresses the problem of the whole induction motor drive efficiency optimization, we need to know the effect of converter losses. For that purpose, we first describe the loss model of the used inverter.

3.7.1. PWM-VSI Inverter Loss Model:

We consider the sine wave PWM-VSI given in the previous section. Therefore, the power losses of the inverter consist of conduction losses and switching losses.

3.7.1.1. The Inverter Conduction Losses:

The conduction losses P_{cond} in IGBT or diode can be expressed as [40]:

$$P_{cond,x} = \frac{1}{T}\int_0^T u_{on}(t).i(t)dt \qquad (3.7).$$

Where:

$P_{cond,x}$: is the conduction losses in device x

T : is the fundamental period

$u_{on}(t)$: is the on-state voltage drop

$i(t)$: is the load current.

The on-state voltage drop can be characterized by a dynamical resistance, r_0, and a constant voltage drop, U_0.

Therefore:

$$P_{cond,x} = \frac{1}{T}\int_0^T \left(U_{0,x} + r_{0,x}.i(t)^{B_{cond,x}}\right).i(t).dt \qquad (3.8).$$

Where:

$B_{cond,x}$ is the curve fitted constant for device x.

3.7.1.2. The Inverter Switching Losses:

It is chosen to describe these losses as [40]:

$$E_{sw,x} = A_{sw,x}.i(t)^{B_{sw,x}} \qquad (3.9).$$

Where:

$A_{sw,x}$ and $B_{sw,x}$ are curve fitting constants for device x.

The expression (3.9) can be used for turn -on and turn-off losses of IGBT as well as for the diode. Also, the constants $U_{0,x}$, $r_{0,x}$, $B_{cond,x}$, $A_{sw,x}$, and $B_{sw,x}$ are determined by applying a first order curve fitting of the measured on-state voltage characteristics and the switching energy losses which are dependent on the load current, these are given in appendix B.

3.7.1.3. The Inverter Total Losses:

The total inverter losses are dependent on the conduction ratio of the diode and IGBT.

$$P_{inv} = 6.f_s. \sum_{t=n\phi}^{t=n\phi+\frac{p-2}{2f_c}} \left\{ \begin{array}{l} A_{sw,T}.i(t)^{B_{sw,T}} + A_{sw,D}.i(t)^{B_{sw,D}} \\ + \int_{\alpha n-\frac{\delta n}{2fc}}^{\alpha n+\frac{\delta n}{2fc}} \left(U_{0,T} + r_{0,T} i(t)^{B_{cond,T}}\right) i(t).dt \\ + \int_{\alpha n+\frac{\delta n}{2fc}}^{\alpha n+1-\frac{\delta n+1}{2fc}} \left(U_{0,D} + r_{0,D} i(t)^{B_{cond,D}}\right) i(t).dt \end{array} \right\} \quad (3.10).$$

Where:

f_s is the fundamental frequency,

δ_n is the duty cycle /conduction time at pulse n,

α_n is the center of pulse n,

$n\phi$ is the pulse corresponding to phase angle ϕ

p : is the number of switching in a fundamental period ($\frac{f_c}{f_s}$)

f_c : is the switching frequency.

3.8. Influence of Converter Losses on Induction Motor Efficiency Optimization:

Based on the inverter loss model, presented in the previous section, and the induction motor analysis under non-sinusoidal power supply, we have calculated these losses for the induction motor alone and the inverter alone at the nominal load current. These calculations concern the series of induction motor power ratings given previously, with the corresponding induction motor parameters and inverter curve fitting constants given in appendix B. The results are illustrated in the following table.

IM. Power Rating	**1.5 kW**	**4.0 kW**	**7.5 kW**	**25 kW**	**50 kW**
Rms .Fund. Current (A)	3.26	8.80	16.69	42.89	66.26
Rms. Har. Current (A)	0.23	0.925	1.54	5.39	23.56
IM. fund. Loss (watts)	324.85	548.18	885.93	1570.3	2903.1
IM. Total Loss (watts)	330.18	566.56	908.88	1618.1	3206
IM. Efficiency	0.8195	0.8758	0.8915	0.9390	0.9395
INV. Losses (watts)	15.08	43.682	93.73	223.77	529.95
Drive losses (watts)	345.26	610.24	1002.6	1841.87	3735.95
Drive Efficiency	0.8128	0.8675	0.8818	0.9276	0.9279

Table3.1. Losses of Induction Motor and Inverter at Full Load for Different Power Levels.

The above calculation results show that for induction motor drives with the size of some kilowatts, as 1.5 kW. 4.0 kW, and 7.5 kW, the converter losses constitute only a small fraction of the total drive losses. But, as the drive size increases, the converter losses increase as well. They still, however, small compared to that of the induction motor. This is the case of 25 kW and 50 kW induction motors.

Consequently, we can conclude that, as far as the small and medium size induction motor drives (below 52 kW), the converter losses can be disregarded. This assumption is valid when the induction motor drive energy efficiency optimization is concerned.

3.9. Conclusion:

From this chapter, it is concluded that power converter, as a power supply of induction motor, has offered a great flexibility of motor speed and torque control, but, since the inverter output voltages and currents are of harmonic content, an additional induction motor harmonic losses are, unfortunately, added.

It is shown, however, that these new losses can be minimized to a low level by appropriately choosing the inverter topology and type. In this context, the sine wave PWM-VSI inverter type is chosen to supply the induction motor with balanced non-sinusoidal voltages, and its losses are considered negligible in energy efficiency optimization of small and medium size (below 52 kW) induction motor drive system.

CHAPTER

4

Power Factor Energy Optimal Control of Induction Motor

4.1. Introduction:

The induction motor efficiency maximization problem would have a theoretical mathematical solution if a complete induction motor model could be known. From a practical point of view, this solution implies three problems [14],[41]:

- The complexity of the complete IM model and the necessity of knowing non-standard IM parameters,
- The great computational effort when a real time control is to be implemented using the complete model,
- The parameter variation with temperature, magnetic non-linearities, etc....

However, several possible induction motor models which would account for its electromagnetic losses have been considered.

In this context, the power factor energy optimal control technique is proposed to minimize the total losses in the induction machine when lightly loaded by optimally adjusting the machine air gap flux, and which will be based on the six parameters equivalent circuit model of the squirrel cage induction motor.

4.2. Power Factor Energy Optimal Control Approach:

The power factor energy efficiency optimization method of induction motor drive system relays on the calculation of induction motor displacement power factor, which can be kept constant when the system is operating at its optimal efficiency [42]. The calculation and even the measurement of this parameter at the level of induction motor requires the distinction between the following two cases:

Case 1: when the induction motor driving the HVAC system is connected to a balanced and sinusoidal three phase power supply, where both voltage and current waveforms are sinusoidal.

In this case, if the induction motor is modelled by a per-phase simplified equivalent circuit given in Fig.4.1, with R_{eq} and X_{eq} being, respectively, the equivalent resistance and reactance of the motor exact equivalent circuit. And if the phase stator voltage $v_s(t)$ is sinusoidal and modelled as: $v_s(t) = V_m.\cos(\omega_s.t)$, with V_m and ω_s are, respectively, the voltage amplitude and the motor synchronous angular speed, the corresponding flowing phase stator current is sinusoidal and can be modelled as: $i_s(t) = I_m.\cos(\omega_s.t - \varphi)$.

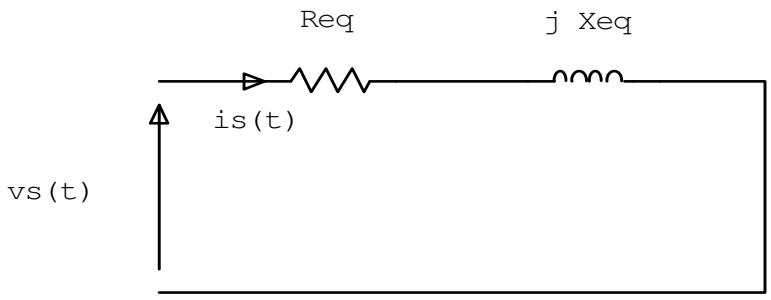

Fig.4.1.Induction Motor Per-Phase simplified Equivalent Circuit with Sinusoidal Power Supply.

Where I_m is the amplitude of stator current and φ is the phase shift angle between the stator voltage and the stator current calculated as;

$$\varphi = \tan^{-1}(\frac{X_{eq}}{R_{eq}}) \tag{4.1}.$$

Therefore, the induction motor has a power factor calculated as:

$$PF = \cos(\varphi) \tag{4.2}.$$

Case 2: when the induction motor driving the HVAC system is powered by a sine wave PWM-VSI power electronic converter described in chapter three. In this case, both stator voltage and stator current waveforms are non-sinusoidal and are harmonic content. If the induction motor is Wye connected, the triplen harmonic components can be eliminated [37]. In this case, the instantaneous induction motor phase voltages are expressed in Fourier series as [37]:

$$V_{an} = \sum_{k=1,5,...}^{\infty} \left(\frac{2.V_1}{k.\pi}\right)\cos\left(\frac{k.\pi}{6}\right).\sin\left(k.\omega.t + \frac{k.\pi}{6}\right) \tag{4.3}.$$

$$V_{bn} = \sum_{k=1,5,...}^{\infty} \left(\frac{2.V_1}{k.\pi}\right)\cos\left(\frac{k.\pi}{6}\right).\sin\left(k.\omega.t + \frac{k.\pi}{2}\right) \tag{4.4}.$$

$$V_{cn} = \sum_{k=1,5,...}^{\infty} \left(\frac{2.V_1}{k.\pi}\right)\cos\left(\frac{k.\pi}{6}\right).\sin\left(k.\omega.t - \frac{7.k.\pi}{6}\right) \tag{4.5}.$$

And the corresponding phase current is given by:

$$I_a = \sum_{k=1,5,...}^{\infty} \left(\frac{2.\mathrm{V}_1}{\mathrm{k}.\pi(\mathrm{R}_{\mathrm{eq}}{}^2 + (k.X_{eq})^2)^{1/2}}.\cos\left(\frac{k\pi}{6}\right).\sin(k\omega.t - \varphi_k)\right) \tag{4.6}.$$

With:

R_{eq} and X_{eq} are the equivalent resistance and reactance of the per-phase equivalent circuit of induction motor and $\varphi_k = \tan^{-1}\left(\frac{k.X_{eq}}{R_{eq}}\right)$ is the phase shift angle between the phase-voltage and the phase-current corresponding to the k^{th} harmonic order.

The power factor energy optimal controller is based on the knowledge of the ***displacement power factor*** of induction motor, which is the cosine of the phase shift angle between the fundamental components of induction motor stator voltage and current.

4.2.1. Induction Motor Displacement Power Factor Calculation:

By referring to the per- phase complete equivalent circuit of induction motor given in Fig.2.2, corresponding to the fundamental component of the inverter voltage output, the following impedance definitions can be given:

$$Z_1 = R_1 + j.X_1 \tag{4.7}$$

$$Z_2 = \frac{R_2}{s} + j.X_2 \tag{4.8}$$

$$Z_m = (R_c \,//\, jX_m) = \frac{j.R_c.X_m}{R_c + j.X_m}$$

$$= R_g + jX_g \tag{4.9}$$

Where:

$$R_g = \frac{R_c.X_m^2}{R_c^2 + X_m^2} \tag{4.9.a}$$

$$X_g = \frac{R_c^2.X_m}{R_c^2 + X_m^2} \tag{4.9.b}$$

And:

$$Z_T = Z_1Z_2 + Z_1Z_m + Z_2Z_m \tag{4.10}$$

The per-phase equivalent input impedance Z_{eq} is:

$$Z_{eq} = \left[(Z_m \,//\, Z_2) + Z_1\right] = \frac{Z_mZ_2}{Z_m + Z_2} + Z_1$$

$$Z_{eq} = R_{eq} + j.X_{eq} \tag{4.11}$$

Where:

$$R_{eq} = \frac{[\,R_2/s.|Z_m|^2 + Rg.(R_2/s)^2 + Rg.X_2^2 + R_1.(Rg + R_2/s)^2 + R_1.(X_g + X_2)^2]}{(Rg + R_2/s)^2 + (Xg + X_2)^2} \quad (4.11.a).$$

$$X_{eq} = \frac{[X_2.|Z_m|^2 + X_g.(R_2/s)^2 + X_g.X_2^2 + X_1.[(R_g + R_2/s)^2 + (X_g + X_2)^2]}{(Rg + R_2/s)^2 + (Xg + X_2)^2} \quad (4.11.b).$$

From the k^{th} harmonic order phase shift angle defined earlier, the displacement power factor angle (φ_1) is expressed as:

$$\varphi_1 = \tan^{-1}\left(\frac{X_{eq}}{R_{eq}}\right) \quad (4.12).$$

And the displacement power factor is:

$$DPF = \cos(\varphi_1) \quad (4.13).$$

It can be noticed that both R_{eq} and X_{eq} are function of supply frequency, therefore, the displacement power factor is also function of supply frequency. Because the induction motor air gap flux and the supply frequency are correlated and are approximately expressed as [43]:

$$\psi_m = \frac{V_1}{\omega_s} \quad (4.14).$$

Where, ψ_m is the air gap flux, V_1 and ω_s are, respectively, the r.m.s value of the fundamental stator voltage and the motor synchronous speed, this means that the induction motor displacement power factor is also function of its air gap flux.

4.2.2. The Simulation Results:

The objective is to see the variation of the motor displacement power factor as a function of induction motor air gap flux.

Simulation results illustrating the variation of induction motor displacement power factor as a function of its air gap flux for all the motors population studied are shown in Fig.4.2, Fig.4.3 and Fig.4.4.

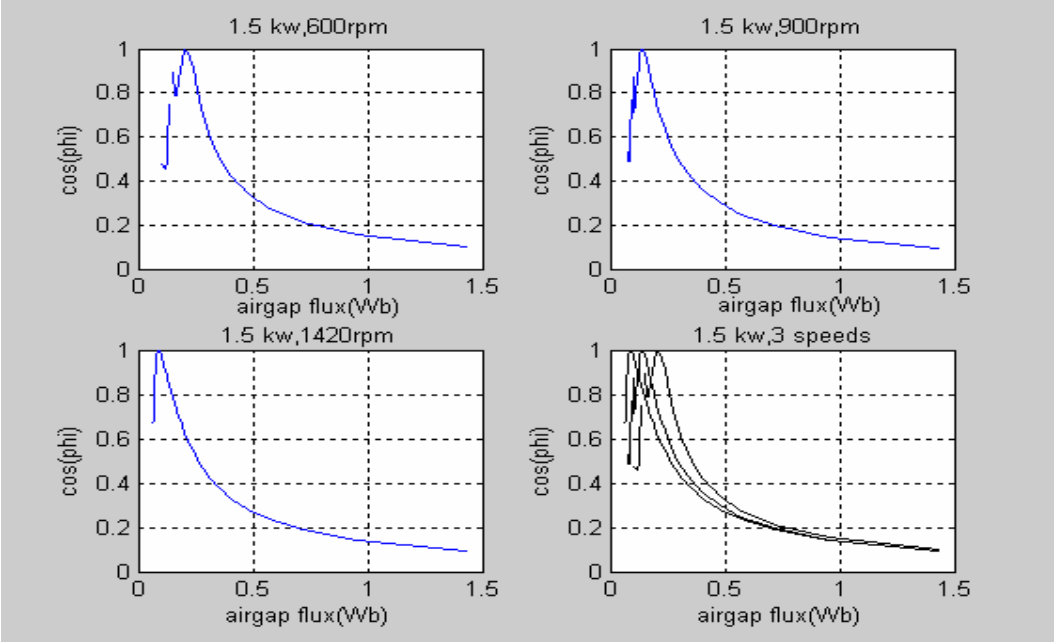

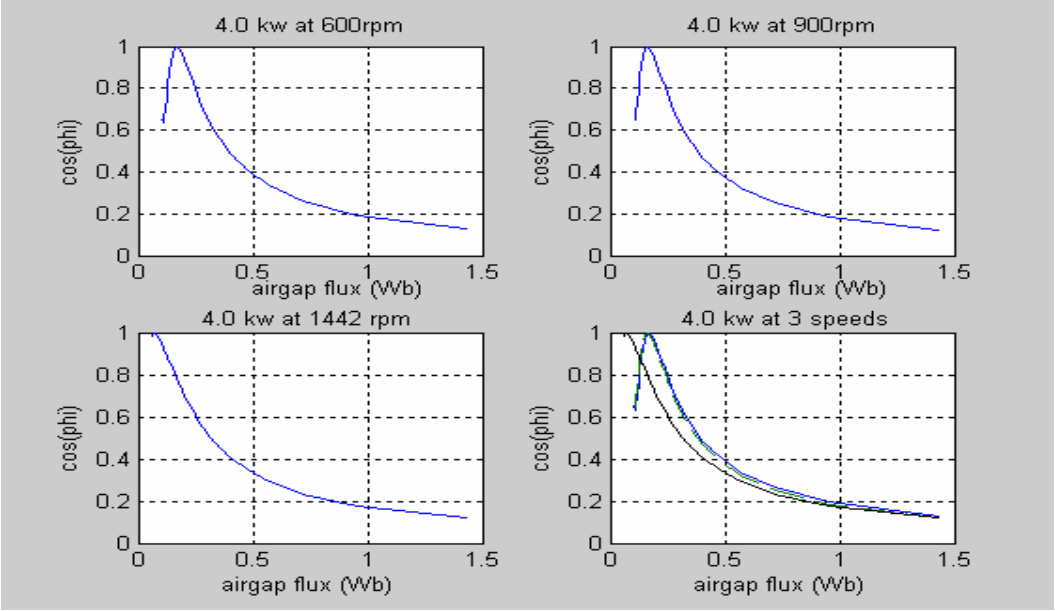

Fig.4.2. Calculated Displacement Power Factor for 1.5 kW, 4.0 kW Induction Motors at three Different Speeds.

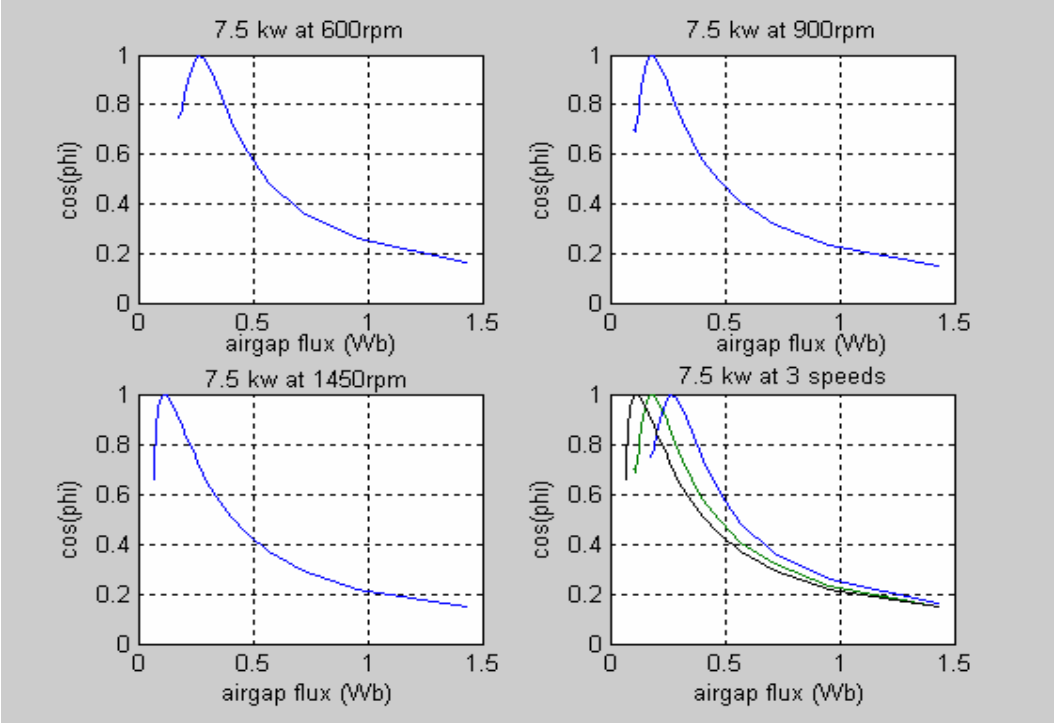

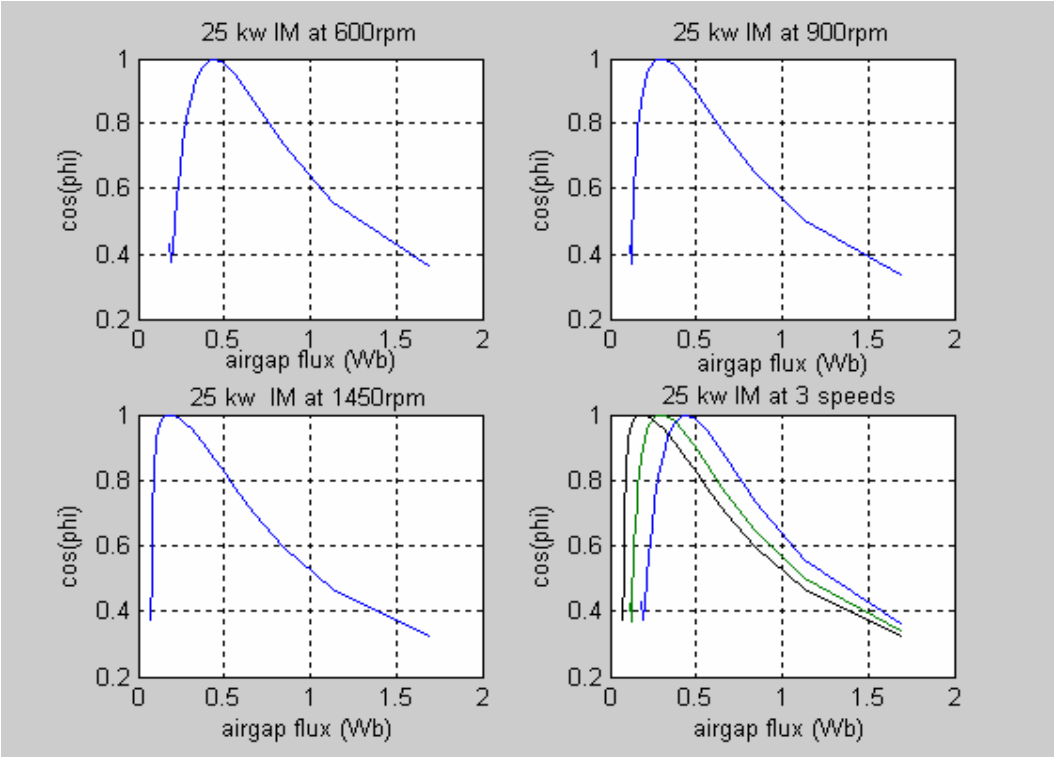

Fig.4.3. Calculated Displacement Power Factor for 7.5 kW, 25 kW Induction Motors at Three Different Speeds.

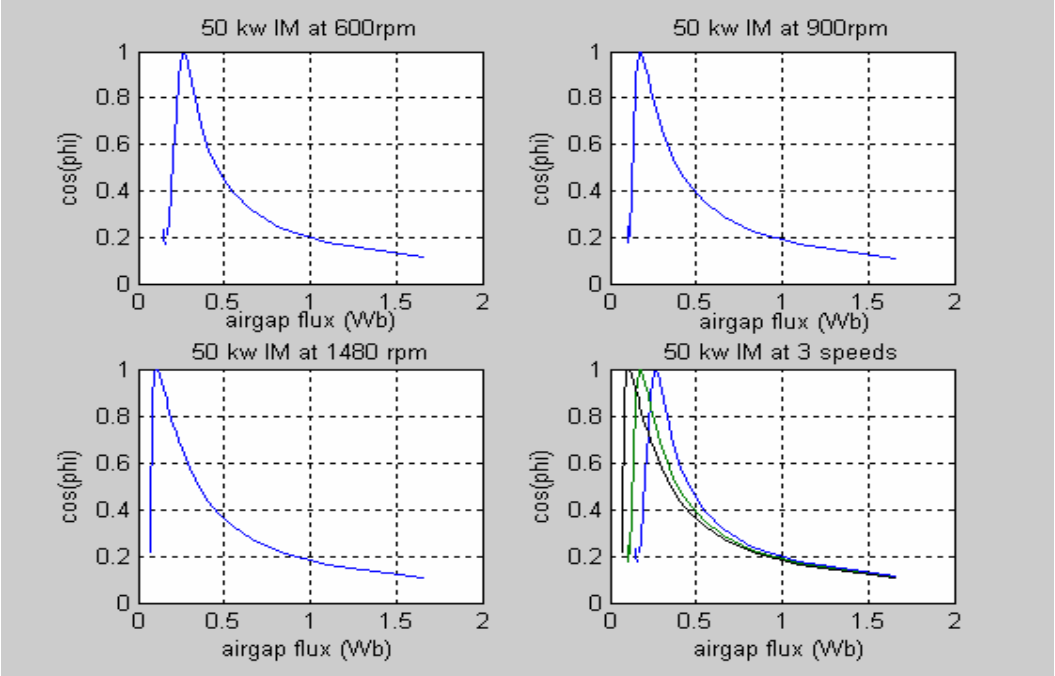

Fig.4.4 Calculated Displacement Power Factor for 50 kW Induction Motor at Three Different Speeds.

4.2.3. Comments and Discussion:

From these simulation results, which show the variation of the induction motor displacement power factor as a function of its magnetization level, we can notice that this power factor has a peak value corresponding to one adjusted value of the air gap flux.

Besides, a very important result can also be deduced; it consists in the similarity of pattern of variation of induction motors displacement power factor as a function of air gap flux at the three different speeds, where, at each speed there is one value of air gap flux level for which the power factor peaks once at a maximum value. At either of the peak value, the power factor abruptly drops.

This result indicates, for this population of induction motors studied, that the displacement power factor can be maintained constant along the speed variation range.

Based on this result, the power factor energy optimal controller is designed. The motor displacement power factor can be kept constant at its (maximum) value with changing load conditions by proper adjustment (tuning) of the flux level.

4.3. Power-Factor Controller Scheme:

The characteristics of the HVAC load allow suitably implementing the power factor energy optimal controller through the use of a simple open-loop scalar control based on the concept of maintaining a constant induction motor air gap flux control. A typical block diagram of this scheme is shown in Fig.4.5.

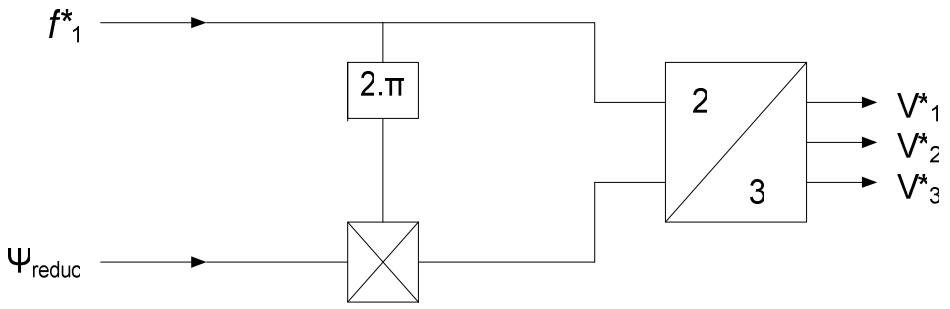

Fig.4.5 . Control Scheme for a Scalar Drive.

With:

f_1^* : being the reference value of the supply frequency,

ψ_{reduc} : the motor air gap flux reduction corresponding to new operating speed.

V_1^* , V_2^* and V_3^* : are the generated reference operating stator voltages corresponding to the new operating point.

With the scalar control scheme, the induction motor efficiency improvement system incorporating the Power Factor controller is shown in Fig.4.6.

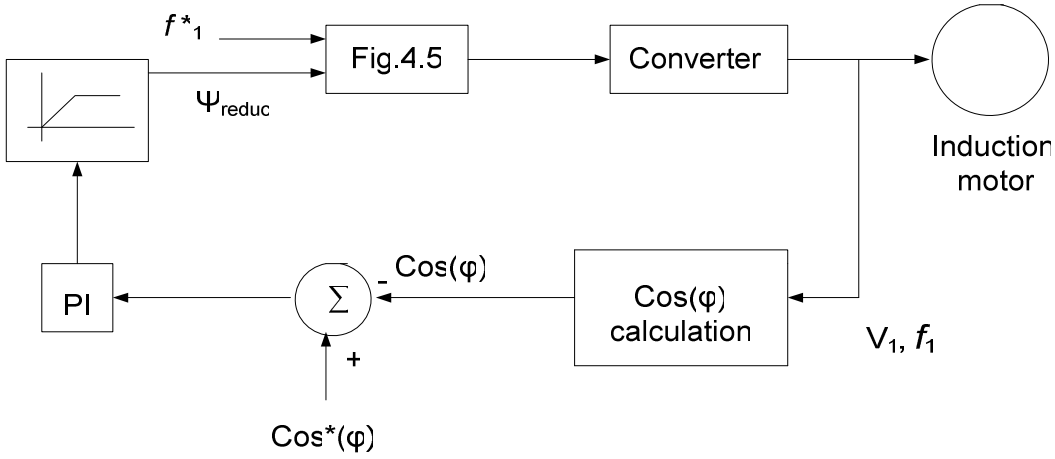

Fig.4.6 Block Diagram of $Cos(\varphi)$ Energy Optimal Controller.

Where:

V_1 and f_1 are, respectively, the voltage r.m.s value and frequency of the fundamental supply voltage of induction motor (IM).

$Cos(\varphi_1)^*$ and $Cos\varphi_1$ are, respectively, the nominal value and the calculated value of induction motor displacement power factor.

The power factor controller is operated in a feed-back control loop configuration, which will drive the induction motor drive system at constant (maximum) power factor when its operating speed is decreased below the rated value. The power factor reference value $Cos(\varphi_1)^*$ is compared to the calculated (or measured) value; the resultant error signal is processed by a proportional plus integral (PI) controller. The output of the controller is the air gap flux reduction signal (ψ_{reduc}) which controls the operation of the PWM-voltage source inverter (VSI), after it passes through the control loop of the scalar drive scheme shown in Fig.4.5.

The proportional-integral (PI) controller is used because of its easy tuning and zero-steady state error. The ψ_{reduc} signal is deduced from the $(\psi, \cos(\varphi_1))$ plane for every induction motor operating speed below the rated value. After that, the controller output is amplitude limited (a ramping circuit can be used) to limit the exceed variation of the control variable.

4.4. Expressing Induction Motor Total Loss:

The behaviour of the a.c induction motor drive is governed by the three independent variables- the motor speed ω_m, the terminal voltage V_1, the terminal frequency f_1 -, the parameters of the motor and its power supply. At any operating point characterized by the speed ω_m and the torque T_e , a combination of the terminal voltage and frequency can be obtained that meets the requirements of the operating point and minimizes the overall losses of the drive, this can be realized by the desired constant power factor energy optimal controller.

The five induction motor power loss components are briefly stated:

1) Stator copper losses, P_{cs} , and Rotor copper losses, P_{cr}, are function primarily of torque,
2) Stator iron loss P_c , a function of stator voltage and frequency;

3) Rotor copper loss P_{cr} , a function primarily of torque and secondarily of slip and temperature;
4) Friction and windage loss P_{fw} , a function of speed;
5) Stray load loss P_s , consisting of additional iron and copper losses due to the quasi-sinusoidal field distribution in the air gap, and additional losses caused by the stator slot effects and skin effect in the conductors. P_s is a function primarily of torque and secondarily of stator voltage, frequency and temperature.

At reduced speed, the losses due to friction and windage with the stray load losses are low. The stator and rotor copper losses and the core losses, which are, hence, dominant losses depend on the stator voltage and frequency can be minimized; thus, overall induction motor losses can be effectively minimized. These controllable losses are expressed as:

$$P_t = I_s^2.R_1 + I_r^2.R_2 + \frac{V_m^2}{R_c} \qquad (4.15).$$

Where I_s and I_r are total r.m.s values of the stator current and the rotor current respectively, and V_m is the voltage drop across the magnetizing branch.

From the previous definitions of the impedances, the fundamental values are calculated as follows:

$$V_m = \frac{V_1.|Z_x|}{|Z_x + Z_1|} \qquad (4.16).$$

Where

$$Z_x = (Z_m // Z_2) = \frac{Z_m Z_2}{Z_m + Z_2} \qquad (4.17).$$

Substituting equation (4.17) into (4.16) yields:

$$V_m = \frac{V_1.|Z_m.Z_2|}{|Z_T|} \qquad (4.18).$$

The magnetizing current can be expressed by:

$$I_m = \frac{V_m}{|Z_m|} \tag{4.19}$$

Using the V_m expression in equation (4.18) leads to:

$$I_m = \frac{V_1 . |Z_2|}{|Z_T|} \tag{4.20}$$

We have also:

$$I_1 = \frac{V_1}{|Z_{eq}|} \tag{4.21}$$

From the equations (4.20) and (4.21) :

$$I_2 = I_1 - I_m = \frac{V_1 . |Z_m|}{|Z_T|} \tag{4.22}$$

By substituting equations (4.18), (4.21) and (4.22) in equation (4.15) we obtain an expression for the total induction motor losses P_t:

$$P_t = V_1 \left\{ R_1 . \left(\frac{|Z_m + Z_2|}{|Z_T|} \right)^2 + R_2 . \left(\frac{|Z_m|}{|Z_T|} \right)^2 + \left(\frac{|Z_m Z_2|}{|Z_T|} \right)^2 . \frac{1}{R_c} \right\} + P_{T.har} \tag{4.23}$$

Where $P_{T.har}$ are the total harmonic power losses.

The impedances Z_m, Z_2 , and Z_T are functions of frequency and slip, by expressing the slip in terms of frequency and the motor speed ω_m, the total power loss expression (4.23) is therefore, a function of induction motor voltage amplitude, frequency and shaft speed.

As a result, with the variation of motor operating speed, the losses can be controlled by adjusting the fundamental terminal voltage V_1 hence by adjusting the air gap flux ψ_m.

4.5. Induction Motor Efficiency Calculation:

The induction motor efficiency will be evaluated without and with the power factor optimizer according to the following efficiency definition:

$$\eta = \frac{P_o}{P_o + P_t} \tag{4.24}$$

Where P_t is the total power loss of the induction motor when fed from a sine wave PWM-VSI inverter, and P_o represents the output mechanical power calculated for the case of 'Fan' type load, where the load torque is proportional to motor speed squared.

4.6. The Simulation Results:

for a variation of induction motor speed and / or torque, from rated values down to zero speed, the variation of its total losses with the corresponding variation of the operating efficiency with and without the use power factor energy efficiency optimization controller are simulated in the following plots for the 1.5 kW, 4.0 kW, 7.5 kW, 25 kW and 50 kW design B, standard squirrel cage induction motors.

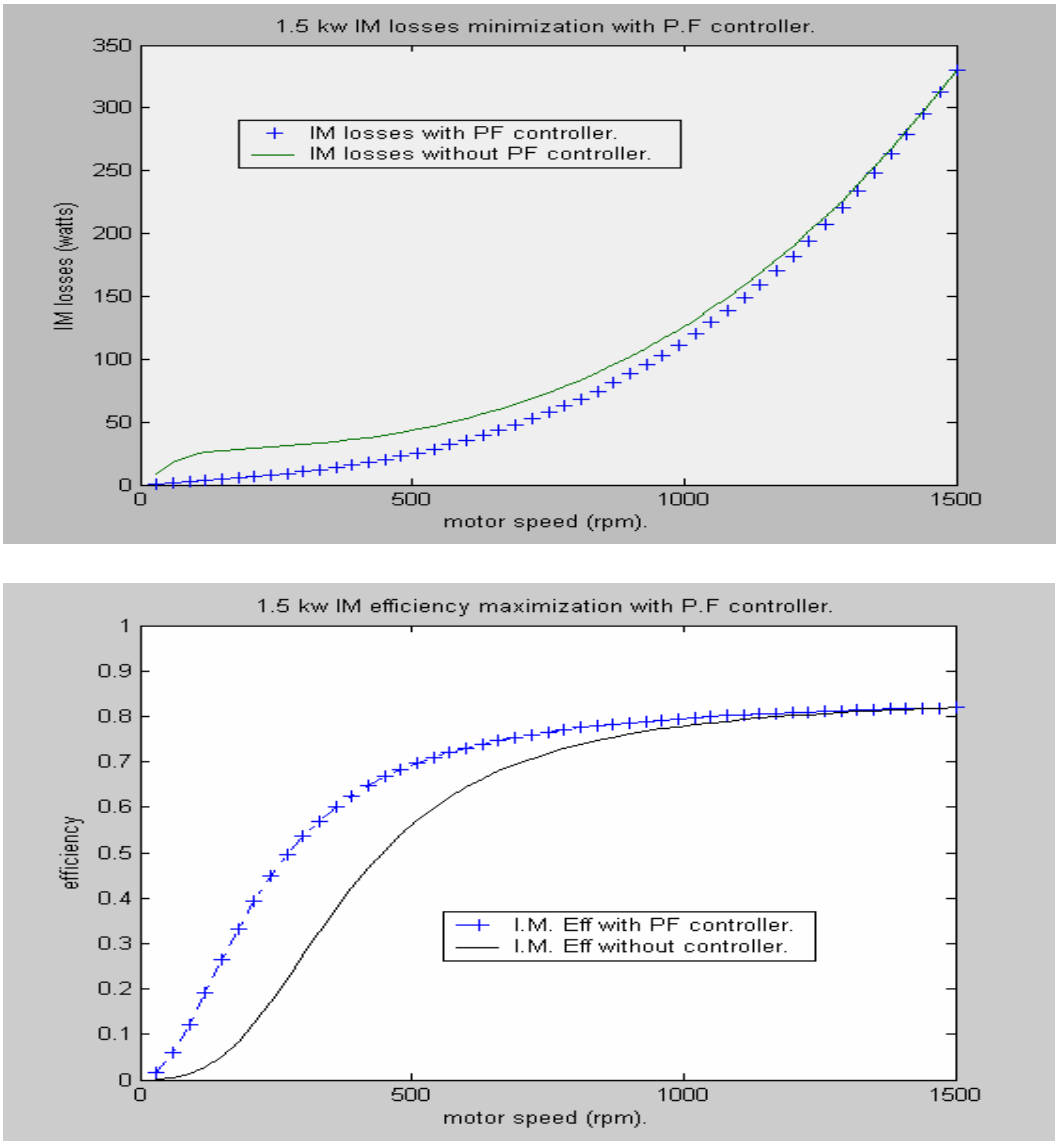

Fig.4.7. 1.5 kW Induction Motor Loss Minimization and Efficiency Improvement with PF Controller.

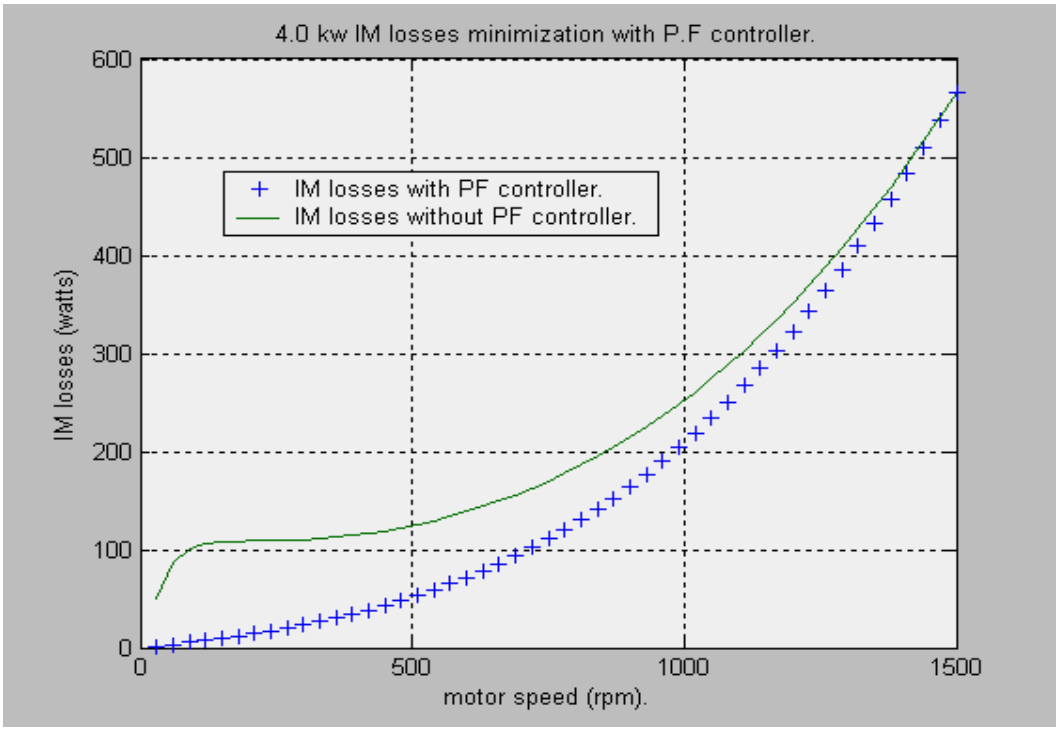

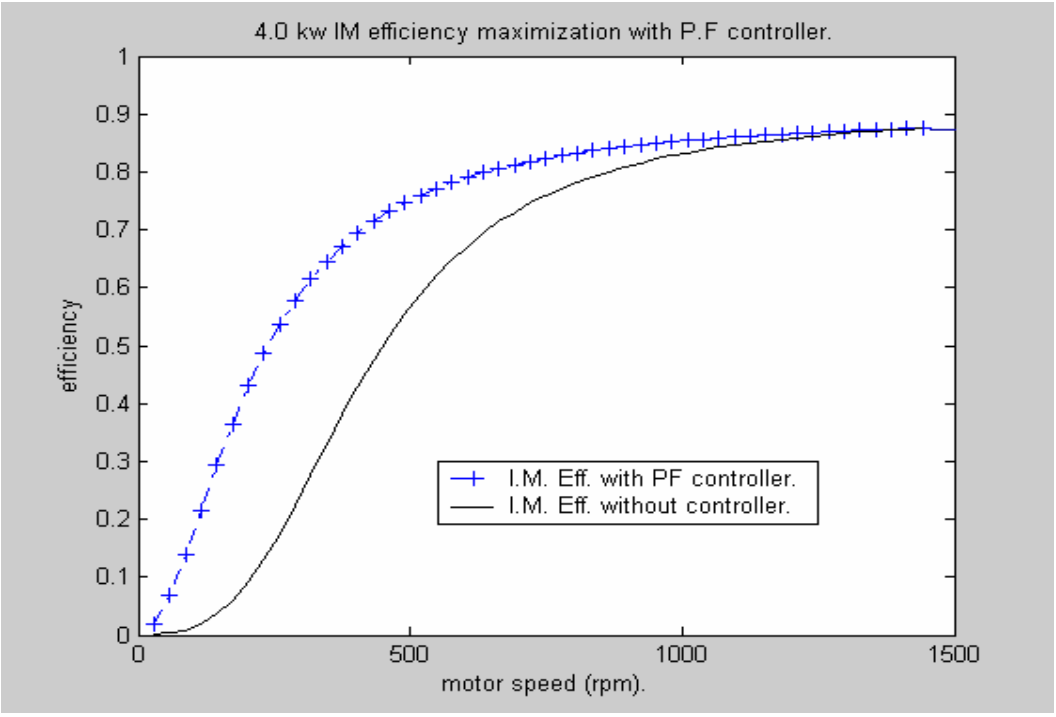

Fig.4.8. 4.0 kW Induction Motor Loss Minimization and Efficiency Improvement with PF Controller.

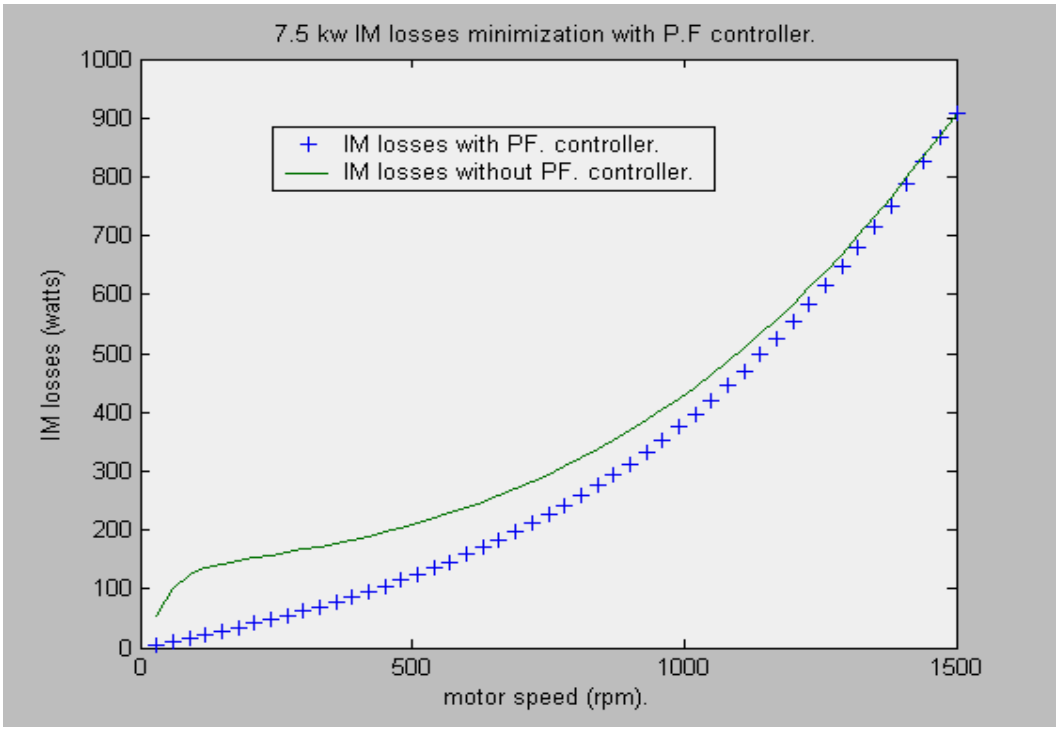

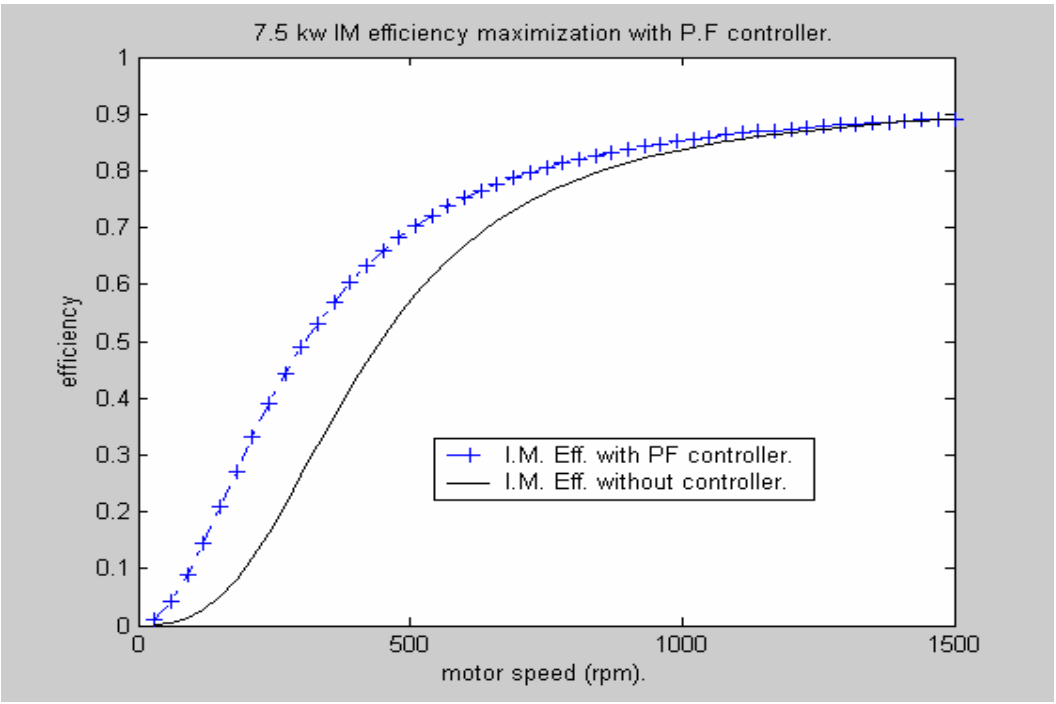

Fig.4.9. 7.5 kW Induction Motor Loss Minimization and Efficiency Improvement with P.F Controller.

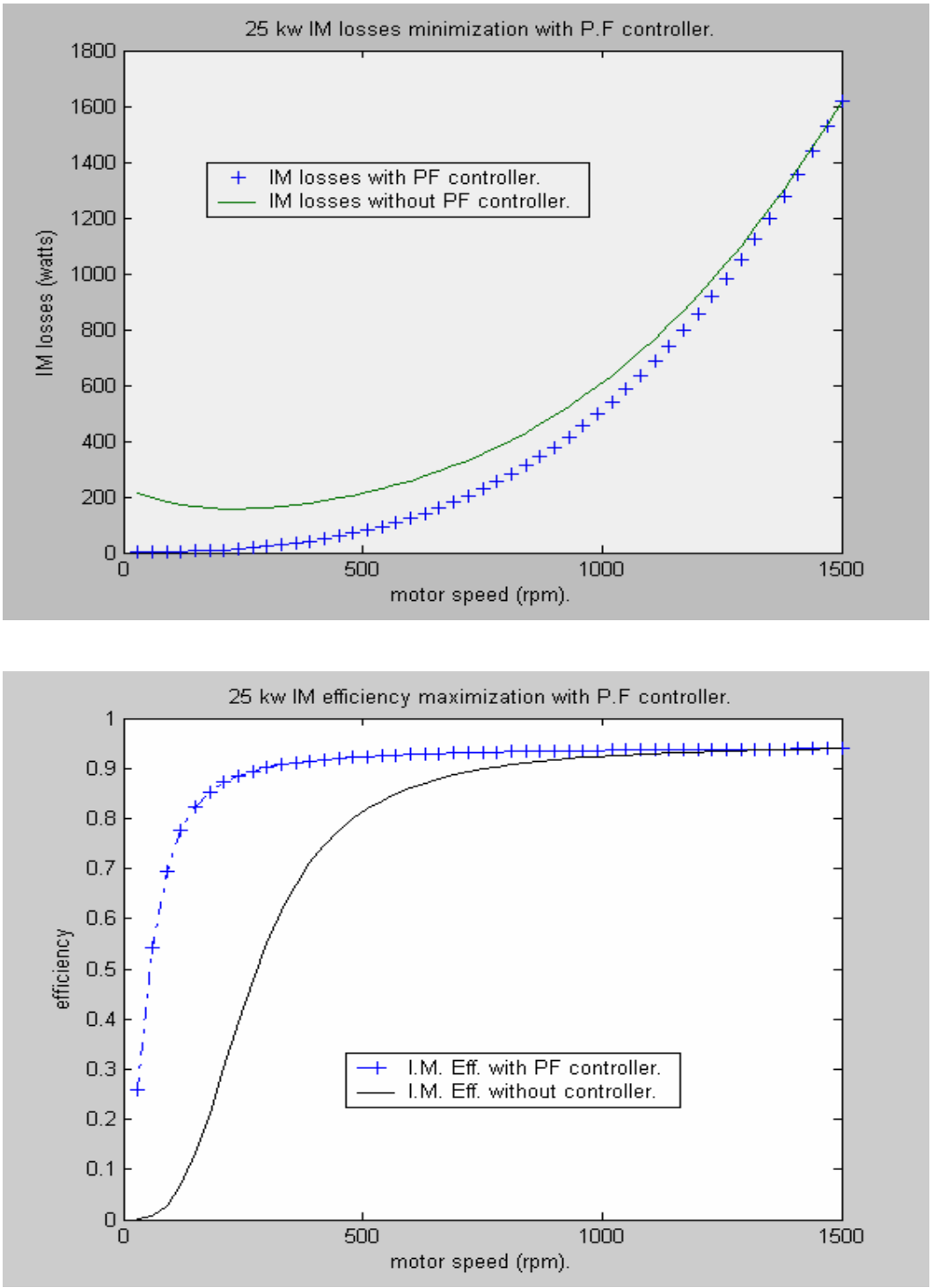

Fig.4.10. 25 kW Induction Motor Loss Minimization and Efficiency Improvement with PF Controller.

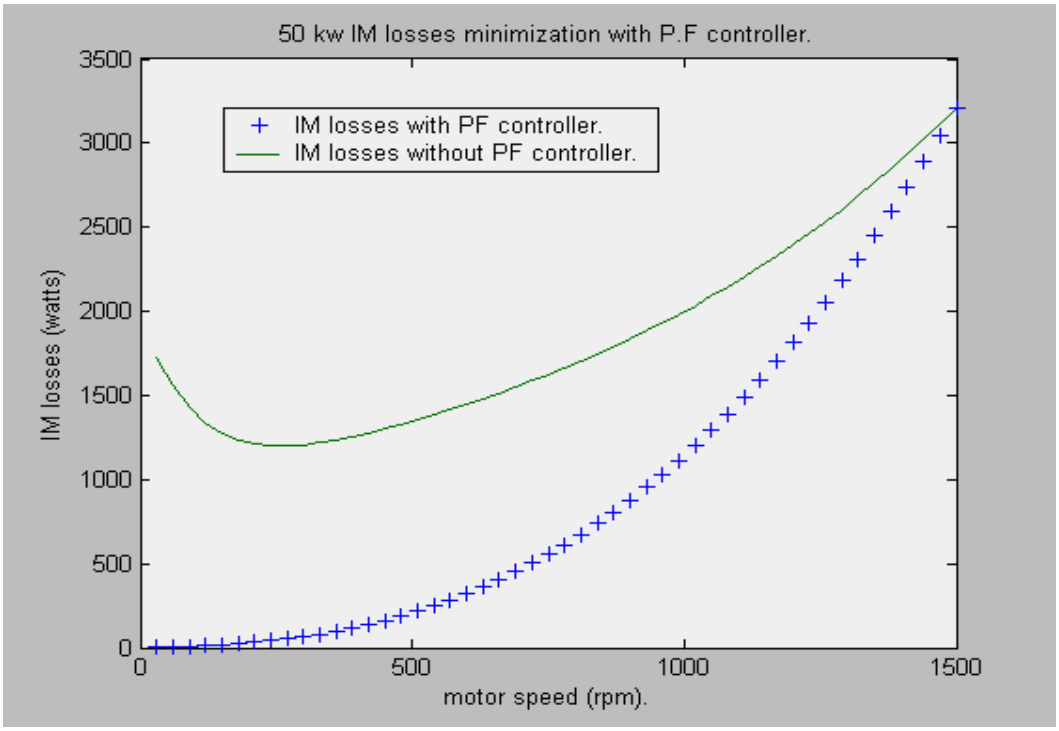

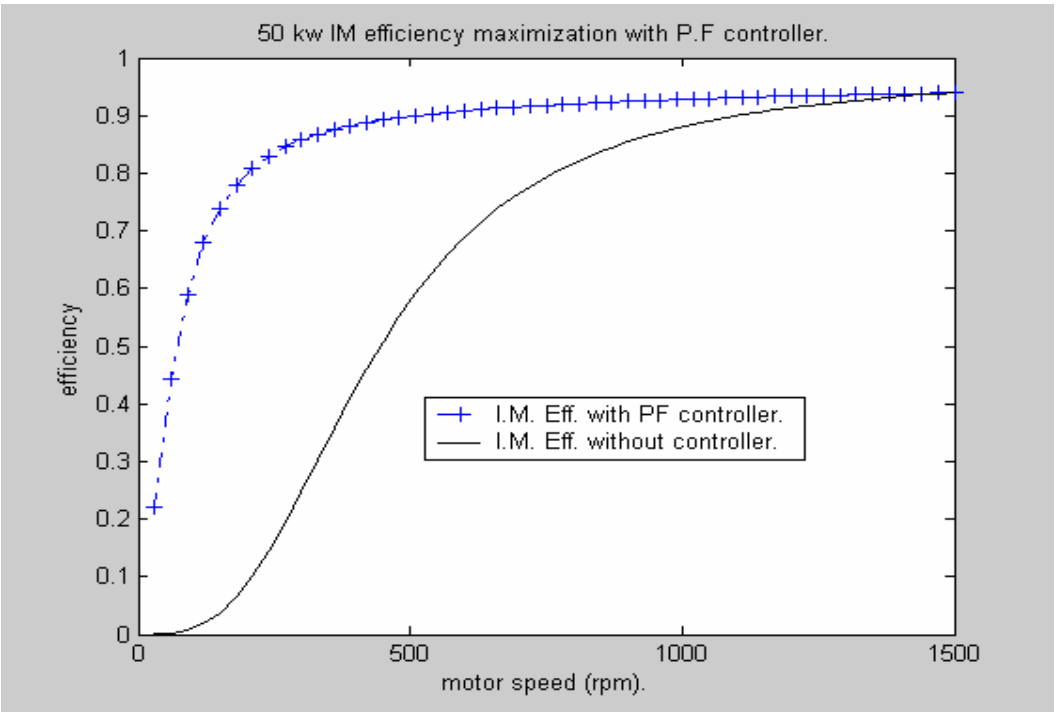

Fig.4.11. 50 kW Induction Motor Loss Minimization and Efficiency Improvement with PF Controller.

4.6.1. Comments and Discussion:

These plots illustrate induction motor controllable loss minimization and its corresponding efficiency improvement that can be achieved by applying the power factor energy optimal controller. The variation of the motor losses and its efficiency as a function of load operating conditions are shown in both cases:

1- When the induction motor drive system is operated with power factor controller, and
2- When the power factor controller action is taken off.

Total losses and motor efficiency throughout the range of speed variation are calculated, and the tables below show efficiency improvements of the population of induction motors studied.

1.5 kW three-phase, 50Hz – 4 poles squirrel cage induction motor Under power factor energy optimal controller.						
Induction motors operating speeds (rpm).	***Induction motor without P.F controller.***		***Induction motor with P.F controller.***		***Achieved Total Losses reduction (w).***	***Achieved Efficiency Improvement***
	Total Losses (w).	***Efficiency***	***Total Losses (w).***	***Efficiency***		
Rated speed.	330.18	0.8195	330.18	0.8195	0.00	0.00
1200	190.16	0.8014	182.01	0.8083	8.15	0.0069
900	101.94	0.7606	88.109	0.7861	13.831	0.0255
600	53.05	0.6439	35.34	0.7308	17.71	0.087
400	39.70	0.5048	20.24	0.6666	19.49	0.1618

Table 4.1. Loss Minimization and Efficiency Improvement of 1.5 kW Induction Motor with Power Factor Controller.

4.0 kW three-phase, 50Hz – 4 poles squirrel cage induction motor Under power factor energy optimal controller.						
Induction motors operating speeds (rpm).	***Induction motor without P.F controller.***		***Induction motor with P.F controller.***		***Achieved Total losses reduction (w).***	***Achieved Efficiency Improvement***
	Total Losses (w).	***Efficiency.***	***Total Losses (w).***	***Efficiency***		
Rated speed.	566.56	0.8757	566.56	0.8756	0.00	0.00
1200	351.66	0.8532	322.66	0.8630	29	0.0098
900	214.75	0.8007	164.37	0.8386	50.38	0.0379
600	138.84	0.6480	71.47	0.7775	67.37	0.1295
400	119.28	0.4748	43.10	0.7060	76.18	0.2312

7.5 kW three-phase, 50Hz – 4 poles Squirrel Cage Induction Motor Under Power Factor Energy Optimal Controller.						
Induction motors operating speeds (rpm).	***Induction motor without P.F controller.***		***Induction motor with P.F controller.***		***Achieved Total losses reduction (w).***	***Achieved Efficiency Improvement***
	Total Losses (w).	***Efficiency***	***Total Losses (w).***	***Efficiency***		
Rated speed.	908.88	0.8915	908.88	0.8915	0.00	0.00
1200	584.48	0.8673	553.6	0.8734	30.88	0.0061
900	368.95	0.8133	312.51	0.8372	56.44	0.0239
600	237.65	0.6656	157.95	0.7497	79.7	0.0841
400	196.28	0.5018	104.49	0.6542	91.79	0.1524

Table 4.2. Loss Minimization and Efficiency Improvement of 4.0 kW and 7.5 kW Induction Motor with Power Factor Controller.

25 kW three-phase, 50Hz – 4 poles squirrel cage induction motor Under Power Factor Energy Optimal Controller.						
Induction motors operating speeds (rpm).	***Induction motor without P.F controller.***		***Induction motor with P.F controller.***		***Achieved Total losses reduction (w).***	***Achieved Efficiency Improvement***
	Total Losses (w).	***Efficiency***	***Total Losses (w).***	***Efficiency***		
Rated speed.	1618.1	0.9390	1618.1	0.9390	0.00	0.00
1200	922.09	0.9326	854.45	0.9372	67.64	0.0049
900	490.93	0.9163	378.94	0.9341	111.99	0.0178
600	257.39	0.8607	124.23	0.9275	133.16	0.0668
400	195.05	0.7743	48.95	0.9198	146.1	0.1446

50 kW three-phase, 50Hz – 4 poles squirrel cage induction motor Under Power Factor Energy Optimal Controller.						
Induction motors operating speeds (rpm).	***Induction motor without P.F controller.***		***Induction motor with P.F controller.***		***Achieved Total losses reduction (w).***	***Achieved Efficiency Improvement***
	Total Losses (w).	***Efficiency***	***Total Losses (w).***	***Efficiency***		
Rated speed.	3206	0.9395	3206	0.9395	0.00	0.00
1200	2396.4	0.9141	1813.3	0.9336	583.1	0.0195
900	1835.9	0.8541	876.58	0.9246	959.32	0.0705
600	1446.9	0.7368	321.93	0.9181	1124.97	0.1813
400	1301.6	0.6903	162.66	0.8870	1138.94	0.1967

Table 4.3. Loss Minimization and Efficiency Improvement of 25 kW and 50 kW Induction Motor with Power Factor Controller.

The obtained results show clearly that when the induction motor drive is energy controlled with the power factor controller, an achievement of motor total loss minimization is possible at every operating point from rated operating point and below; it is zero or negligible at or near rated speed, but gets increasingly more important at lower operating speeds.

The efficiency, on the other hand, shows a remarkable improvement by several percent when the drive is lightly loaded.

It can be also deduced from the results that the pattern of efficiency improvement and its relative magnitude are basically similar for all induction motors studied.

4.7. Conclusion:

In this chapter, the power factor approach for induction motor energy efficiency optimization control is studied. The method is based on the calculation of the induction motor displacement power factor by referring to the motor per-phase complete equivalent circuit including the core loss parameter.

The principle of operation of the controller is based on the fact that optimal efficiency operation is correlated with the induction motor displacement power factor being constant at its nominal value. Keeping the power factor constant allows us to readily adjust the amount of increase or decrease of the needed magnetization level depending on whether the motor loading is decreased or increased.

The simulation results obtained when the controller is used with the induction motor driving a fan type load have shown a very appreciable efficiency improvement below rated speed.

This efficiency improvement goes on getting, as expected, more important as speed is decreased (light loading).

CHAPTER

5

Model-Based Energy Optimal Control of Induction Motor

5.1. Introduction:

In the preceding chapter, we have described the power factor energy efficiency optimization controller, which is based on the steady-state equivalent circuit model of the induction motor. In this chapter an other approach known as: loss-model based method is studied and simulated.

5.2. Loss-Model-Based Energy Optimal Controller:

The model-based energy optimal control approach is a method for minimizing the total copper and iron losses in a variable speed and /or torque induction motor drive system. The method is based on a simple induction motor loss model that includes the iron losses, and which only requires the knowledge of conventional induction motor parameters.

When the model is built, the equations required to quantify the induction motor total losses are deduced, and based on these equations, an algorithm based on the field-oriented scheme is proposed. This algorithm allows the electromagnetic losses in a variable speed and torque induction motor drive system to be minimized and its efficiency to be improved at operating conditions below the rated values.

5.2.1. Induction Motor Loss Model In d-q Reference Frame:

Fig.5.1 shows the steady-state equivalent circuit of a given induction motor in the d-q coordinates which rotate synchronously with an electrical angular velocity ω_s .

The equivalent circuits include the effects of the copper and iron losses. The copper losses are represented by the stator and rotor resistances R_1 and R_2, whereas the iron losses are represented by the resistance R_c.

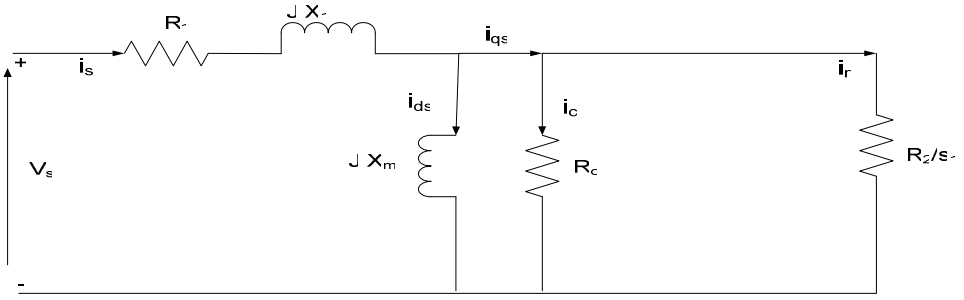

Fig.5.1 Steady State Rotor-Flux Oriented Model of Induction Motor Including core Losses [7].

This model adopted for the induction motor is obtained by defining the d-axis of the coordinate in the direction of the rotor magnetic flux (field oriented frame); therefore, the magnetic flux in the q-axis direction is zero [13],[44].

For simplification, it is assumed that all motor parameter are constant; magnetic saturation and temperature effects are ignored.

5.2.2. Model-Based Loss Minimization Algorithm (LMA):

When the steady-state operation is considered, the induction motor losses consist of copper and iron losses. With the aid of the d-q model of induction motor, these loss components can be computed as well as the torque and efficiency as a function of i_{qs} and i_{ds}, as follows:

- ***Stator copper losses:***

$$P_{cus} = R_1(i_{qs}^2 + i_{ds}^2) \tag{5.1}$$

- ***Rotor copper losses:***

$$P_{cur} = R_2\left(i_{qs} - i_c\right)^2 = R_2\left(i_{qs} - \frac{\omega_s.L_m}{R_c}.i_{ds}\right)^2$$

$$P_{cur} = R_2\left(i_{qs}^2 + (\omega_s.L_m)^2.\frac{1}{R_c^{\,2}}i_{ds}^2 - 2.L_m\omega_s.i_{qs}.i_{ds}\right). \tag{5.2}$$

- ***Iron losses:***

$$P_c = (\omega_s.L_m)^2.\frac{1}{R_c}.i_{ds}^{\,2} \tag{5.3}$$

- ***Total losses:***

$$P_t = P_{cus} + P_{cur} + P_c$$

$$P_t = (R_1 + R_2).i_{qs}^2 + \left((\omega_s.L_m)^2.\frac{1}{R_c} + R_1 + (\omega_s.L_m)^2.\frac{R_2}{R_c^2}\right).i_{ds}^2 - 2.\omega_s.L_m.\frac{R_2}{R_c}.i_{ds}.i_{qs} \tag{5.4}$$

From this expression, the induction motor total losses are a function of i_{qs} and i_{ds}, which can be rearranged in the following loss components:

$$P_{loss,d} = \left((\omega_s.L_m)^2.\frac{1}{R_c} + R_1 + (\omega_s.L_m)^2.\frac{R_2}{R_c^2}\right).i_{ds}^2 \tag{5.4.a}$$

$$P_{loss,q} = (R_1 + R_2).i_{qs}^2 \tag{5.4.b}$$

$$P_{loss,dq} = -2.\omega_s.L_m.\frac{R_2}{R_c}.i_{ds}.i_{qs} \qquad (5.4.c).$$

- Induction motor developed torque:

$$T_d = p\left(\frac{L_m.i_{ds}}{(R_c + R_2)}\left(R_c.i_{qs} - L_m.\omega_s.i_{ds}\right)\right) \qquad (5.5).$$

Where p is the number of pole pairs.

In the standard efficiency induction motor, we can assume that the core loss component is much higher than the rotor cupper loss component:

$$R_c >> R_2,$$

and:

$$R_c >> L_m{}^2.\omega_s.i_{ds}^2$$

Then:

$$T_d \cong pL_m.i_{qs}.i_{ds} \qquad (5.6).$$

The equation (5.6) of the developed torque is usually accepted as a good approximation [7], [13], [14].

If we substitute the equation (5.6) into (5.4), we can express the total power losses of the induction motor as a function of i_{ds}, T_d and ω_s as:

$$P_t = \left\{\left[(\omega_s.L_m)^2.\frac{1}{R_c} + R_1 + (\omega_s.L_m)^2.\frac{R_2}{R_c^2}\right].i_{ds}^2 + \left(\frac{T_d}{p.M_d}\right)^2.(R_1 + R_2).\frac{1}{i^2{}_{ds}} - 2.\omega_s.L_m.\frac{R_2}{R_c}(\frac{T_d}{p.M_d})\right\} \qquad (5.7).$$

In steady-state operation, and at a given torque and speed, the total losses is a function only of current flux component, i_{ds}.

At rated operating speed, we depict in Fig.5.2 the simulation results of the induction motor total losses as a function of i_{ds} for, as an example, the 7.5 kW and 50 kW induction motors.

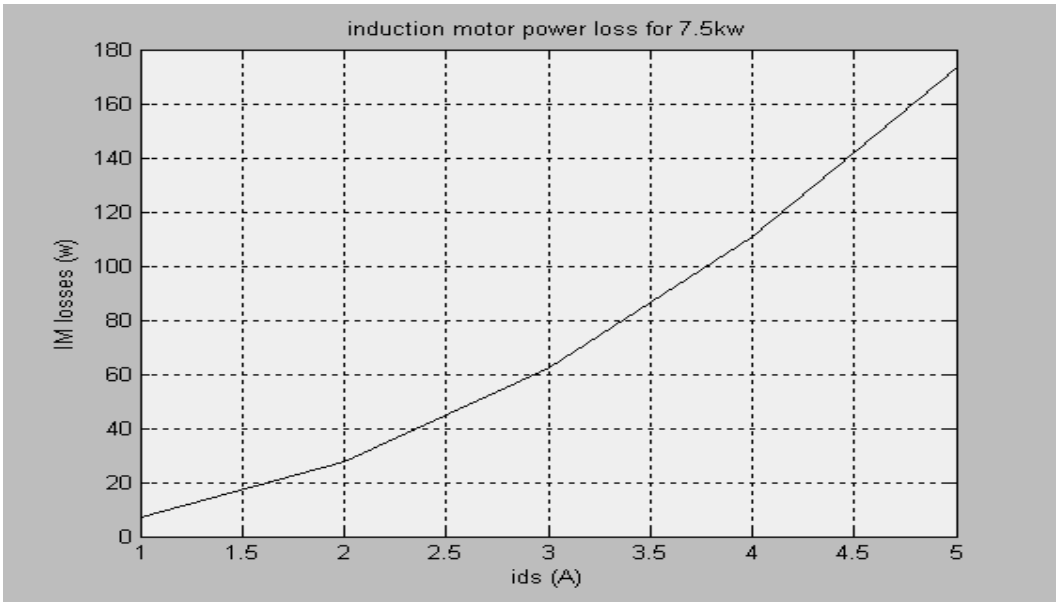

Fig.5.2. Variation of Total Losses with Current-Flux Component for 7.5 kW and 50 kW Induction Motor.

It can be seen from these plots that the optimal value of the current flux component i_{ds} exists for minimizing the electromagnetic power losses of the induction motor.

5.2.3. Condition for minimizing Induction Motor Total Losses:

The condition of minimizing the induction motor total losses is derived as follows:

By defining the current ratio $K_{\min}$ as:

$$i_{qs} = K_{\min}.i_{ds} \tag{5.8}$$

Using the torque expression and the definition of $K_{\min}$, the induction motor total losses becomes:

$$P_t = \frac{T_d}{p.M_d}\left[\left((\omega_s.L_m)^2.\frac{1}{R_c} + R_1 + (\omega_s.L_m)^2.\frac{R_2}{R_c^2}\right).\frac{1}{(K_{\min})} + (R_1 + R_2).K_{\min} - 2.\omega_s.L_m.\frac{R_2}{R_c}\right] \tag{5.9}$$

By differentiating P_t with respect to $K_{\min}$, we obtain:

$$\frac{dP_t}{dK_{\min}} = \frac{T_d}{pL_m}\left(-\left((\omega_s.L_m)^2.\frac{1}{R_c} + R_1 + (\omega_s.L_m)^2.\frac{R_2}{R_c^2}\right).\frac{1}{(K_{\min})^2} + (R_1 + R_2)\right) \tag{5.10}$$

The optimal candidate of P_t requires:

$$\frac{dP_t}{dK_{\min}} = 0 \tag{5.11}$$

This gives:

$$(R_1 + R_2).K^2{}_{\min} = (\omega_s.L_m)^2.\frac{1}{R_c} + R_1 + (\omega_s.L_m)^2.\frac{R_2}{R_c^2} \Rightarrow P_{loss,q} = P_{loss,d} \tag{5.12}$$

The equation (5.12) gives the condition for optimal induction motor total losses, from which we can have:

$$K_{\min} = \sqrt{\frac{(\omega_s.L_m)^2.\frac{1}{R_c} + R_1 + (\omega_s.L_m)^2.\frac{R_2}{R_c^2}}{(R_1 + R_2)}} \tag{5.13}$$

This is called the Loss Minimization Factor (LMF).

The induction motor total losses are, thus, minimal when the motor loss depending on the current direct with the rotor flux i_{ds}, $P_{loss,d}$, is equal to the loss depending on the current in quadrature to the rotor flux i_{qs}, $P_{loss,q}$.

5.2.4. Model-Based Control Scheme:

The optimization equation (5.9) can be practically solved by implementing the system configuration shown in Fig.5.3 [13].

This is known as the loss-model-based energy optimal controller of the induction motor drive system.

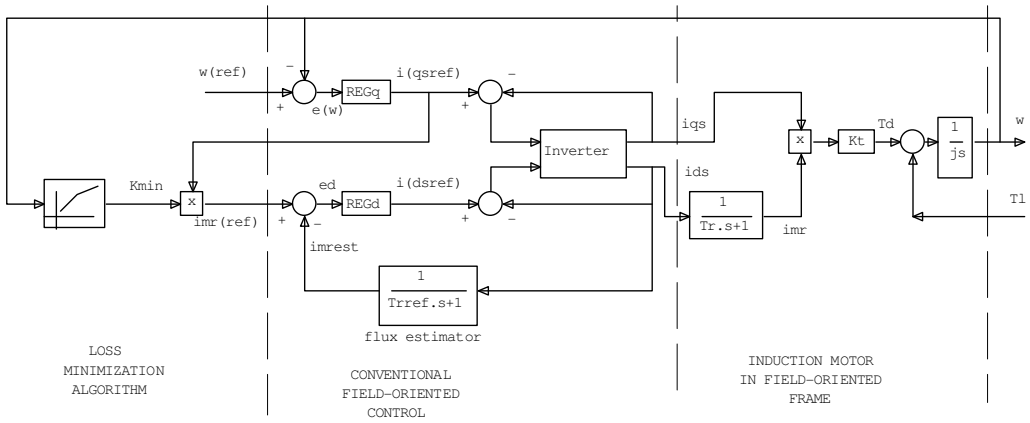

Fig.5.3. Block Diagram of Field Oriented Controller and induction motor in Field-Oriented Frame.

Where:

ω, T_1 : are the operating speed and torque of induction motor.

T_d , ω_{ref} : are, respectively the motor developed torque and the speed reference value.

i_{ds} , i_{qs} : are, respectively, the direct and quadrature components of the stator current and i_{dsref} , i_{qsref} being their respective reference values.

i_{mrest} : is estimated value of the direct component of stator current.

i_{mr} and i_{mrref} are, respectively, the magnetizing rotor current and its reference value.

T_r : is the rotor time constant,

J : is the induction motor constant of inertia.

In this controller system, the reference value of the current i_{qs}, $i_{qsref.}$, is determined by the torque control loop. On the other hand, when the induction motor is in steady-state operation, we have $i_{ds} = i_{mr}$, as a consequence, the reference of the current i_{mr}, $i_{mrref.}$, is calculated from the expression (5.8). If this calculated value exceeds the

rated value, the rated value, i_{mr}, will be used as a reference to avoid magnetic saturation, but when $i_{mrref.}$ is equal to the rated value, the (LMA) algorithm works exactly as in a conventional Field-Oriented Control (FOC).

This implementation of the controller requires, in addition to the field oriented scheme of the induction motor, a torque control loop, which may be needed when high dynamic performance loads are driven by the induction motor. But, as far as the HVAC load systems are concerned, which are not dynamically demanding, the LMA is adequate to be implemented with the simple scalar control scheme depicted in the following figure.

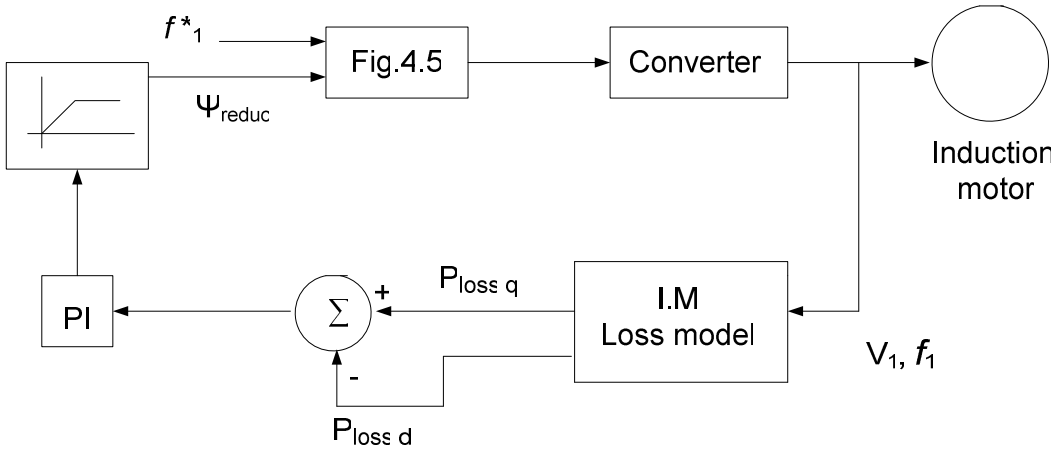

Fig.5.4. Block Diagram for Energy Optimal Scalar Model Based Control.

Where:

f_1^* : the frequency control variable.

V_1 and f_1: are, respectively, the voltage r.m.s value and frequency of the fundamental voltage supply.

$P_{loss,d}$ and $P_{loss,q}$ are, respectively, the loss component depending on the current direct with the rotor flux i_{ds}, and the loss component depending on the current in quadrature to the rotor flux i_{qs}.

ψ_{reduc} is the induction motor air gap flux at the new operating speed.

Based on this block diagram illustrating the operating mechanism of the model-based control system, the following simulation results showing the induction motor total losses and its efficiency variation with load conditions are presented.

5.3. Induction Motor Efficiency Computation using Model-Based Control Approach:

Using equations (5.6) and (5.9), the induction motor efficiency can be calculated as follows:

$$\eta = \frac{T_d.\omega_m}{T_d.\omega + P_t} = \frac{L_m.i_{qs}.i_{ds}.\omega_m}{L_m.i_{qs}.i_{ds}.\omega_m + P_t} \qquad (5.14).$$

This equation of efficiency combined the total power losses equation are used to calculate the power losses and efficiencies for the 1.5 kW, 4.0 kW, 7.5 kW, 25 kW and 50 kW induction motors, represented in the following plots.

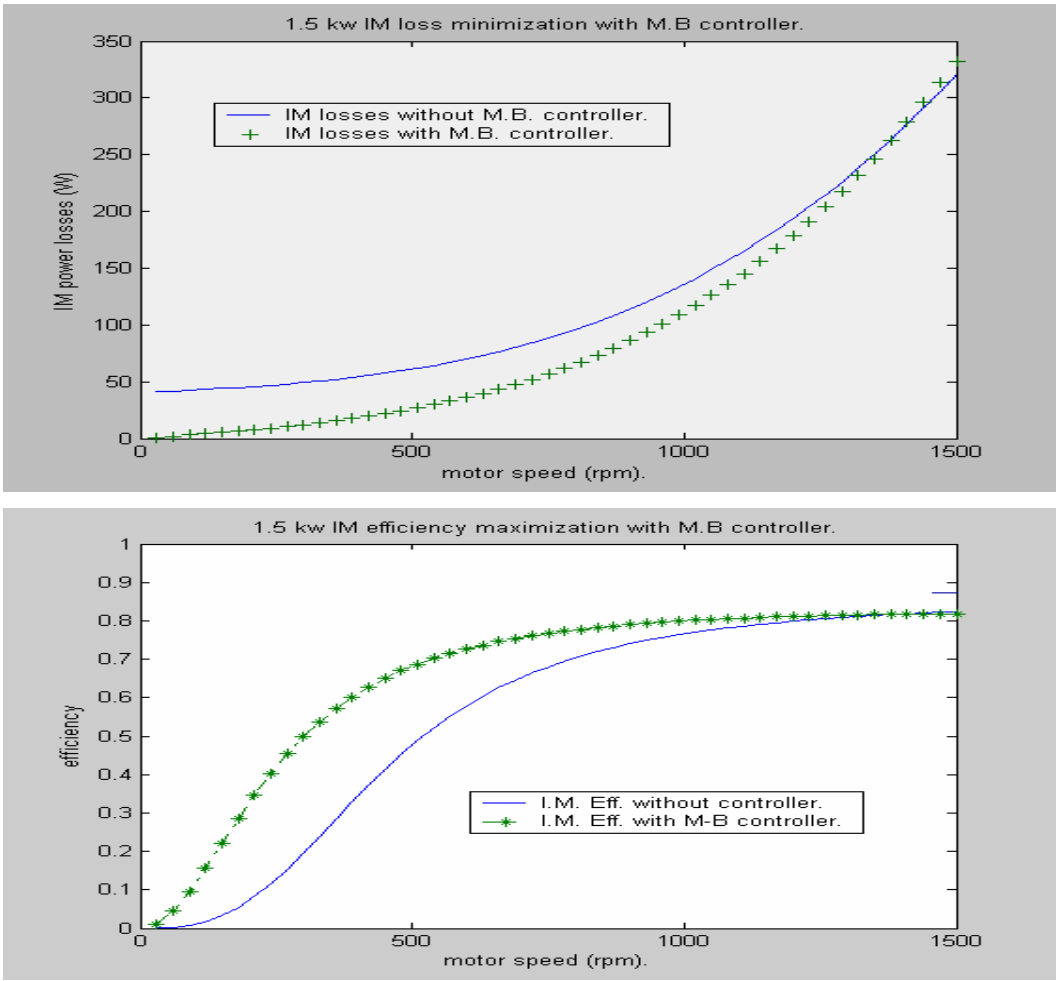

Fig.5.5. 1.5 kW Induction Motor Loss Minimization and Efficiency Improvement with Model-Based Controller.

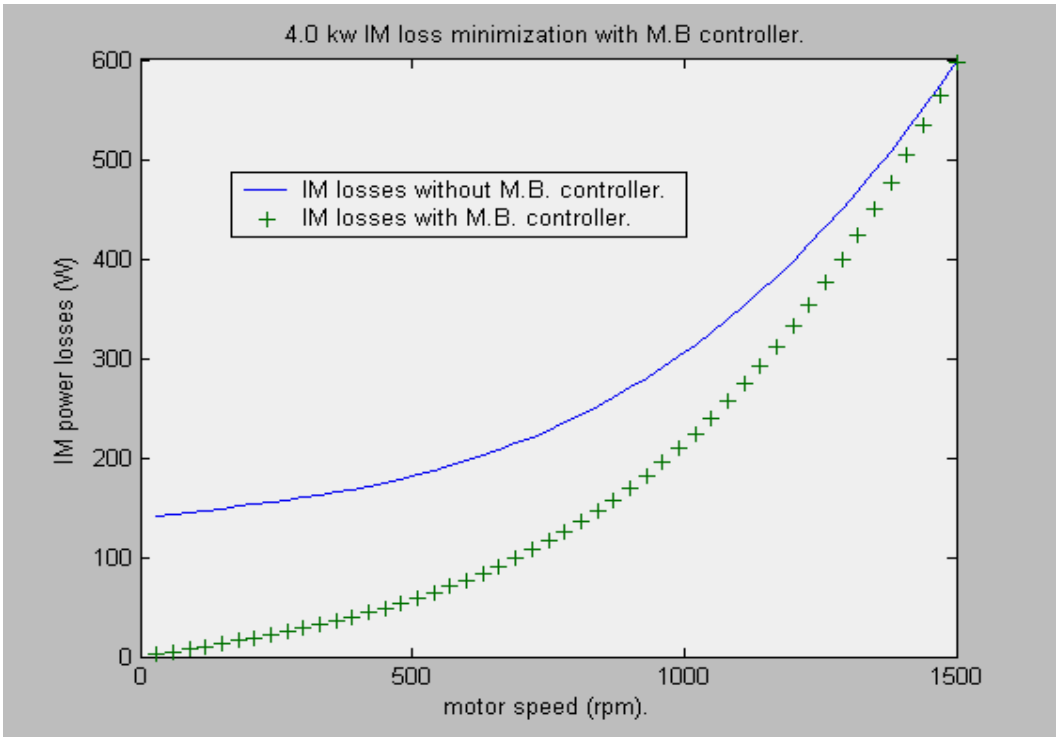

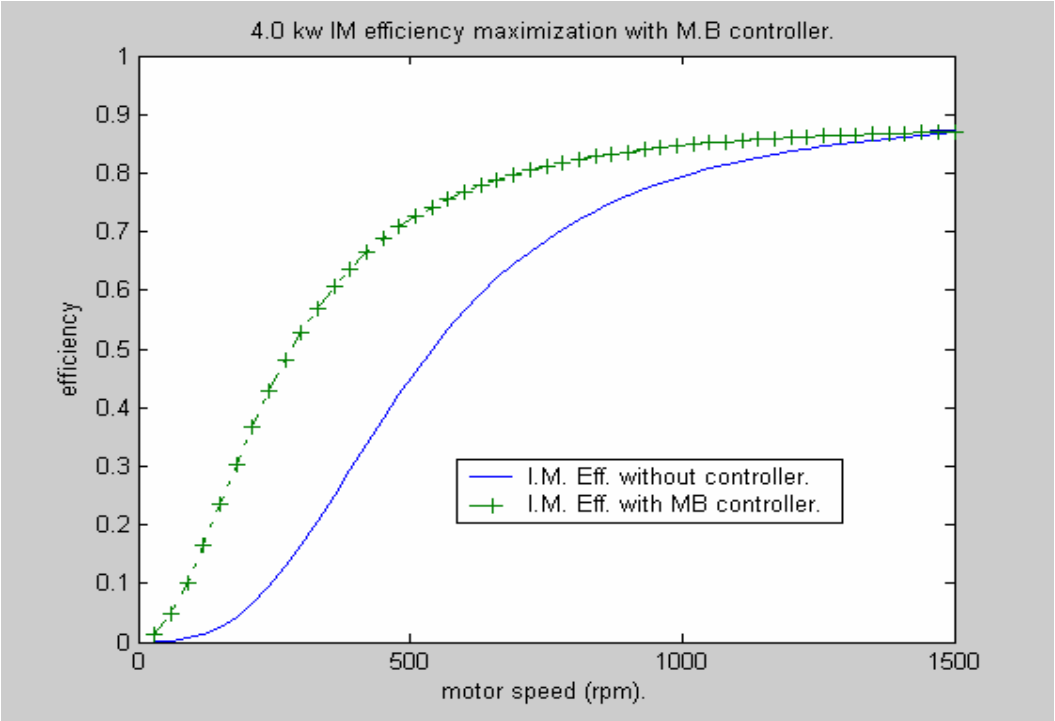

Fig.5.6. 4.0 kW Induction Motor Loss Minimization and Efficiency Improvement with Model-Based Controller.

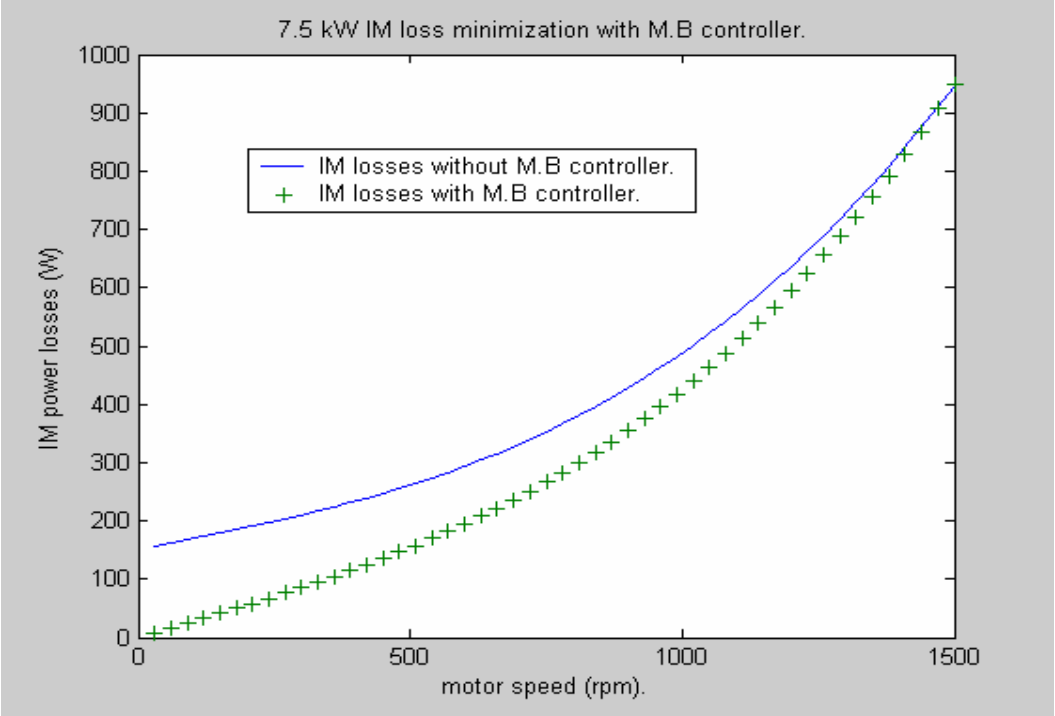

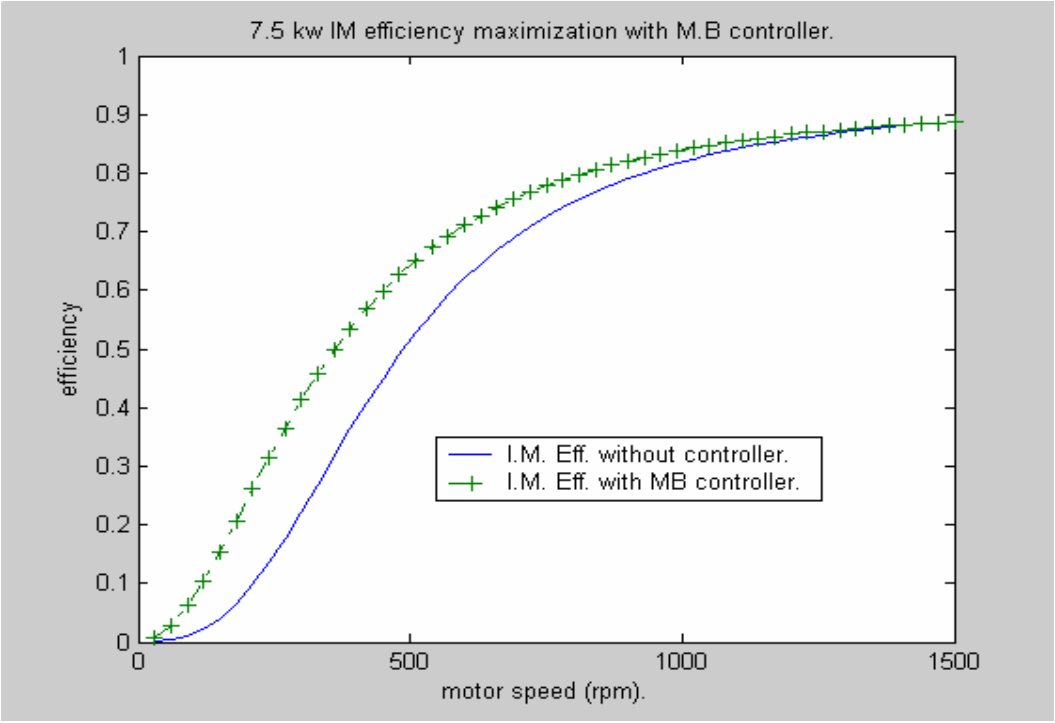

Fig.5.7. 7.5 kW Induction Motor Loss Minimization and Efficiency Improvement with Model-Based Controller.

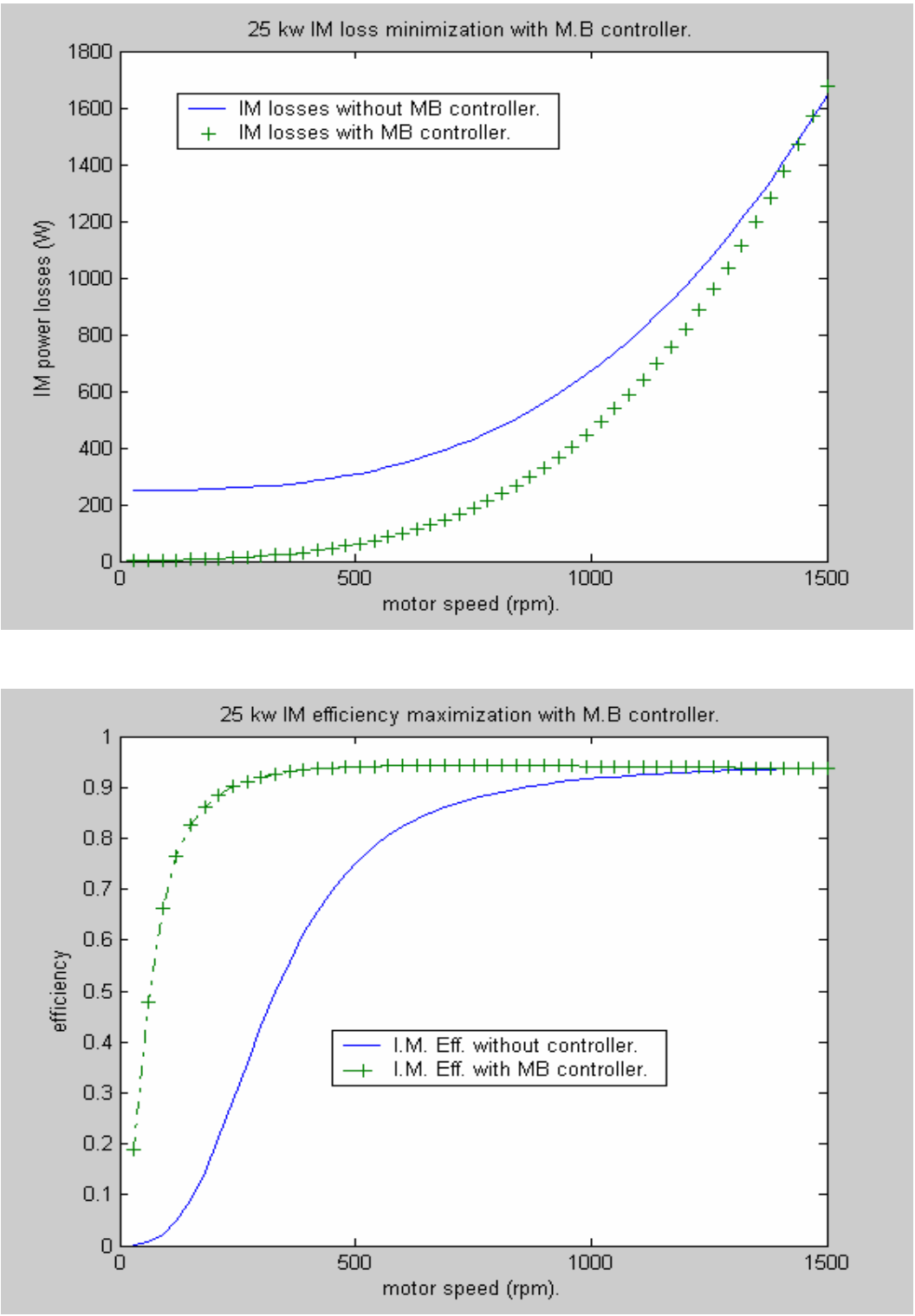

Fig.5.8. 25 kW Induction Motor Loss Minimization and Efficiency Improvement with Model-Based Controller.

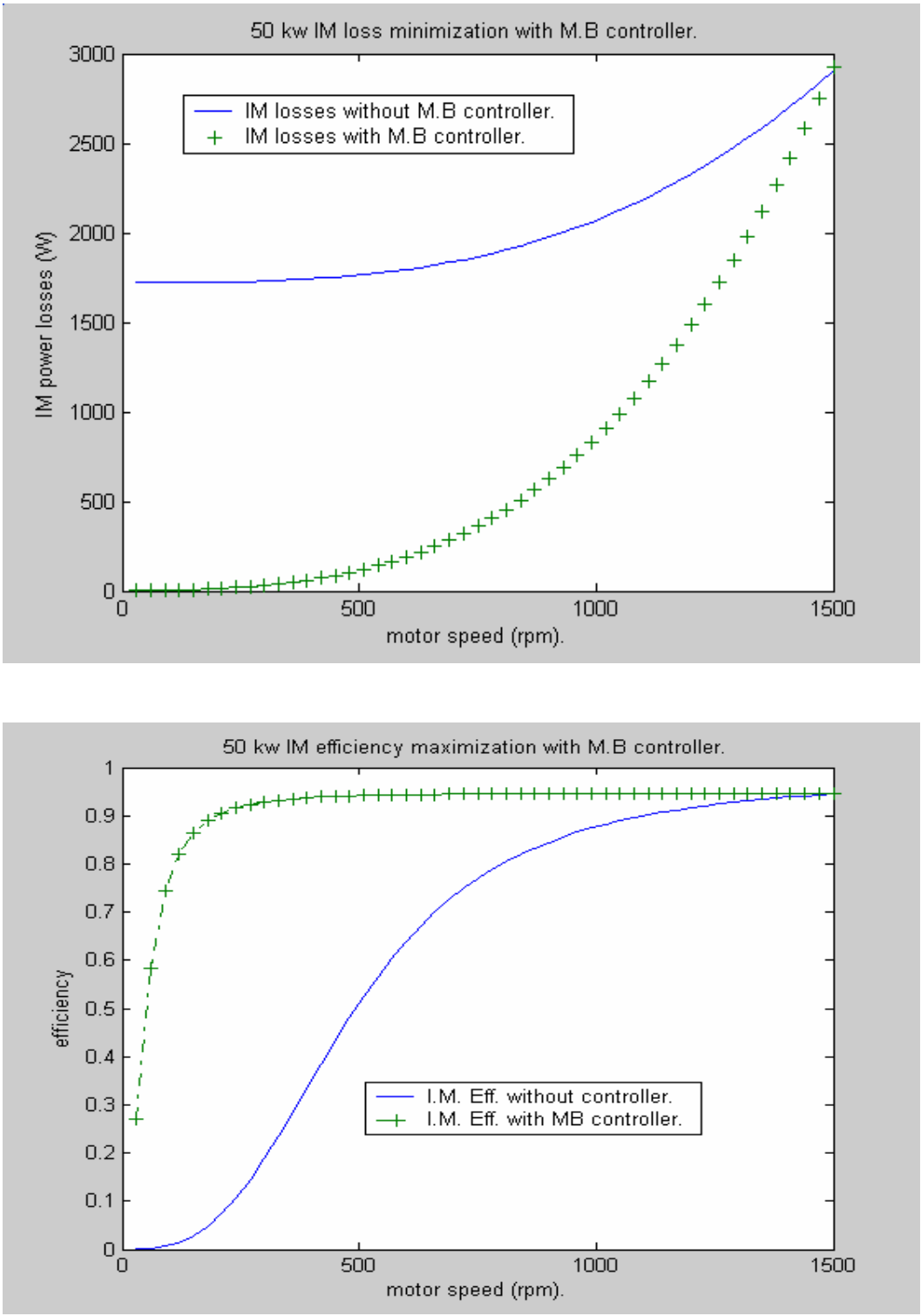

Fig.5.9. 50 kW Induction Motor Loss Minimization and Efficiency Improvement with Model-Based Controller.

5.3.1. Comments and Discussion:

The above plots show the induction motor total losses minimization and the corresponding efficiency improvement that can be achieved with the loss-model-based energy optimal controller. In order to show a clear picture, the simulation results are given in both cases: with and without the controller. In the following tables we illustrate these results of loss minimization and efficiency improvement at different operating load conditions below the rated speed and torque values for all induction motors studied.

1.5 kW three-phase, 50Hz – 4 poles squirrel cage induction motor Under Model-Based energy optimal controller.						
Induction motors operating speeds (rpm).	***Induction motor without M.B controller.***		***Induction motor with M.B controller.***		***Achieved Total losses reduction (w).***	***Achieved Efficiency Improvement***
	Total Losses (w).	***Efficiency***	***Total Losses (w).***	***Efficiency***		
Rated speed.	330.78	0.8195	332.4	0.8189	0.00	0.00
1200	193.51	0.8014	178.6	0.8112	14.91	0.0098
900	113.88	0.7606	86.12	0.7899	27.76	0.0293
600	69.82	0.6439	36.12	0.7265	33.7	0.0826
400	57.38	0.5048	21.77	0.6502	35.61	0.1454

Table 5.1. Loss Minimization and Efficiency Improvement of 1.5 kW Induction Motor with Model-Based Controller.

4.0 kW three-phase, 50Hz – 4 poles squirrel cage induction motor Under Model-Based energy optimal controller.						
Induction Motor operating speeds (rpm).	***Induction motor without M.B controller.***		***Induction motor with M.B controller.***		***Achieved Total Losses reduction (w).***	***Achieved Efficiency Improvement***
	Total Losses (w).	***Efficiency***	***Total Losses (w).***	***Efficiency***		
Rated speed.	598.4	0.8757	596.86	0.8753	0.00	0.00
1200	397.9	0.8532	332.17	0.8596	65.73	0.0064
900	270.25	0.8007	169.12	0.8347	101.13	0.034
600	197.05	0.6480	77.04	0.7643	120.01	0.1163
400	175.13	0.4748	48.89	0.6792	126.24	0.2044

7.5 kW three-phase, 50Hz – 4 poles squirrel cage induction motor Under Model-Based energy optimal controller.						
Induction motors operating speeds (rpm).	***Induction motor without M.B controller.***		***Induction motor with M.B controller.***		***Achieved Total losses reduction (w).***	***Achieved Efficiency Improvement***
	Total Losses (w).	***Efficiency***	***Total Losses (w).***	***Efficiency***		
Rated speed.	945.89	0.8915	943.83	0.8915	0.0000	0.00
1200	636.48	0.8673	595.41	0.8695	41.07	0.0022
900	427.51	0.8133	354.95	0.8246	72.56	0.0113
600	293.61	0.6656	194.78	0.7161	98.83	0.0505
400	246.98	0.5018	135.44	0.6025	111.54	0.1007

Table 5.2. Loss Minimization and Efficiency Improvement of 4.0 kW and 7.5 kW Induction Motor with Model-Based Controller.

25 kW three-phase, 50Hz – 4 poles squirrel cage induction motor Under Model-Based energy optimal controller.						
Induction motors operating speeds (rpm).	***Induction motor without M.B controller.***		***Induction motor with M.B controller.***		***Achieved Total losses reduction (w).***	***Achieved Efficiency Improvement***
	Total Losses (w).	***Efficiency***	***Total Losses (w).***	***Efficiency.***		
Rated speed.	1647.1	0.9390	1647.1	0.9388	0.00	0.00
1200	970.6	0.9314	939.57	0.9326	31.03	0.0012
900	558.87	0.9163	378.96	0.9241	179.91	0.0078
600	345.52	0.8607	112.25	0.9240	233.27	0.0633
400	292.51	0.7743	51.24	0.9188	241.27	0.1445

50 kW three-phase, 50Hz – 4 poles squirrel cage induction motor Under Model-Based energy optimal controller.						
Induction motors operating speeds (rpm).	***Induction motor without M.B controller.***		***Induction motor with M.B controller.***		***Achieved Total losses reduction (w).***	***Achieved Efficiency Improvement***
	Total Losses (w).	***Efficiency***	***Total Losses (w).***	***Efficiency.***		
Rated speed.	3195.5	0.9395	3195.5	0.9397	0.00	0.00
1200	2790.9	0.9141	1622.1	0.9382	1138.8	0.0241
900	2368.7	0.8541	681.96	0.9308	1686.74	0.0767
600	2154.2	0.7368	207.93	0.9264	1946.27	0.1896
400	2102.7	0.6903	93.66	0.9255	2009.04	0.2352

Table 5.3. Loss Minimization and Efficiency Improvement of 25 kW and 50 kW Induction Motor with Power Factor Controller.

It is clear from these results that the application of the model-based energy efficiency optimization controller allows an efficiency improvement of the squirrel cage induction motor when it is operated at speeds and / or torque below the rated operating conditions.

Results show also that the lower the drive operating speed further from the rated value, the higher the efficiency improvement is achieved.

Similar conclusions can be said from plots concerning the 1.5 kW and 4.0 kW induction motors. As for the 25 kW and 50 kW induction motors, we notice that the motor efficiency obtained with the controller is maintained almost constant at its rated value over a comparatively wider speed range.

5.4. Conclusion:

In this chapter, the loss-model-based energy efficiency optimization control approach is studied. The method is based on the loss model built for the induction motor in the d-q reference frame with the rotor flux oriented in the d-axis direction. According to this model, the total losses of the induction motor, including the core losses, can be calculated and minimized at every operating condition below rated condition.

The application of the model-based controller with the induction motor power ratings under study can lead to substantial efficiency improvement at partial loads.

Figures of several additional percentages in efficiency improvement are achieved, for example, a value of 5 % can be given for the 7.5 kW induction motor running at speed of 600 r.p.m, where the pattern of efficiency improvement is basically similar for all induction motors studied.

CHAPTER

6

Comparison between Power Factor and Model-Based Controllers Performances

6.1. Introduction:

The results of induction motor loss minimization and efficiency improvement using power factor and model-based energy efficiency controllers are given and discussed in the preceding two chapters. It is now in order to make a brief comparison between the two energy efficiency optimizers respective performances.

6.2. Comparison between Power Factor and Model Based Controllers:

Plots of achievable efficiency improvement using power factor and model-based energy optimal controllers are shown in the figures: Fig.6.1, Fig.6.2 and Fig.6.3 below for the five cases of induction motors studied.

The plots show the efficiency of induction motors without any energy optimizer; i.e. when the motor is simply speed controlled by variable frequency converter, and the efficiency when the motor is optimally controlled in order to maximize efficiency using the power factor and model-based controllers.

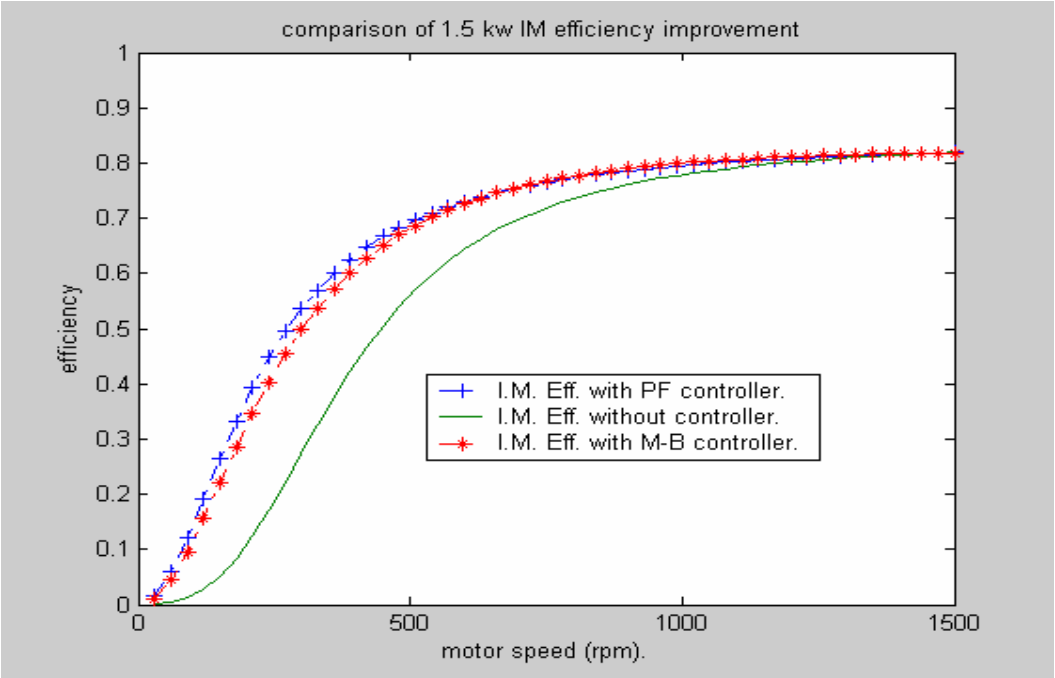

Fig.6.1. Comparison of 1.5 kW Induction Motor Efficiency Improvement with the Power Factor and Model-Based Energy Optimal Controllers.

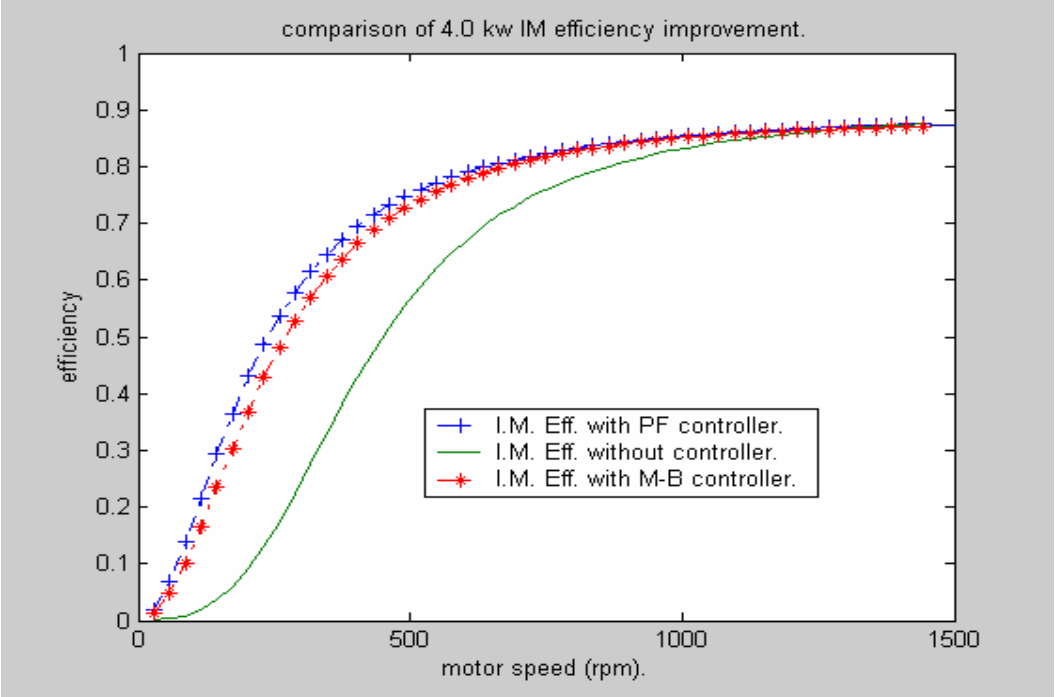

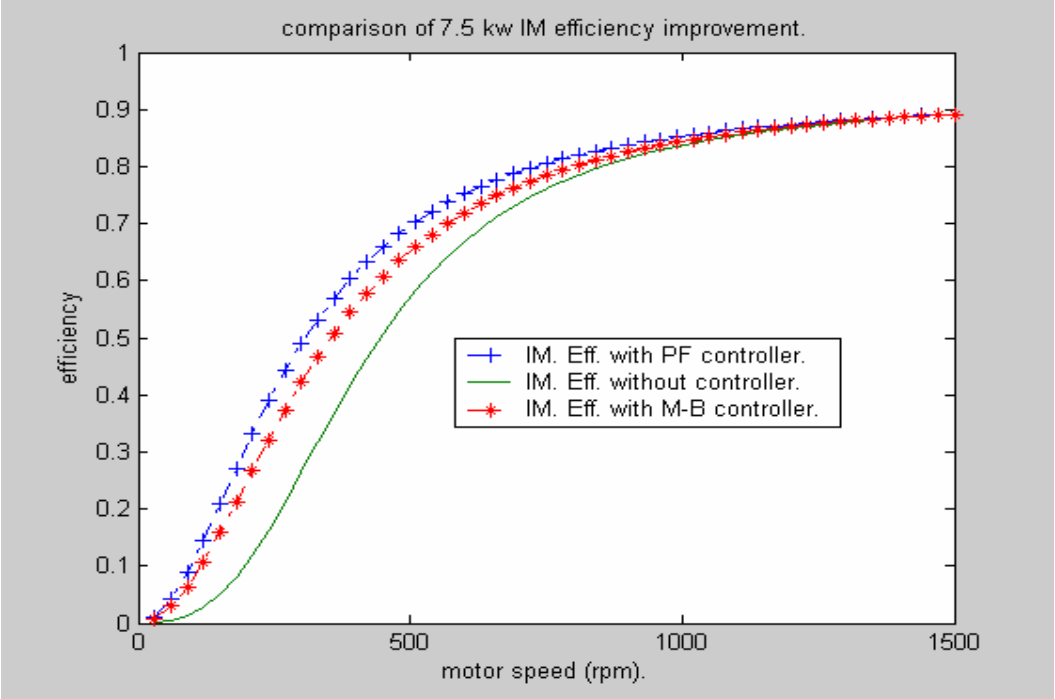

Fig.6.2. Comparison of 4.0 kW and 7.5 kW Induction Motor Efficiency Improvement with the Power Factor and Model-Based Energy Optimal Controllers.

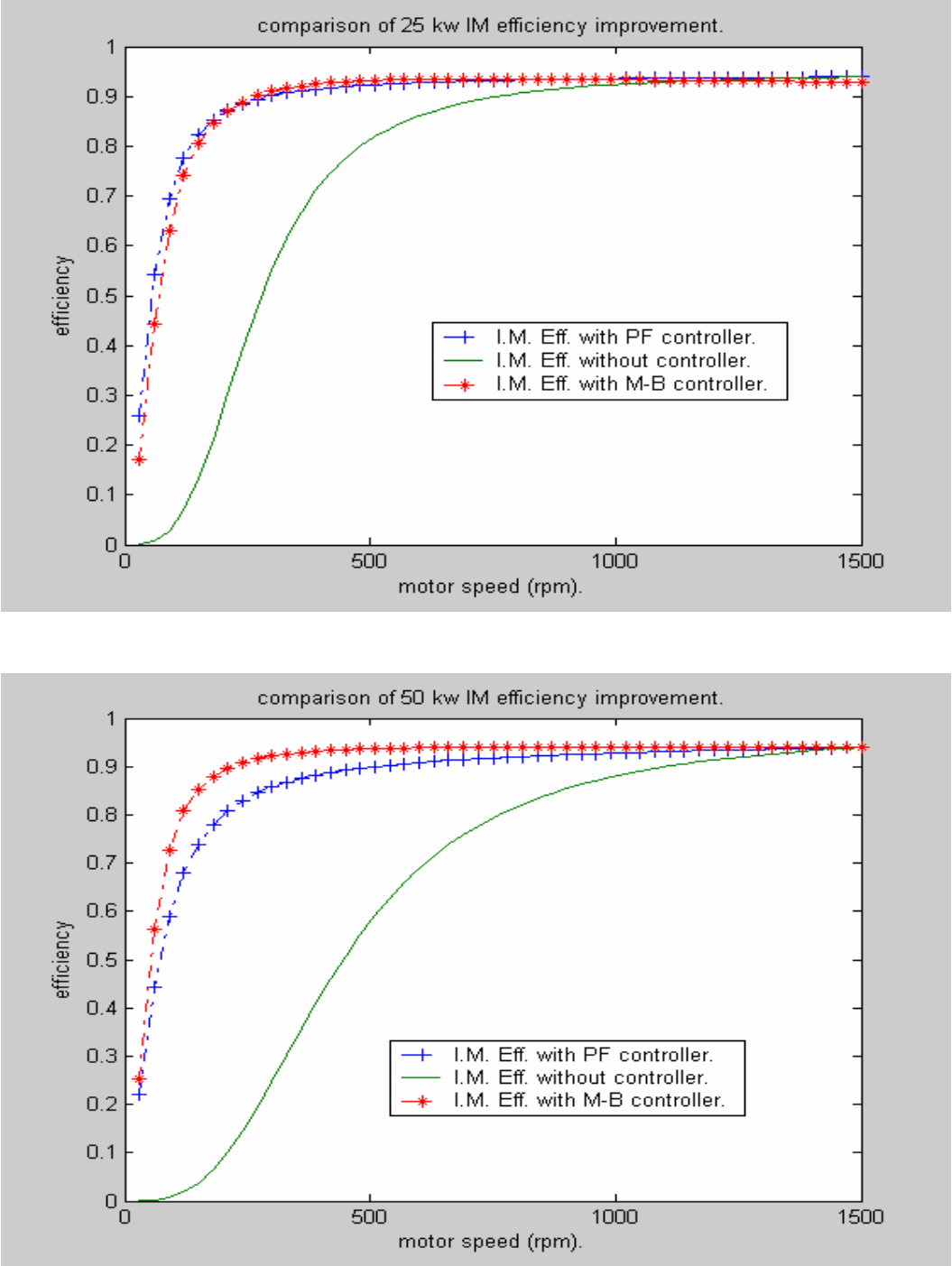

Fig.6.3. Comparison of 25 kW and 50 kW Induction Motor Efficiency Improvement with the Power Factor and Model-Based Energy Optimal Controllers.

6.2.1. Comments and Discussion:

It appears from these plots that both controllers have essentially the positive impact on efficiency improvement for all induction motors studied.

The following table can be deduced, which shows, quantitatively, the achievable efficiency improvement for the five motors using the two energy optimal controllers.

Induction motor power ratings	*Induction motor percent loading (rpm)*	*Efficiency improvement with **P.F** Controller*	*efficiency improvement With **M-B** Controller*
1.5 kW	Rated speed	0.00	0.00
	1200	0.0069	0.0098
	900	0.0255	0.0293
	600	0.087	0.0826
	400	0.1618	0.1454
4.0 kW	Rated speed	0.00	0.00
	1200	0.0098	0.0064
	900	0.0379	0.034
	600	0.1295	0.1163
	400	0.2312	0.2044
7.5 kW	Rated speed	0.00	0.00
	1200	0.0061	0.0022
	900	0.0239	0.0113
	600	0.0841	0.0505
	400	0.1524	0.1007
25 kW	Rated speed	0.00	0.00
	1200	0.0049	0.0012
	900	0.0178	0.0078
	600	0.0668	0.0633
	400	0.1446	0.1445
50 kW	Rated speed	0.00	0.00
	1200	0.0195	0.0241
	900	0.0705	0.0767
	600	0.1813	0.1896
	400	0.1967	0.2352

Table 6.1. Efficiency Improvement Comparison between Power Factor and Model-Based Controllers.

The margin of efficiency improvement is considerable with some noticeable differences in efficiency improvement achievable by the two energy efficiency control approaches appear at lower speeds for different motor power levels.

However, the overall performances achievable using either controllers are very much comparable, with slightly better performances achieved when using power factor controller, where a value of 8 % of efficiency improvement is achieved when using power factor controller compared with the value of 5 % of efficiency improvement achieved using model-based controller for 7.5 kW induction motor running at speed of 600 rpm can be given. This is not the case, however, for the case of 50 kW motor, where we see that the better efficiency improvement is achieved with the model-based controller.

6.2. Conclusion:

In view of these results, both power factor and model-based energy efficiency control techniques have exhibited a very interesting level of efficiency improvement for all induction motors population studied.

Results show that a slightly better efficiency improvement is achieved using power controller for 1.5 kW, 4.0 kW and 7.5 kW induction motors. As for 50 kW motor, the model-based controller predicted results are better.

On overall, we can conclude that both controllers are of a comparable level of performance.

General Conclusion

General Conclusion:

In this present work, the problem of efficiency optimization of the squirrel cage induction motor drive driving HVAC loads is addressed. HVAC loads dynamics are not demanding but efficiency improvement margins can be very important, particularly under light load conditions below rated speed.

The energy efficiency optimization of induction motor drive system consists of minimizing the drive total losses at each operating point below the full load operating point.

First, the loss components of the induction motor fed from a sine wave, balanced three phase power supply are quantified and analyzed. The induction motor losses consist of five components: stator and rotor copper losses, core losses, friction and windage losses and stray load losses. Under steady-state running conditions, design B squirrel cage type induction motor slip is about 0.05 p.u, which is the dominant type induction motor design for the population concerned, therefore the rotor frequency will not exceed the value of 2.5 Hz, which makes the rotor core losses very small, a fact that has led us to consider this loss component negligible.

The stray load losses, on the other hand, are important if the induction motor operating slip is large, which not the case in our study, justifying, therefore, our neglecting them. The remaining loss components, including the friction and windage losses, which are function of induction motor running speed, are considered controllable and can therefore be minimized.

The objective of this study being the optimization of the induction motor drive system efficiency, in addition to the induction motor loss components calculation, it is also required to estimate converter losses. The induction motor driving a fan type load is assumed supplied by a low harmonic content sine wave PWM-VSI power supply. The aim is to evaluate the converter total losses and compare their relative importance against those of the induction motor to gauge their effect on the drive energy efficiency optimization algorithms.

Based on closed form expressions of converter switching and conducting losses, the converter total losses are calculated when feeding induction motors of the following power levels: 1.5 kW, 4.0 kW, 7.5 kW, 25 kW and 50 kW. The obtained results have

shown that the converter total losses at full load operating point exhibit different relative proportions when compared to that of the induction motors; these results are found dependent on the motor size, where the percent ratio of the converter total losses to the motor losses at full load reaches the value of 4.5 % for the 1.5 kW induction motor and attains 15.48 % for the 50 kW motor power rating.

In view of these results, the total converter losses for the population of induction motors below 52 kW are considered small and, therefore, can be neglected without affecting the efficacy of the energy efficiency optimization algorithms.

Two energy optimal control techniques are applied in an attempt of achieving efficiency optimization; these are the power factor controller and the loss-model-based energy optimal controller.

The power factor energy efficiency controller is first presented; it is based on the calculation of induction motor displacement power factor according to the motor six-parameter per-phase exact equivalent circuit model including the core losses.

The principle of operation of the controller is based on the idea that optimal efficiency operation is ensured by maintaining the induction motor displacement power factor constant at its nominal value, whatever the load operating point is below the rated value. Therefore, the induction motor efficiency can be improved by a suitable reduction of the motor air gap flux when the system operates at speeds below the rated speed.

The simulation results of controlling the induction motor total losses and its operating efficiency by power factor energy optimal controller have shown very clearly that, at light load steady-state operating conditions, the total losses can be minimized for every operating point below the rated operating speed and a corresponding efficiency improvement is achieved throughout the range of speed variation from the rated operating speed down to minimum speed for all the motors studied.

The largest induction motor total losses minimization and efficiency improvement is in the region where the motor is running under light load conditions at reduced speeds.

The loss-model-based method of energy efficiency optimization control requires building the induction motor loss model in the d-q reference frame with the rotor flux oriented in the d-axis direction. In this model, the motor loss components, including

the core losses, are modelled with the induction motor decoupled and its total losses are expressed as a function of direct and quadrature components of the stator current, .

The principle of operation of the model-based method as an energy efficiency optimization technique is based on achieving a loss balance between the induction motor losses depending on the current direct with the rotor flux and that depending on the current in quadrature to the rotor flux. This balance is the unique condition for minimum total losses when the induction motor is lightly loaded.

The simulation results obtained when the model-based is used to energy optimally control the total losses and efficiency of induction motor driving a fan type load have shown, as for the case of power factor controller, an achievement of a very substantial energy efficiency improvement, in particular within the lower speed range.

When the two studied energy optimal controllers are compared, we can say that both control methods can achieve a high level of performance in terms of efficiency improvement. Though, slightly better results are obtained with the power factor controller for the 1.5 kW, 4.0 kW and 7.5 kW induction motors. However, for 50 kW induction motor, the model-based predicted performance is better.

On overall, results obtained indicate a comparable level of performance for the two optimization techniques, with the power factor controller being the stronger candidate for practical implementation because of its simplicity and cost effectiveness.

Appendices

Appendix A: Glossary of Terms and Supporting Information.

A.1. Abbreviations:

ac- Alternating Current.

A- Amperes.

ASD- Adjustable Speed Drive.

CSI- Current Source Inverter.

dc- Direct Current.

DPF- Displacement Power Factor.

EMF-Electromagnetic Force.

Eff. - Efficiency.

FOC : Field Oriented Controller.

hp- Horse Power.

HVAC- Heating, Ventilation and Air Conditioning.

Hz- Hertz

IM- Induction Motor**.**

IEEE- Institute of Electrical and Electronics Engineers.

IGBT- Insulate Gate Bipolar Transistor.

Kw- Kilowatts.

KWH- Kilowatt Hours.

KVA- Kilovolt-Amperes.

KVAR- Kilovolt-Amperes Reactive**.**

MMF- Magneto-Motive Force.

NEC- National Electrical Code**.**

NEMA- National Electrical Manufacturers Association**.**

PF- Power Factor**.**

PWM- Pulse Width Modulation.

r.p.m- Revolutions per Minute.

SCR- Silicon Controlled Rectifier**.**

Vac- Volts Alternating Current**.**

Vdc- Volts Direct Current.

VFD- Variable Frequency Drive (see ASD).

VSI- Voltage Source Inverter.

A.2. Terms:

Refer to IEEE standard dictionary of electrical and electronics terms for additional electrical related definitions

***Adjustable Speed Drive*:** electronic equipment that controls the speed of a motor by adjusting the frequency of the motor's power supply. Some adjustable speed drives also control current and phase angle to control other elements of motor performance.

Ambient Temperature : The temperature of surrounding air.

Breakdown Torque: The maximum torque a motor will produce and is also referred as maximum torque and pull-out torque.

Constant Power: A driven load for which shaft power is maintained at a controlled or preset level for a range of operating speeds.

Constant Torque: A driven load for which load torque is maintained as a controlled or preset level for a range of operating speeds.

Current Source Inverter: The ASD provides stepped current waveforms to the motor.

Driven Load: The machine or equipment that the motor is driving.

Efficiency: The ratio of output power to the input power, with a value somewhere between 0 and 1.

Energy Optimal Control: The method of motor control by adjusting its magnetization level.

Friction and Windage: The power loss within any rotating electrical machine caused by bearing and friction, air friction against rotating surfaces, and the movement of air circulating fans.

Full Load Current: The current required by the motor to produce full load torque at the motor's rated speed.

Full Load Torque: The torque required to produce rated horse power at full load speed.

Full Load Speed: The speed at which rated horse power is developed.

Horse Power: A unit of measure of the motor power. One horse power equals 746 watts.

Inrush Current: The high current drawn by a motor during start-up.

Load Torque: The torque required by a driven load to achieve or maintain a given speed.

Locked Rotor Current: The current drawn by a motor with the rotor stopped (locked) and full voltage applied.

Locked Rotor Torque: The torque produced by a motor when the rotor is stationary and full power is applied to the motor.

Losses: Energy that is not transmitted through a machine in a useful form.

Percent Slip: The percentage reduction in speed below synchronous speed.

Rectifier: A circuit that converts ac to dc.

Running Torque: The torque required to maintain the drive process or machine after it accelerates to the desired operating speed.

Shaft Power: The mechanical power transmitted from the motor shaft to the driven load.

Slip: The percentage difference between synchronous and operating speeds.

Starting Torque: The torque produced by a motor at rest when power is applied.

Synchronous Speed: The maximum speed for an ac motor.

Variable Torque: A driven load for which load torque changes with shaft speed.

Appendix B: Induction Motors and Inverter Parameters.

B.1. Induction Motor Equivalent Circuit Parameters:

In the following table, we illustrate the impedance parameters of the population of induction motors studied

IM. Power rating			*R1 (ohms)*	*R2 (ohms)*	*Rc (ohms)*	*X1 (ohms)*	*X2 (ohms)*	*Xm (ohms)*
kW	*Line voltage (V)*	*Rated speed (r.p.m)*						
1.5	*380*	*1420*	*7.9*	*5.8*	*2424*	*5.9*	*10.4*	*145.5*
4.0	*380*	*1440*	*1.37*	*1.1*	*699*	*1.53*	*2.5*	*44.3*
7.5	*380*	*1450*	*0.67*	*0.71*	*649*	*0.94*	*1.5*	*20.3*
25	*450*	*1450*	*0.10*	*0.17*	*557*	*0.3*	*0.5*	*23.6*
50	*440*	*1480*	*0.067*	*0.04*	*64.2*	*0.0885*	*0.0885*	*19.6*

Table B.1. Induction Motor Equivalent Circuit Parameters

B.2. Curve Fitting Determined Parameters of PWM-VSI Inverter:

The following are the curve fitting determined parameters of PWM-VSI inverter [40].

$A_{sw,on,T}$	$0.085.10^{-3}$
$B_{sw,on,T}$	1.0
$A_{sw,off,T}$	$0.118.10^{-3}$
$B_{sw,off,T}$	1.0
$U_{O,T}$ [V]	1.54
$r_{O,T}[\Omega]$	0.169
$B_{con,T}$	0.94
$A_{sw,on,D}$	0
$B_{sw,on,D}$	1.0
$A_{sw,off,D}$	$0.33.10^{-3}$
$B_{sw,off,D}$	0.58
$U_{O,D}$ [V]	0.66
$r_{O,D}[\Omega]$	0.166
$B_{con,D}$	0.7

Table B.2. Curve Fitting Determined Parameters of the PWM-VSI Inverter with IGBT Devices.

Appendix C: Air Gap MMF Harmonics.

C.1. Time Harmonic MMF Waves:

When a non-sinusoidal balanced power supply is used to feed induction motors, the output voltages or currents waveforms are harmonic content. Assuming that a converter has an output phase current of the fifth harmonic component, consequently, each phase establishes a standing mmf wave having the same spatial distribution as the fundamental, but pulsates at five times the supply frequency; therefore the fifth harmonic mmf of the first coil is given by:

$$F_1 = F_{(1,5)p}.\cos\theta.\sin 5.\omega.t \qquad \text{(C.1).}$$

Where $F_{(1,5)p}$ is the maximum amplitude of the fundamental space mmf wave due to the fifth current harmonic, and similarly the fifth harmonic mmf from the two other coils is given by:

$$F_2 = F_{(1,5)p}.\cos(\theta - 2\pi/3).\sin 5(\omega.t - 2\pi/3) \qquad \text{(C.2).}$$

$$F_3 = F_{(1,5)p}.\cos(\theta - 4\pi/3).\sin 5(\omega.t - 4\pi/3) \qquad \text{(C.3).}$$

Where as, due to the entire winding, the resultant mmf is obtained by adding the three mmf contributions and as the same as the previous manipulation, we end up with the following equation:

$$F = 3/2.F_{(1,5)p}\sin(5\omega.t + \theta) \qquad \text{(C.4)}$$

This confirms that the fifth harmonic currents produce a rotating mmf at a speed of rotate given by:

$$d\theta/dt = -5\omega_s \qquad \text{(C.4.1).}$$

Which means that the wave is moving at five times the synchronous speed in the opposite direction of the fundamental mmf. And also for the seventh harmonic currents produce a rotating mmf waves that moves at seven times synchronous speed:

$$d\theta/dt = 7\omega_s \qquad \text{(C.4.2).}$$

with the same direction as the fundamental mmf.

In general, we can state that the current harmonic of order **k = (3n+1)**, where n is an integer, produce forward rotating mmf waves, while harmonics of order **k = (3n-1)** produce backward mmf waves, where the speed of a time harmonic field is always k times the synchronous speed.

C.2. Space Harmonic mmf Waves due to Harmonic Components:

The presence of harmonic currents in the phase of integral slot winding not only produce fundamental component of special mmf, but the time and space harmonic mmf waves are presented simultaneously. So, additional rotating mmf waves are produced by the space harmonic distribution of mmf resulting from the time harmonic in the phase currents. For example, the fifth harmonic currents in each of the three phases produce the seventh harmonic space mmfs as follows:

$$F_1 = F_{(7,5)p} \cos 7.\theta \sin 5\omega.t \qquad \text{(C.5).}$$

$$F_2 = F_{(7,5)p}.\cos 7(\theta - 2\pi/3).\sin 5(\omega.t - 2\pi/3) \qquad \text{(C.6).}$$

$$F_3 = F_{(7,5)p} \cos 7(\theta - 4\pi/3)\sin 5(\omega.t - 4\pi/3) \qquad \text{(C.7).}$$

Following the same procedure for the entire winding $(F = F_1 + F_2 + F_3)$, therefore:

$$F = 3/2.F_{(7,5)p}.\sin(5\omega.t + 7\theta) \qquad \text{(C.8).}$$

This result clarifies that the seventh space harmonic mmf waves rotating backward at five seventh of synchronous speed.

C.3. Positive, Negative and Zero Sequences Harmonics:

It is deduced that the direction of rotation of the harmonic field is determined by the phase sequence of the harmonic currents.

C.3.1. Negative Sequence Harmonic:

Consider the fundamental three phase voltage components presented as follows:

$$\left.\begin{aligned} V_{AN} &= V_1 \sin \omega.t \\ V_{BN} &= V_1 \sin(\omega.t - 2\pi/3) \\ V_{CN} &= V_1 \sin(\omega.t - 4\pi/3) \end{aligned}\right\} = \text{ABC sequence}$$

These components produce the main field wave in the air gap rotating at synchronous speed. Their corresponding fifth harmonic phase voltages are given by:

$$\left.\begin{aligned} V_{AN} &= V_1 \sin 5\omega.t \\ V_{BN} &= V_1 \sin 5.(\omega.t - 2.\pi/3) = V_1 \sin(5.\omega.t - 4\pi/3) \\ V_{CN} &= V_1 \sin 5.(\omega.t - 4\pi/3) = V_1 \sin(5\omega.t - 2\pi/3) \end{aligned}\right\} = \text{ACB sequence}$$

These equations show the phase sequence of the fifth harmonic voltage $ACB \equiv CBA$ which is opposite to that of the fundamental sequence (ABC). Generally it can be shown that the

phase sequence of the harmonic voltages and currents of order k =(6n-1) is opposite to the fundamental ABC sequence, and they are known as negative sequence harmonics that are caused by the same winding of the fundamental and they have the same number of poles.

Because the phase sequence is opposite and the frequency is k times that of the fundamental, they produce harmonic field waves in the air gap which rotate at k times the fundamental synchronous speed in the opposite direction to the main field.

C.3.2. Positive Sequence Harmonics:

$$\left.\begin{aligned} V_{AN} &= V_1 \sin 7\omega.t \\ V_{BN} &= V_1 \sin 7(\omega.t - 2\pi/3) = V_1 \sin(7\omega.t - 2\pi/3) \\ V_{CN} &= V_1 \sin 7(\omega.t - 4\pi/3) = V_1 \sin(7\omega.t - 4\pi/3) \end{aligned}\right\} = \text{ABC sequence}$$

These equations show that the phase sequence of the seventh harmonic voltages ABC rotates with the same direction of that of the fundamental. Generally it can be shown that the phase sequence of the harmonic voltages and currents of order k = (6n+1) are in the same direction as that of the fundamental ABC sequence, and they are known as positive sequence harmonics that are caused by the same winding of the fundamental, and they have the same number of poles.

Because their frequency is k times that of the fundamental, they produce field waves rotate at a speed of k times the fundamental synchronous speed in the same direction to the main field.

C.3.3. Zero Sequence Harmonics:

The harmonic currents of order k = (6n-3) or k = 3n do not produce any fundamental air gap mmf because they are in exact time phase in each of the three windings, that is why they are called zero sequence harmonics, and they are also termed as tripplen harmonics.

Appendix D: Induction Motor Model in d-q Reference Frame.

Fig.C.1 shows the steady-state d- and q-axis equivalent circuits in the d-q coordinates which rotate synchronously with an electrical angular velocity ω.

The equivalent circuits include the effects of the copper and iron losses. The copper losses are represented by the stator and rotor resistances R_s and R_r, whereas the stator and rotor iron losses are represented by (R_{qls}, R_{dls}) and (R_{qlr}, R_{dlr}) respectively.

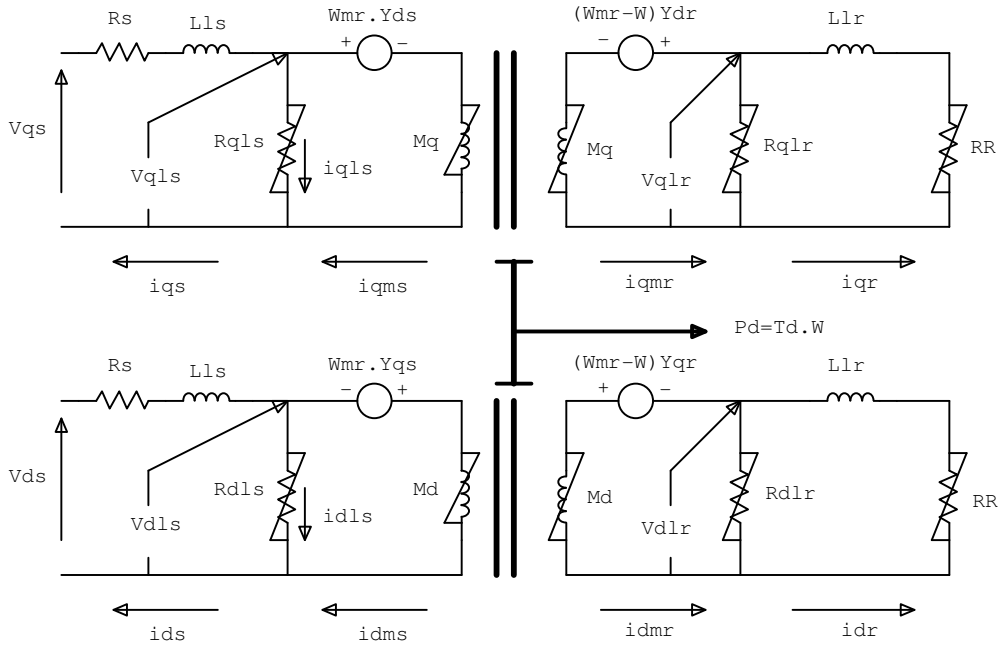

Fig.D.1. Induction Motor Equivalent Circuit In d-q Coordinates.

In order to have simplified equations, the d-axis of the coordinate will be defined in the direction of the rotor magnetic flux (field oriented frame). Therefore, the magnetic flux in the q-axis direction is zero [15]. Furthermore, and in order to have a simple induction motor model, the following simplifications have been made:

- Due to the fact that the leakage magnetic flux is small compared to the magnetizing flux, the leakage inductances, L_{ls} and L_{lr}, will be neglected,
- The resistors that represent the rotor iron losses will be considered as a part of the rotor resistance (R_R will be replaced by $R_r = R_R \,//\, R_{qlr}$),

- Every IM parameter will be considered constant, ignoring effects such as magnetic saturation and temperature.

We can state also that the currents observed from the field oriented frame are constant and consequently the inductor voltage drops are zero.

With the stated assumptions and the help of the equivalent circuit of Fig.D.1, the following equations can be deduced:

$$\begin{aligned} Y_{qr} &= 0 \\ &= M_q (i_{qms} + i_{qmr}) \\ &= Y_{qs} \end{aligned} \qquad \text{(D.1).}$$

Where Y_{qr} and Y_{qs} are the rotor and stator flux in the q- equivalent circuit; M_q is the mutual inductance between stator and rotor in the q- equivalent circuit.

From (D.1), it follows,

$$i_{qms} = -i_{qmr} \qquad \text{(D.2).}$$

In steady-state and using the field-oriented frame, the voltages across M_d and M_q, in the stator and rotor are always zero [13], therefore,

$$i_{dms} = i_{ds}, \qquad \text{(D.3).}$$

$$\begin{aligned} i_{dls} &= 0 \\ &= i_{dmr}. \end{aligned} \qquad \text{(D.4).}$$

From Fig.C.1, it follows,

$$\begin{aligned} Y_{ds} &= Y_{dr} \\ &= M_d (i_{dms} + i_{dmr}) \end{aligned} \qquad \text{(D.5).}$$

Where Y_{ds} and Y_{dr} are the stator and rotor flux in the d-equivalent circuit.

From (D.3) and (D.4), it follows,

$$\begin{aligned} Y_{ds} &= Y_{dr} \\ &= M_d i_{ds} \end{aligned} \qquad \text{(D.6).}$$

From Fig.D.1 and (D.1) – (D.6), the equivalent circuit of Fig.D.2 can be justified.

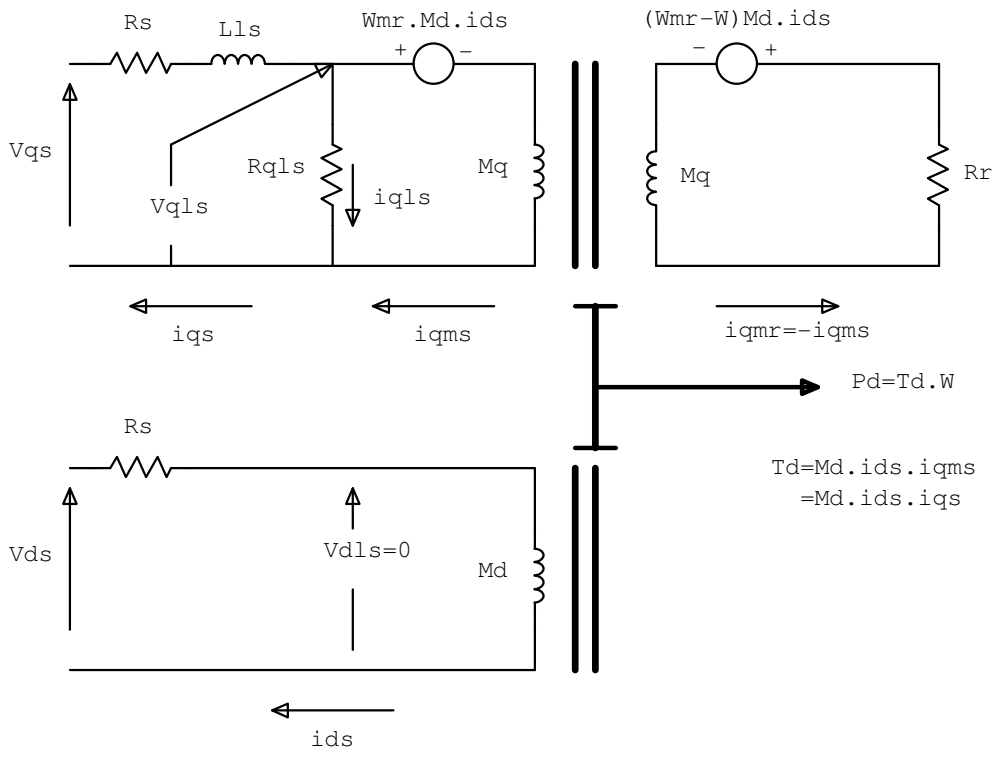

Fig.D.2. Steady-State Induction Motor Equivalent Circuit in Field Oriented Frame.

From (D.4), it can be concluded that, in the equivalent d-axis circuit, the iron losses are zero. This is the reason why R_{dls} has been eliminated in Fig.D.2. Therefore, the iron losses are concentrated in the equivalent q-axis circuit.

References:

[1] F. R. Bergseth, S. S. Vekata, “Introduction to Electric Energy Devices.”, first edition, Prentice Hall Inc., Englewood Cliffs, New Jersey 07632, 1987.

[2] S. A. Nasar, L. E. Unnewehr, “Electromechanics and Electric Machines.”, first edition, John Wiley and Sons, New York, 1979.

[3] www.inphotonics.com «Variable Speed Drive Theory", 2000.

[4] R. Gabriel, W. Leonard and C. Nordby, “Field-Oriented Control of a Standard AC Motor using Microprocessors .”, IEEE *Trans. Ind. App*., Vol. IA-16, pp. 186-192, Mar. / Apr., 1980.

[5] B. K. Bose, “High Performance Control of Induction Motor Drives.”, Department of Electrical Engineering, the University of Tennessee, Knoxville, U.S.A., 1988.

[6] www.inphotonics.com, “Induction Motor Control Theory”, 2000.

[7] F. Abrahamsen, F. Blaabjerg, J. K. Pedersen, P.Z. Grabowski and P. Thoegersen, “On the Energy Optimized Control of Standard and High Efficiency Induction Motors in CT and HVAC Applications”, IEEE *Trans. Ind. Applicat*., Vol. 34, pp. 822-831, July / Aug. 1998.

[8] www.abb.com, www.tic.toshiba.com, “Adjustable Speed Drives.”, 2001.

[9] H. N. Hickok, “Adjustable Speed- a Tool for Saving Energy Losses in Pumps, Fans, Blowers and Compressors”, IEEE / IAS Trans., vol. 21, pp. 124-136, Jan./Feb. 1985.

[10] R. W. Haines, D.C. Hittle, «Control Systems for Heating, Ventilating and Air Conditioning.”, Chapman and Hall, One Penn Plaza, New York, Fifth Edition, 1983.

[11] H. A. Al. Rachidi, A. Gastli, and A. Al-Badi, “Optimization of Variable Speed Induction Motor Efficiency using Artificial Neural Networks”, Electrical Engineering Department, College Of Engineering, Sultan Qaboos University, 2003.

[12] A. Cuckoo, D. Galler, „Control Means for Minimization of Losses in AC and DC Drives.“, IEEE *Trans.* On *Ind. App*., Vol. IA-19, No. 4, July / August 1983.

[13] G.O. Garcia, J. C. Mendes Luis, R. M. Stephan and E. H. Watanabe, “An Efficient Controller for an Adjustable Speed Induction Motor Drives.”, IEEE *Trans*. On *Ind. Elect.* Vol. 41, No. 5, pp. 533-539, Oct. 1994.

[14] G.O. Garcia, J. C. Mendes Luis, R.M. Stephan and E.H. Watanabe, "Fast Efficiency Maximizer for Adjustable-Speed Induction Motor Drives.", Electrical Engineering Program, Federal University Of Rio De Janeiro, Brazil, IEEE Trans. On Indust. Electron., 1992.

[15] J.C. Moreira, V. Blasko, and T. A. Lipo, "Low Cost Efficiency Minimizer for an Induction Motor Drive.", Dep. Of Electrical and Computer Engineering, University of Wisconsin, Madison, Wisconsin 53706, U.S.A, IEEE Press, 1989.

[16] G. C. D. Sousa, B. K. Bose, "Fuzzy Logic Based On-Line Efficiency Optimization Control of an Indirect Vector Controlled Induction Motor Drive", IEEE Trans. Ind. Electron., vol. 42, pp. 192-198, 1995.

[17] C. Minh Ta, Y. Hori, « Convergence Improvement of Efficiency Optimization Control of Induction Motor Drives.", IEEE *Trans. Ind. App.*, Vol.37, No.6, pp. 1746-1753, Nov. / Dec. 2001.

[18] D. Griffiths, "Principles and Problems of Electrical Machines.", Prentice Hall International (UK) Limited, 1995.

[19] M.G. Say, "Alternating Current Machines", Fifth Edition, English Language Book Society / Longman, (ELBS), 1983.

[20] V. Ostovic, "Computer –Aided Analysis of Electric Machines, a Mathematica Approach.", Prentice Hall International (UK), First Edition, 1994.

[21] W. Shepherd, L.N. Hulley and D. T. W.Liang, "Power Electronics and Motor Control.", Dep. of Electronic and Electrical Engineering, University of Bradford, England, Cambridge University Press, Second Edition, 1995.

[22] P. C. Crause, O. Wasynczuk, S. Sudhoff, "Analysis of Electric Machinery.", published by McGraw Hill, New York, first edition, 1986.

[23] D.V. Richardson, "Rotating Electric Machinery and Transformer Technology.", Reston Publishing Company Inc., a Prentice Hall Company, Reston, Virginia 22090, 1978.

[24] A. T. De Almeida, F. Ferreira, "Efficiency Testing of Electric Induction Motors.", ISR, Dep. Eng. Electronica University of Coimbra, Polo 2, 3030 Coimbra, Portugal.

[25] G. McPherson, "An Introduction to Electrical Machines and Transformers.", first ed. John Weily and Sons Inc., New York, 1981.

[26] Say, "Electrical Engineering Hand Book", London, 1976.

[27] D. A. Conkling, “Energy Efficient Motors and Adjustable Speed drives”, AIR FORCE PAMPHLET 32-1192, civil engineering, 1 February 2000.

[28] T. A. Lipo and D.W. Novotny, “Induction Motor Application Considerations for Adjustable Speed Drives.”, Dep. of Electrical and Computing Engineering, University of Wisconsin, Madison, August, 1988

[29] D. Finny, “Variable Frequency AC Motor Drive Systems.”, Peter Peregrinus Ltd., London, United Kingdom, 1991.

[30] P. S. Bimbhra, “Electrical Machinery, Theory, Performance and Applications”, Khanna Publishers, 2-B, Nath Market, Nait Sarak, Dehi.110006 (India), 2-nd Edition, 1990.

[31] B. K. Bose, “Power Electronics and AC Drives.”, Prentice Hall Englewood Cliffs, New Jersey 07632, 1986.

[32] M. P. Berizintu, D. Rotor, and G. Culea, “Energetic Rate Optimization of the Electric drives with Speed Control for the Turbo Machines.”, The University of Bacau, 5500, Bacau, Romania, 1995.

[33] H. E. Jordan, “Energy Efficient Electric Motors and their Applications’, Publishing Corporation, New York, Second Edition, 1997.

[34] ROBINCON, “Power Factor and Harmonics.”, Robincon Corporation, Technical Document,1987.

[35] S. K. Sen, “Electrical Machinery.”, Khanna Publisher, Nait Sarak. Delhi (India) 1989.

[36] B. K. Bose, “Power Electronics and Variable Frequency Drives, Technology and Applications.”, IEEE Press, 1997.

[37] M. H. Rashid, “Power Electronics, Circuits, Devices and Applications.”, Prentice Hall International Inc., Second Edition, 1993.

[38] L. H. Walker, P. M. Espelage, “A High-Performance Controlled Current Inverter Drives.”, IEEE *Trans. Ind. App.*, Vol. IA-16, pp. 193-202, Mar. / Apr. 1980

[39] B.K. Bose, "Power Electronic Control of AC Motors", Pergaman Press, New York, 1988.

[40] F. Blaabjerg, U. Jaeger, S. Munk-Nielsen, and J. K. Pedersen, "Power Losses in PWM-VSI Inverter using NPT and PT IGBT Devices", IEEE Trans. on Power Electron., Vol. 10, No.03, May, 1995.

[41] A. Khaldoun, “Commande Vectorielle d’un Moteur Asynchrone a Cage avec Adaptation par Logique Floue de la Résistance Rotorique et Minimisation des Pertes Totales.”,

Thèse de Magister, Laboratoire de Recherche sur L'Electrification des Entreprises Industrielles (LREEI), F.H.C, Université de Boumerdes, 2001.

[42] F. Abrahamsen, F. Blaabjerg, .J.K. Pedersen, and P. Thoegersen,, "Efficiency-Optimized Control of Medium Size Induction Motor Drives.", IEEE *Trans. Ind. Applicat.*, Vol. 37, No. 6, pp. 1761-1767, Nov. / Dec. 2001.

[43] B. K. Bose, "Adjustable Speed AC Drive Systems", IEEE Press, 1981.

[44] Moromoto, Y. Tog, J. Takeda, and T. Hirasa, "Loss Minimization Control of Permanent Magnet Synchronous Motor Drive.", IEEE *Trans. On Ind. Elect*, Vol. 41, No. 5, pp. 511-516, Oct. 1994.